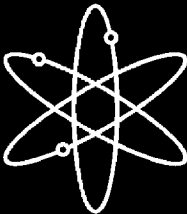# Effect of LWR Coolant Environments on the Fatigue Life of Reactor Materials

Draft Report for Comment

Argonne National Laboratory

U.S. Nuclear Regulatory Commission
Office of Nuclear Regulatory Research
Washington, DC 20555-0001

Effect of LWR Coolant Environments on the Fatigue Life of Reactor Materials

Draft Report for Comment

Prepared by
O. K. Chopra and W. J. Shack

Argonne National Laboratory
9700 South Cass Avenue
Argonne, IL 60439
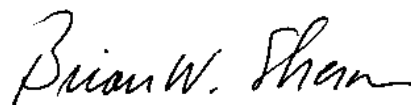

H. J. Gonzalez, NRC Project Manager

Abstract

The ASME Boiler and Pressure Vessel Code provides rules for the design of Class 1 components of nuclear power plants. Figures I–9.1 through I–9.6 of Appendix I to Section III of the Code specify design curves for applicable structural materials. However, the effects of light water reactor (LWR) coolant environments are not explicitly addressed by the Code design curves. The existing fatigue strain–vs.–life (ε–N) data illustrate potentially significant effects of LWR coolant environments on the fatigue resistance of pressure vessel and piping steels. Under certain environmental and loading conditions, fatigue lives in water relative to those in air can be a factor of 15 lower for austenitic stainless steels and a factor of ≈30 lower for carbon and low-alloy steels. This report summarizes the work performed at Argonne National Laboratory on the fatigue of piping and pressure vessel steels in LWR environments. The existing fatigue ε–N data have been evaluated to identify the various material, environmental, and loading parameters that influence fatigue crack initiation, and to establish the effects of key parameters on the fatigue life of these steels. Statistical models are presented for estimating fatigue life as a function of material, loading, and environmental conditions. The environmental fatigue correction factor for incorporating the effects of LWR environments into ASME Section III fatigue evaluations is described. The report also presents a critical review of the ASME Code fatigue design margins of 2 on stress (or strain) and 20 on life and assesses the possible conservatism in the current choice of design margins.

Foreword

This report summarizes, reviews, and quantifies the effects of the light-water reactor (LWR) environment on the fatigue life of reactor materials, including carbon steels, low-alloy steels, and austenitic stainless steels. The primary purpose of this report is to provide the background and technical bases to support Draft Regulatory Guide DG-1144, "Guidelines for Evaluating Fatigue Analyses Incorporating the Life Reduction of Metal Components Due to the Effects of the Light-Water Reactor Environment for New Reactors."

Previously published related reports include NUREG/CR-5704, "Effects of LWR Coolant Environments on Fatigue Design Curves of Austenitic Stainless Steels"; NUREG/CR-6717, "Environmental Effects on Fatigue Crack Initiation in Piping and Pressure Vessel Steels"; NUREG/CR-6787, "Mechanism and Estimation of Fatigue Crack Initiation in Austenitic Stainless Steels in LWR Environments"; NUREG/CR-6815, "Review of the Margins for ASME Code Fatigue Design Curve — Effects of Surface Roughness and Material Variability"; and NUREG/CR-6583, "Effects of LWR Coolant Environments on Fatigue Design Curves of Carbon and Low-Alloy Steels." By contrast to these previously published reports, this report provides a review of the existing fatigue data for carbon steels, low-alloy steels, and austenitic stainless steels to define the potential effects of key material, loading, and environmental parameters on the fatigue life of the steels. This report also updates the statistical models that are used to estimate the fatigue curves as a function of those parameters. In addition, this report presents a procedure for incorporating environmental effects into fatigue evaluations. The database described in this report (and its predecessors) reinforces the position espoused by the U.S. Nuclear Regulatory Commission (NRC) that the design curves for the fatigue life of pressure boundary and internal components fabricated from stainless steel should be revised, and a guideline for incorporating the LWR environmental effects in the fatigue life evaluations should be developed. Toward that end, this report proposes a method for establishing reference curves and safety factors for use in evaluating the fatigue life of reactor components exposed to LWR coolants and operational experience.

Data described in this review have been used to define fatigue design curves that include the LWR environmental effect. Specifically, the published data indicate that the existing code curves are nonconservative for austenitic stainless steels (e.g. 304, 316, and 316NG). The new stainless steel fatigue design curves presented herein are endorsed (through Draft Regulatory Guide DG-1144) for incorporation in fatigue analyses for new reactors. However, because of significant conservatism in quantifying other plant-related variables (such as cyclic behaviour, including stress and loading rates) involved in cumulative fatigue life calculations, the design of the current fleet of reactors is satisfactory, and the plants are safe to operate.

Brian W. Sheron, Director
Office of Nuclear Regulatory Research
U.S. Nuclear Regulatory Commission

Contents

Figures

xiii

Tables

Executive Summary

Section III, Subsection NB, of the ASME Boiler and Pressure Vessel Code contains rules for the design of Class 1 components of nuclear power plants. Figures I–9.1 through I–9.6 of Appendix I to Section III specify the Code design fatigue curves for applicable structural materials. However, Section III, Subsection NB–3121 of the Code states that the effects of the coolant environment on fatigue resistance of a material were not intended to be addressed in these design curves. Therefore, the effects of environment on the fatigue resistance of materials used in operating pressurized water reactor (PWR) and boiling water reactor (BWR) plants, whose primary–coolant pressure boundary components were designed in accordance with the Code, are uncertain.

The current Section–III design fatigue curves of the ASME Code were based primarily on strain–controlled fatigue tests of small polished specimens at room temperature in air. Best–fit curves to the experimental test data were first adjusted to account for the effects of mean stress and then lowered by a factor of 2 on stress and 20 on cycles (whichever was more conservative) to obtain the design fatigue curves. These factors are not safety margins but rather adjustment factors that must be applied to experimental data to obtain estimates of the lives of components. Recent fatigue–strain–vs.–life (ε–N) data obtained in the U.S. and Japan demonstrate that light water reactor (LWR) environments can have potentially significant effects on the fatigue resistance of materials. Specimen lives obtained from tests in simulated LWR environments can be much shorter than those obtained from corresponding tests in air.

This report reviews the existing fatigue ε–N data for carbon and low–alloy steels and wrought and cast austenitic stainless steels (SSs) in air and LWR environments. The effects of various material, loading, and environmental parameters on the fatigue lives of these steels are summarized. The results indicate that in air, the ASME mean curve for low–alloy steels is in good agreement with the available experimental data, and the curve for carbon steels is somewhat conservative. However, in air, the ASME mean curve for SSs is not consistent with the experimental data at strain amplitudes <0.5% or stress amplitudes <975 MPa (<141 ksi); the ASME mean curve is nonconservative.

The fatigue lives of both carbon and low–alloy steels and austenitic SSs are decreased in LWR environments; the reduction depends on some key material, loading, and environmental parameters. The fatigue data are consistent with the much larger database on enhancement of crack growth rates in these materials in LWR environments. The key parameters that influence fatigue life in these environments, e.g., temperature, dissolved–oxygen (DO) level in water, strain rate, strain (or stress) amplitude, and, for carbon and low–alloy steels, S content of the steel, have been identified. Also, the range of the values of these parameters within which environmental effects are significant has been clearly defined. If these critical loading and environmental conditions exist during reactor operation, then environmental effects will be significant and need to be included in the ASME Code fatigue evaluations.

Statistical models developed earlier to predict fatigue lives of small smooth specimens of carbon and low–alloy steels and wrought and cast austenitic SSs as a function of material, loading, and environmental parameters have been updated/revised by drawing upon a larger fatigue ε–N database. The functional form and bounding values of these parameters were based on experimental observations and data trends. An approach that can be used to incorporate the effects of LWR coolant environments into the ASME Code fatigue evaluations, based on the environmental fatigue correction factor, F_{en}, is discussed. The fatigue usage for a specific stress cycle of load set pair based on the Code fatigue design curves is multiplied by the correction factor to account for environmental effects.

The report also presents a critical review of the ASME Code fatigue design margins of 2 on stress and 20 on life and assesses the possible conservatism in the current choice of design margins. Although these factors were intended to be somewhat conservative, they should not be considered safety margins. These factors cover the effects of variables that can influence fatigue life but were not investigated in the experimental data that were used to obtain the fatigue design curves. Data available in the literature have been reviewed to evaluate the margins on cycles and stress that are needed to account for such differences and uncertainties. Monte Carlo simulations were performed to determine the margin on cycles needed to obtain a fatigue design curve that would provide a somewhat conservative estimate of the number of cycles to initiate a fatigue crack in reactor components. The results suggest that for both carbon and low–alloy steels and austenitic SSs, the current ASME Code requirements of a factor of 20 on cycle to account for the effects of material variability and data scatter, as well as size, surface finish, and loading history in low cycle fatigue, contain at least a factor of 1.7 conservatism. Thus, to reduce this conservatism, fatigue design curves have been developed from the ANL statistical model by first correcting for mean stress effects, and then reducing the mean–stress adjusted curve by a factor of 2 on stress or 12 on cycles, whichever is more conservative. These design curves are consistent with the existing fatigue ε–N data. A detailed procedure for incorporating environmental effects into fatigue evaluations is presented.

Abbreviations

ANL	Argonne National Laboratory
ANN	Artificial Neural Network
ASME	American Society of Mechanical Engineers
BWR	Boiling Water Reactor
CGR	Crack Growth Rate
CUF	Cumulative Usage Factor
DO	Dissolved Oxygen
EAC	Environmentally Assisted Cracking
ECP	Electrochemical Potential
EPR	Electrochemical Potentiodynamic Reactivation
EPRI	Electric Power Research Institute
GE	General Electric Co.
IHI	Ishikawajima-Harima Heavy Industries
KWU	Kraftwerk Union Laboratories
LWR	Light Water Reactor
MA	Mill Annealed
MEA	Materials Engineering Associates
MHI	Mitsubishi Heavy Industries
MPA	Materialprufungsanstalt
MSC	Microstructurally Small Crack
NRC	Nuclear Regulatory Commission
ORNL	Oak Ridge National Laboratory
PVRC	Pressure Vessel Research Council
PWR	Pressurized Water Reactor
RCS	Reactor Coolant System
RT	Room Temperature
SCC	Stress Corrosion Cracking
SICC	Strain Induced Corrosion Cracking
SS	Stainless Steel
UTS	Ultimate Tensile Strength

Acknowledgments

1. Fatigue Analysis

The American Society of Mechanical Engineers (ASME) Boiler and Pressure Vessel Code Section III, Subsection NB, which contains rules for the design of Class 1 components for nuclear power plants, recognizes fatigue as a possible mode of failure in pressure vessel steels and piping materials. Fatigue has been a major consideration in the design of rotating machinery and aircraft, where the components are subjected to a very large number of cycles (e.g., high–cycle fatigue) and the primary concern is the endurance limit, i.e., the stress that can be applied an infinite number of times without failure. However, cyclic loadings on a reactor pressure boundary component occur because of changes in mechanical and thermal loadings as the system goes from one load set (e.g., pressure, temperature, moment, and force loading) to another. The number of cycles applied during the design life of the component seldom exceeds 10^5 and is typically less then a few thousand (e.g., low–cycle fatigue). The main difference between high–cycle and low–cycle fatigue is that the former involves little or no plastic strain, whereas the latter involves strains in excess of the yield strain. Therefore, design curves for low–cycle fatigue are based on tests in which strain rather than stress is the controlled variable.

The ASME Code fatigue evaluation procedures are described in NB-3200, "Design by Analysis," and NB-3600, "Piping Design." For each stress cycle or load set pair, an individual fatigue usage factor is determined by the ratio of the number of cycles anticipated during the lifetime of the component to the allowable cycles. Figures I–9.1 through I–9.6 of the mandatory Appendix I to Section III of the ASME Boiler and Pressure Vessel Code specify fatigue design curves that define the allowable number of cycles as a function of applied stress amplitude. The cumulative usage factor (CUF) is the sum of the individual usage factors, and ASME Code Section III requires that the CUF at each location must not exceed 1.

The ASME Code fatigue design curves, given in Appendix I of Section III, are based on strain–controlled tests of small polished specimens at room temperature in air. The design curves have been developed from the best–fit curves to the experimental fatigue–strain–vs.–life (ε–N) data, which are expressed in terms of the Langer equation[1] of the form

$$\varepsilon_a = A1\left(N\right)^{-n1} + A2 , \tag{1}$$

where ε_a is the applied strain amplitude, N is the fatigue life, and A1, A2, and n1 are coefficients of the model. Equation 1 may be written in terms of stress amplitude S_a instead of ε_a. The stress amplitude is the product of ε_a and elastic modulus E, i.e., $S_a = E \cdot \varepsilon_a$. The current ASME Code best–fit or mean curve described in the Section III criteria document[2] for various steels is given by

$$S_a = \frac{E}{4\sqrt{N_f}} \ln\left(\frac{100}{100 - A_f}\right) + B_f , \tag{2}$$

where E is the elastic modulus, N_f is the number of cycles to failure, and A_f and B_f are constants related to reduction in area in a tensile test and endurance limit of the material at 10^7 cycles, respectively. The current Code mean curve for carbon steel is expressed as

$$S_a = 59{,}734 \, (N_f)^{-0.5} + 149.2, \tag{3}$$

for low-alloy steel, as

$$S_a = 49,222 \ (N_f)^{-0.5} + 265.4, \tag{4}$$

and for austenitic SSs, as

$$S_a = 58,020 \ (N_f)^{-0.5} + 299.9. \tag{5}$$

Note that because most of the data used to develop the Code mean curve were obtained on specimens that were tested to failure, in the Section III criteria document, fatigue life is defined as cycles to failure. Accordingly, the ASME Code fatigue design curves are generally considered to represent allowable number of cycles to failure. However, in Appendix I to Section III of the Code the design curves are simply described as stress amplitude (S_a) vs. number of cycles (N).

In the fatigue tests performed during the last three decades, fatigue life is defined in terms of the number of cycles for tensile stress to decrease 25% from its peak or steady–state value. For typical cylindrical specimens used in these studies, this corresponds to the number of cycles needed to produce an $\approx$ 3–mm–deep crack in the test specimen. Thus, the fatigue life of a material is actually being described in terms of three parameters, viz., strain or stress, cycles, and crack depth. The best–fit curve to the existing fatigue ε–N data describes, for given strain or stress amplitude, the number of cycles needed to develop a 3–mm deep crack. The fatigue ε–N data are typically expressed by rewriting Eq. 1 as

$$\ln(N) = A - B \ln(\varepsilon_a - C), \tag{6}$$

where A, B, and C are constants; C represents the fatigue limit of the material; and B is the slope of the log-log plot of fatigue ε–N data. The ASME Code mean–data curves (i.e., Eqs. 3-5) may be expressed in terms of Eq. 6 as follows. The fatigue life of carbon steels is given by

$$\ln(N) = 6.726 - 2.0 \ln(\varepsilon_a - 0.072), \tag{7}$$

for low-alloy steels, by

$$\ln(N) = 6.339 - 2.0 \ln(\varepsilon_a - 0.128), \tag{8}$$

and, for austenitic SSs, by

$$\ln(N) = 6.954 - 2.0 \ln(\varepsilon_a - 0.167). \tag{9}$$

The Code fatigue design curves have been obtained from the best–fit (or mean–data) curves by first adjusting for the effects of mean stress using the modified Goodman relationship given by

$$S'_a = S_a \left(\frac{\sigma_u - \sigma_y}{\sigma_u - S_a} \right) \quad \text{for } S_a < \sigma_y, \tag{10}$$

and

$$S'_a = S_a \quad \text{for } S_a > \sigma_y, \tag{11}$$

where S'_a is the adjusted value of stress amplitude, and σ_y and σ_u are yield and ultimate strengths of the material, respectively. Equations 10 and 11 assume the maximum possible mean stress and typically give a conservative adjustment for mean stress. The fatigue design curves are then obtained by reducing the fatigue life at each point on the adjusted best-fit curve by a factor of 2 on strain (or stress) or 20 on cycles, whichever is more conservative.

The factors of 2 and 20 are not safety margins but rather adjustment factors that should be applied to the small–specimen data to obtain reasonable estimates of the lives of actual reactor components. As described in the Section III criteria document,[2] these factors were intended to account for data scatter (including material variability) and differences in surface condition and size between the test specimens and actual components. In comments about the initial scope and intent of the Section III fatigue design procedures Cooper[3] states that the factor of 20 on life was regarded as the product of three subfactors:

Scatter of data (minimum to mean)	2.0
Size effect	2.5
Surface finish, atmosphere, etc.	4.0

Although the Section III criteria document[2] states that these factors were intended to cover such effects as environment, Cooper[3] further states that the term "atmosphere" was intended to reflect the effects of an industrial atmosphere in comparison with an air-conditioned laboratory, not the effects of a specific coolant environment. Subsection NB–3121 of Section III of the Code explicitly notes that the data used to develop the fatigue design curves (Figs. I–9.1 through I–9.6 of Appendix I to Section III) did not include tests in the presence of corrosive environments that might accelerate fatigue failure. Article B–2131 in Appendix B to Section III states that the owner's design specifications should provide information about any reduction to fatigue design curves that is necessitated by environmental conditions.

Existing fatigue ε–N data illustrate potentially significant effects of light water reactor (LWR) coolant environments on the fatigue resistance of carbon and low–alloy steels and wrought and cast austenitic SSs.[4-44] Under certain environmental and loading conditions, fatigue lives of carbon and low–alloy steels can be a factor of 30 lower in the coolant environment than in air. Therefore, the margins in the ASME Code may be less conservative than originally intended.

The fatigue ε–N data are consistent with the much larger database on enhancement of crack growth rates (CGRs) in these materials in simulated LWR environments. The key parameters that influence fatigue life in these environments, e.g., temperature, dissolved–oxygen (DO) level in water, strain rate, strain (or stress) amplitude, and, for carbon and low–alloy steels, S content of the steel, have been identified. Also, the range of the values of these parameters within which environmental effects are significant has been clearly defined. If these critical loading and environmental conditions exist during reactor operation, then environmental effects will be significant and need to be included in the ASME Code fatigue evaluations. Experience with nuclear power plants worldwide indicates that the critical range of loading and environmental conditions that leads to significant environmental effects on fatigue crack initiation are observed during plant operation.[44-60]

Many failures of reactor components have been attributed to fatigue; examples include piping, nozzles, valves, and pumps.[45-52] The mechanism of cracking in feedwater nozzles and piping has been attributed to corrosion fatigue or strain–induced corrosion cracking (SICC).[53-55] A review of significant occurrences of corrosion fatigue damage and failures in various nuclear power plant systems has been presented in an Electric Power Research Institute (EPRI) report.[44] In piping components, several failures were associated with thermal loading due to thermal stratification and striping. Thermal stratification is

caused by the injection of low–flow, relatively cold feedwater during plant startup, hot standby, or variations below 20% of full power, whereas thermal striping is caused by rapid, localized fluctuations of the interface between hot and cold feedwater. Significant cracking has also occurred in nonisolable piping connected to a PWR reactor coolant system (RCS). In most cases, thermal cycling was caused by interaction of hot RCS fluid from turbulent penetration at the top of the pipe, and cold valve leakage fluid that had stratified at the bottom of the pipe. Lenz et al.[54] have shown that in feedwater lines, strain rates are 10^{-3}–10^{-5}%/s due to thermal stratification and 10^{-1}%/s due to thermal shock. They also have reported that thermal stratification is the primary cause of crack initiation due to SICC. Full–scale mock-up tests to generate thermal stratification in a pipe in a laboratory have confirmed the applicability of laboratory data to component behavior.[43,61] A recent study conducted on SS pipe bend specimens in simulated PWR primary water at 240°C concluded that reactor coolant environment can have a significant effect on the fatigue life of SSs.[108]

Thermal loading due to flow stratification or mixing was not included in the original design basis analyses. Regulatory evaluation has indicated that thermal–stratification cycling can occur in all PWR surge lines.[62] In PWRs, the pressurizer water is heated to ≈227°C. The hot water, flowing at a very low rate from the pressurizer through the surge line to the hot–leg piping, rides on a cooler water layer. The thermal gradients between the upper and lower parts of the pipe can be as high as 149°C.

Two approaches have been proposed for incorporating the environmental effects into ASME Section III fatigue evaluations for primary pressure boundary components in operating nuclear power plants: (a) develop new fatigue design curves for LWR applications, or (b) use an environmental fatigue correction factor to account for the effects of the coolant environment.

In the first approach, following the same procedures used to develop the current fatigue design curves of the ASME Code, environmentally adjusted fatigue design curves are developed from fits to experimental data obtained in LWR environments. Interim fatigue design curves that address environmental effects on the fatigue life of carbon and low–alloy steels and austenitic SSs were first proposed by Majumdar et al.[63] Fatigue design curves based on a more rigorous statistical analysis of experimental data were developed by Keisler et al.[64] These design curves have subsequently been updated on the basis of updated statistical models.[4,6,37,38] However, because, in LWR environments, the fatigue life of carbon and low–alloy steels and austenitic SSs depends on several loading and environmental parameters, such an approach would require developing several design curves to cover all possible conditions encountered during plant operation. Defining the number of these design curves or the loading and environmental conditions for the curves is not easy.

The second approach, proposed by Higuchi and Iida,[13] considers the effects of reactor coolant environments on fatigue life in terms of an environmental fatigue correction factor, F_{en}, which is the ratio of fatigue life in air at room temperature to that in water under reactor operating conditions. To incorporate environmental effects into fatigue evaluations, the fatigue usage factor for a specific stress cycle or load set pair, based on the ASME Code design curves, is multiplied by the environmental fatigue correction factor. Specific expressions for F_{en}, based on the Argonne National Laboratory (ANL) statistical models, have been developed.[38] Such an approach is relatively simple and is recommended in this report.

This report presents an overview of the existing fatigue ε–N data for carbon and low–alloy steels and wrought and cast austenitic SSs in air and LWR environments. The data are evaluated to (a) identify the various material, environmental, and loading parameters that influence fatigue crack initiation and (b) establish the effects of key parameters on the fatigue life of these steels. Statistical models, presented

in earlier reports, for estimating fatigue life as a function of material, loading, and environmental conditions have been updated using a larger database. The F_{en} approach for incorporating effects of LWR environments into ASME Section III fatigue evaluations is described. The report also presents a critical review of the ASME Code fatigue design margins of 2 on stress (or strain) and 20 on life and assesses the possible conservatism in the current choice of design margins.

2. Fatigue Life

The formation of surface cracks and their growth to an engineering size (3–mm deep) constitute the fatigue life of a material, which is represented by the fatigue ε–N curves. Fatigue life has conventionally been divided into two stages: initiation, expressed as the number of cycles required to form microcracks on the surface; and propagation, expressed as cycles required to propagate the surface cracks to engineering size. During cyclic loading of smooth test specimens, surface cracks 10 μm or longer form early in life (i.e., <10% of life) at surface irregularities either already in existence or produced by slip bands, grain boundaries, second–phase particles, etc.[4,5] Thus, fatigue life may be considered to constitute propagation of cracks from 10 to 3000 μm long.
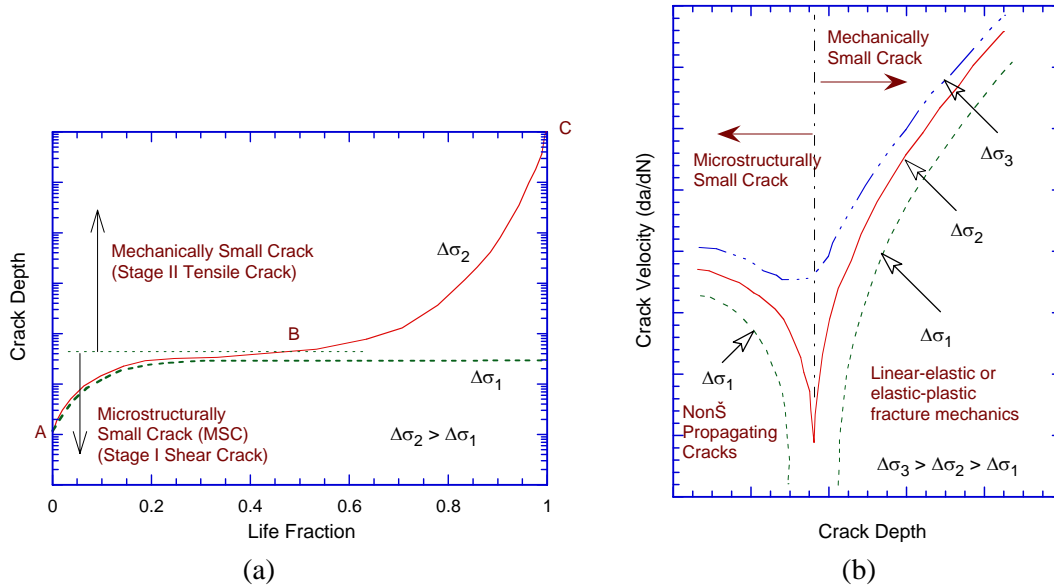
Figure 1.   Schematic illustration of (a) growth of short cracks in smooth specimens as a function of fatigue life fraction and (b) crack velocity as a function of crack depth.

A schematic illustration of the initiation and propagation stages of fatigue life is shown in Fig. 1. The initiation stage involves growth of "microstructurally small cracks" (MSCs), characterized by decelerating crack growth (Region AB in Fig. 1a). The propagation stage involves growth of "mechanically small cracks," characterized by accelerating crack growth (Region BC in Fig. 1a). The growth of the MSCs is very sensitive to microstructure.[5] Fatigue cracks greater than a critical depth show little or no influence of microstructure and are considered mechanically small cracks. Mechanically small cracks correspond to Stage II (tensile) cracks, which are characterized by striated crack growth, with the fracture surface normal to the maximum principal stress. Various criteria, summarized in Section 5.4.1 of Ref. 6, have been used to define the crack depth for transition from microstructurally to mechanically small crack. The transition crack depth is a function of applied stress (σ) and microstructure of the material; actual values may range from 150 to 250 μm. At low enough stress levels ($\Delta\sigma_1$), the transition from MSC growth to accelerating crack growth does not occur. This circumstance represents the fatigue limit for the smooth specimen. Although cracks can form below the fatigue limit, they can grow to engineering size only at stresses greater than the fatigue limit. The fatigue limit for a material is applicable only for constant loading conditions. Under variable loading conditions, MSCs can grow at high stresses ($\Delta\sigma_3$) to depths larger than the transition crack depth and then can continue to grow at stress levels below the fatigue limit ($\Delta\sigma_1$).

7

Studies on the formation and growth characteristics of short cracks in smooth fatigue specimens in LWR environments indicate that the decrease in fatigue life in LWR environments is caused primarily by the effects of the environment on the growth of MSCs (i.e., cracks <200 µm deep) and, to a lesser extent, on the growth of mechanically small cracks.[4,7] Crack growth rates measured in smooth cylindrical fatigue specimens of A533–Gr B low–alloy steel and austenitic Type 304 SSs in LWR environments and air are shown in Fig. 2. The results indicate that in LWR environments, the period spent in the growth of MSCs (region ABC in Fig. 1a) is decreased. For the A533–Gr B steel, only 30–50 cycles are needed to form a 100–mm crack in high–DO water, whereas ≈450 cycles are required to form a 100–mm crack in low–DO water and more than 3000 cycles in air. These values correspond to average growth rates of ≈2.5, 0.22, and 0.033 µm/cycle in high–DO water, low–DO water, and air, respectively. Relative to air, CGRs for A533–Gr B steel in high–DO water are nearly two orders of magnitude higher for crack sizes <100 µm, and one order of magnitude higher for crack sizes >100 µm.
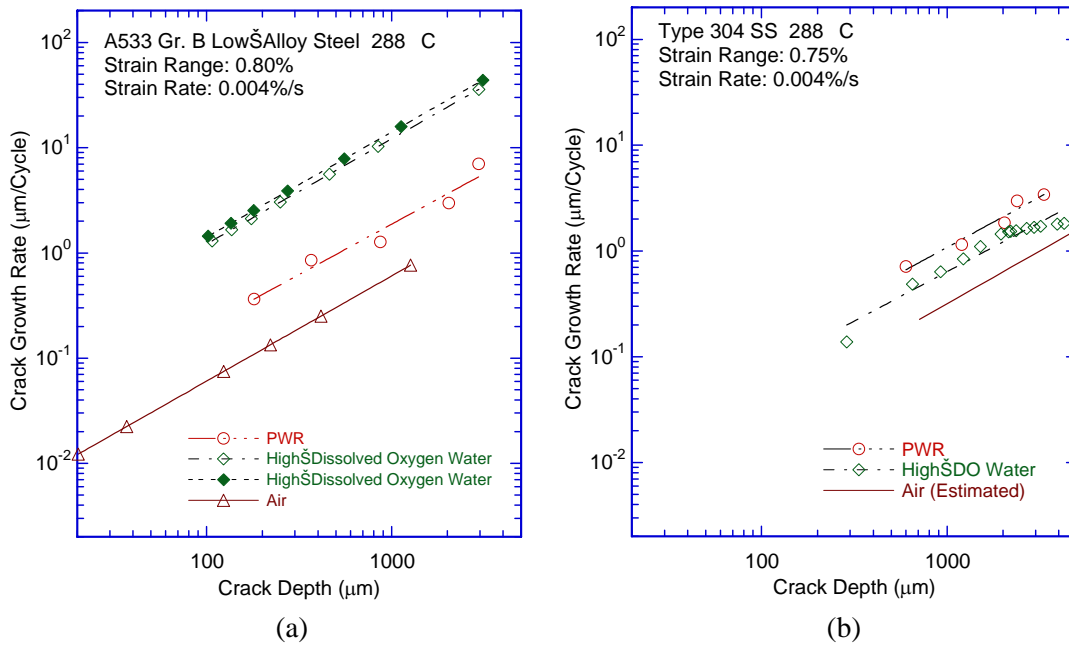
Figure 2. Crack growth rates plotted as a function of crack depth for (a) A533–Gr B low–alloy steel and (b) Type 304 SS in air and LWR environments.

The fatigue ε-N data for carbon and low-alloy steels in air and LWR environments have been examined from the standpoint of fracture mechanics and CGR data.[65,66] Fatigue life is considered to consist of an initiation stage, composed of the growth of microstructurally small cracks, and a propagation stage, composed of the growth of mechanically small cracks. The growth of the latter has been characterized in terms of the J-integral range ΔJ and crack growth rate data in air and LWR environments. The estimated values show good agreement with the experimental ε-N data for test specimens in air and water environments.

3. Fatigue Strain vs. Life Data

The existing fatigue ε–N data developed at various establishments and research laboratories worldwide have been compiled by the Pressure Vessel Research Council (PVRC), Working Group on ε–N Curve and Data Analysis. The database used in the ANL studies is an updated version of the PVRC database. A summary of the sources included in the updated PVRC database, as categorized by material type and test environment, is presented in Table 1.

Unless otherwise mentioned, smooth cylindrical gauge specimens were tested under strain control with a fully reversed loading, i.e., strain ratio of –1. Tests on notched specimens or at values of strain ratio other than –1 were excluded from the fatigue ε–N data analysis. In nearly all tests, fatigue life is defined as the number of cycles, N_{25}, necessary for tensile stress to drop 25% from its peak or steady–state value. For the specimen size used in these studies, e.g., 5.1–9.5 mm (0.2–0.375 in.) diameter cylindrical specimens, this corresponds to a ≈3–mm–deep crack. Some of the earlier tests in air were carried out to complete failure of the specimen, and life in some tests is defined as the number of cycles for peak tensile stress to decrease by 1–5%. Also, in fatigue tests that were performed using tube specimens, life was represented by the number of cycles to develop a leak. For the tests where fatigue life was defined by a criterion other than 25% drop in peak tensile stress (e.g., 5% decrease in peak tensile stress or complete failure), fatigue lives were normalized to the 25% drop values before performing the fatigue data analysis.[4]

Table 1.   Sources of the fatigue ε–N data on reactor structural materials in air and water environments.

Source	Material	Environment	Reference
General Electric Co.	Carbon steel, Type 304 SS	Air and BWR water	8–11
Japan; including Ishikawajima-Harima Heavy Industries (IHI) Co., Mitsubishi Heavy Industries (MHI) Ltd., Hitachi Research Laboratory	Carbon and low-alloy steel, wrought and cast austenitic SS, Alloy 600	Air, BWR, and PWR water	JNUFAD[*] database, 12–32
Argonne National Laboratory	Carbon and low-alloy steel, wrought and cast austenitic SS	Air, BWR, and PWR water	4–7, 33–39
Materials Engineering Associates (MEA) Inc.	Carbon steel, austenitic SS	Air and PWR water	40–42
Germany; including MPA	Carbon steel		43–44
France; including studies sponsored by Electricite de France (EdF)	Austenitic SS	Air and PWR water	67–69
Jaske and O'Donnell	Austenitic SS, Ni-alloys	Air	70
Others	Austenitic SS	Air	71,72

---

[*]Primate communication from M. Higuchi, Ishikawajima–Harima Heavy Industries Co. Japan, to M. Prager of the Pressure Vessel Research Council, 1992. The old database "Fadal" has been revised and renamed "JNUFAD."

An analysis of the existing fatigue ε–N data and the procedures for incorporating environmental effects into the Code fatigue evaluations has been presented in several review articles[73–84] and ANL topical reports.[4,6,7,37–39] The key material, loading, and environmental parameters that influence the fatigue lives of carbon and low–alloy steels and austenitic stainless steels have been identified, and the range of these key parameters where environmental effects are significant has been defined.

How various material, loading, and environmental parameters affect fatigue life and how these effects are incorporated into the ASME Code fatigue evaluations are discussed in detail for carbon and low-alloy steels, and wrought and cast SSs in Sections 4 and 5, respectively.

4 Carbon and Low–Alloy Steels

The primary sources of relevant ε–N data for carbon and low–alloy steels are the tests performed by General Electric Co. (GE) in a test loop at the Dresden 1 reactor;[8,9] work sponsored by EPRI at GE;[10,11] the work of Terrell at Mechanical Engineering Associates (MEA);[40–42] the work at ANL on fatigue of pressure vessel and piping steels;[4–7,33–39] the large JNUFAD database for "Fatigue Strength of Nuclear Plant Component" and studies at Ishikawajima-Harima Heavy Industries (IHI), Hitachi, and Mitsubishi Heavy Industries (MHI) in Japan;[12–30] and the studies at Kraftwerk Union Laboratories (KWU) and Materialprufungsanstalt (MPA) in Germany.[43–44] The database is composed of ≈1400 tests; ≈60% were obtained in the water environment and the remaining in air. Carbon steels include ≈12 heats of A333–Grade 6, A106–Grade B, A516–Grade 70, and A508–Class 1 steel, while the low–alloy steels include ≈16 heats of A533–Grade B, A302–Gr B, and A508–Class 2 and 3 steels.

4.1 Air Environment

4.1.1 Experimental Data

In air, the fatigue lives of carbon and low–alloy steels depend on steel type, temperature, and for some compositions, applied strain rate and sulfide morphology. Fatigue ε–N data from various investigations on carbon and low–alloy steels are shown in Fig. 3. The best-fit curves based on the ANL statistical models (Eqs. 15 and 16 from Section 4.1.8) and the ASME Section III mean–data curves (at room temperature) are also included in the figures. The results indicate that, although significant scatter is apparent due to material variability, the fatigue lives of these steels are comparable at less than 5 x 10^5 cycles, and those of low–alloy steels are greater than carbon steels for >5 x 10^5 cycles. Also, the fatigue limit of low–alloy steels is higher than that of carbon steels.
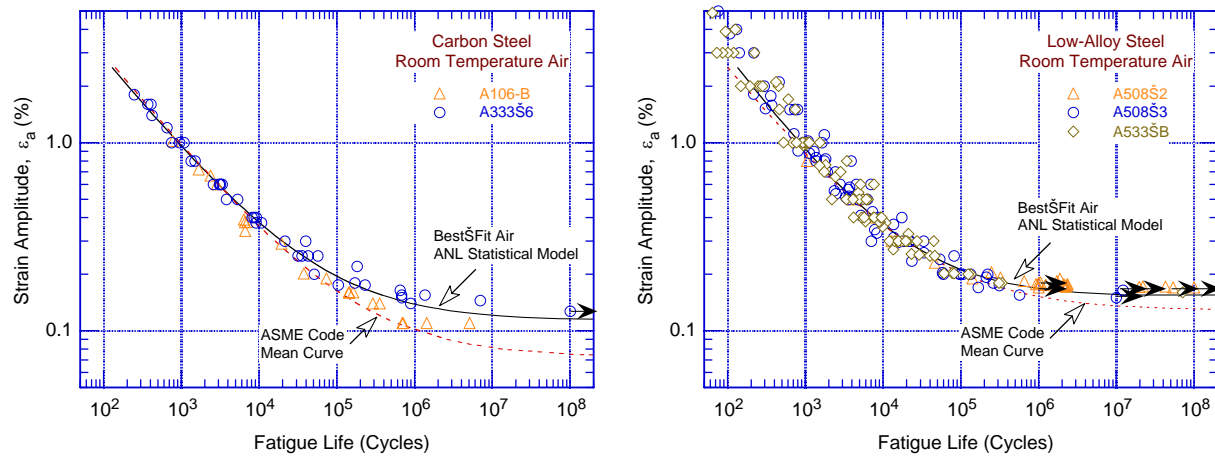
Figure 3.   Fatigue strain vs. life data for carbon and low–alloy steels in air at room temperature (JNUFAD database and Refs. 4,12,13,40).

The existing fatigue ε–N data for low–alloy steels are in good agreement with the ASME mean data curve. The existing data for carbon steels are consistent with the ASME mean data curve for fatigue life ≤5 x 10^5 cycles and are above the mean curve at longer lives. Thus, above 5 x 10^5 cycles, the Code mean curve is conservative with respect to the existing fatigue ε–N data.

- *The current Code mean data curves are either consistent with the existing fatigue ε–N data or are somewhat conservative under some conditions.*

4.1.2   Temperature

In air, the fatigue life of both carbon and low–alloy steels decreases with increasing temperature; however, the effect is relatively small (less than a factor of 1.5). Fatigue ε–N data from the JNUFAD database and other investigations in air at 286–300°C are shown in Fig. 4. For each grade of steel, the data represent several heats of material. The best-fit curves for carbon and low-alloy steels at room temperature (Eqs. 15 and 16 from Section 4.1.8) and at 289°C (Eqs. 13 and 14 from Section 4.1.8) are also included in the figures. The results indicate a factor of ≈1.5 decrease in fatigue life of both carbon and low–alloy steels as the temperature is increased from room temperature to 300°C. As discussed later in Section 4.1.6, the greater–than–predicted difference between the best-fit air curve at room temperature and the data for A106–Gr B steel at 289°C is due to heat–to–heat variability and not temperature effects.

- *The effect of temperature is not explicitly considered in the mean data curve used for obtaining the fatigue design curves; variations in fatigue life due to temperature are accounted for in the subfactor for "data scatter and material variability."*
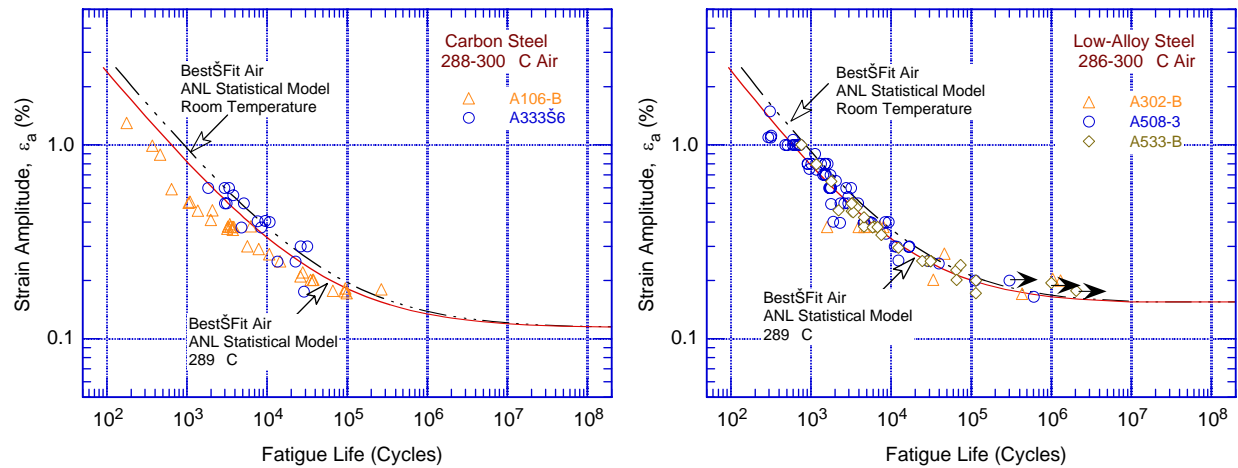
Figure 4.   Fatigue strain vs. life data for carbon and low–alloy steels in air at 288°C (JNUFAD database, and Refs. 4,12,13,41-42).

4.1.3   Strain Rate

The effect of strain rate on the fatigue life of carbon and low-alloy steels in air appears to depend on the material composition. The existing data indicate that in the temperature range of dynamic strain aging (200–370°C), some heats of carbon and low–alloy steel are sensitive to strain rate; with decreasing strain rate, the fatigue life in air may be either unaffected,[4] decrease for some heats,[85] or increase for others.[86] The C and N contents in the steel are considered to be important. Inhomogeneous plastic deformation can result in localized plastic strains. This localization retards blunting of propagating cracks that is usually expected when plastic deformation occurs and can result in higher crack growth rates.[85] The increases in fatigue life have been attributed to retardation of CGRs due to crack branching and suppression of the plastic zone. Formation of cracks is easy in the presence of dynamic strain aging.[86]

- *Variations in fatigue life due to the effects of strain rate are not explicitly considered in the fatigue design curves, they are accounted for in the subfactor for "data scatter and material variability."*

12
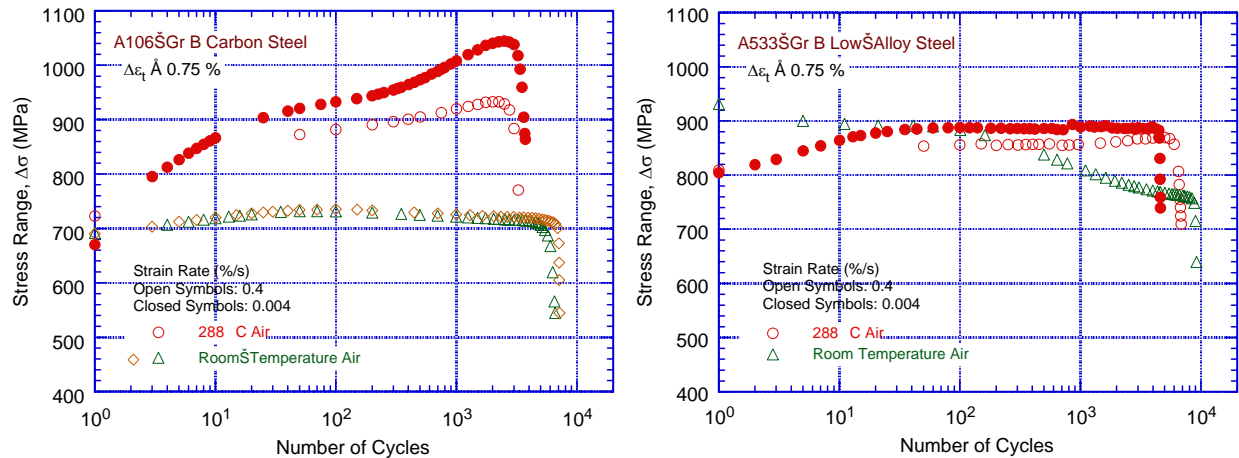
Figure 5.   Effect of strain rate and temperature on cyclic stress of carbon and low–alloy steels.

4.1.4   Sulfide Morphology

Some high–S steels exhibit very poor fatigue properties in certain orientations because of structural factors such as the distribution and morphology of sulfides in the steel. For example, fatigue tests on a high–S heat of A302–Gr. B steel in three orientations[*] in air at 288°C indicate that the fatigue life and fatigue limit in the T2 orientation are lower than those in the R and T1 orientations.[4] At low strain rates, fatigue life in the T2 orientation is nearly one order of magnitude lower than in the R orientation. In the orientation with poor fatigue resistance, crack propagation is preferentially along the sulfide stringers and is facilitated by sulfide cracking.

• *Variations in fatigue life due to differences in sulfide morphology are accounted for in the subfactor for "data scatter and material variability."*

4.1.5   Cyclic Strain Hardening Behavior

The cyclic stress–strain response of carbon and low–alloy steels varies with steel type, temperature, and strain rate. In general, these steels show initial cyclic hardening, followed by cyclic softening or a saturation stage at all strain rates. The carbon steels, with a pearlite and ferrite structure and low yield stress, exhibit significant initial hardening. The low–alloy steels, with a tempered bainite and ferrite structure and a relatively high yield stress, show little or no initial hardening and may exhibit cyclic softening with continued cycling. For both steels, maximum stress increases as applied strain increases and generally decreases as temperature increases. However, at 200–370°C, these steels exhibit dynamic strain aging, which results in enhanced cyclic hardening, a secondary hardening stage, and negative strain rate sensitivity.[85,86] The temperature range and extent of dynamic strain aging vary with composition and structure.

The effect of strain rate and temperature on the cyclic stress response of A106–Gr B carbon steel and A533–Gr B low-alloy steel is shown in Fig. 5. For both steels, cyclic stresses are higher at 288°C than at room temperature. At 288°C, all steels exhibit greater cyclic and secondary hardening because of dynamic strain aging. The extent of hardening increases as the applied strain rate decreases.

---

[*]Both transverse (T) and radial (R) directions are perpendicular to the rolling direction, but the fracture plane is across the thickness of the plate in the transverse orientation and parallel to the plate surface in the radial orientation.

13

- *The cyclic strain hardening behavior is likely to influence the fatigue limit of the material; variations in fatigue life due to the effects of strain hardening are not explicitly considered in the fatigue design curves, they are accounted for in the subfactor for "data scatter and material variability."*

4.1.6 Surface Finish

The effect of surface finish must be considered to account for the difference in fatigue life expected in an actual component with industrial–grade surface finish, compared with the smooth polished surface of a test specimen. Fatigue life is sensitive to surface finish; cracks can initiate at surface irregularities that are normal to the stress axis. The height, spacing, shape, and distribution of surface irregularities are important for crack initiation. The most common measure of roughness is average surface roughness R_a, which is a measure of the height of the irregularities. Investigations of the effects of surface roughness on the low–cycle fatigue of Type 304 SS in air at 593°C indicate that fatigue life decreases as surface roughness increases.[87,88] The effect of roughness on crack initiation $N_i(R)$ is given by

$$N_i(R_q) = 1012 \, R_q^{-0.21}, \tag{12}$$

where the root–mean–square (RMS) value of surface roughness R_q is in µm. Typical values of R_a for surfaces finished by different metalworking processes in the automotive industry[89] indicate that an R_a of 3 µm (or an R_q of 4 µm) represents the maximum surface roughness for drawing/extrusion, grinding, honing, and polishing processes and a mean value for the roughness range for milling or turning processes. For carbon steel or low–alloy steel, an R_q of 4 µm in Eq. 12 (the R_q of a smooth polished specimen is ≈0.0075 µm) would decrease fatigue life by a factor of ≈3.[87]

Fatigue test has been conducted on a A106–Gr B carbon steel specimen that was intentionally roughened in a lathe, under controlled conditions, with 50-grit sandpaper to produce circumferential scratches with an average roughness of 1.2 µm and an R_q of 1.6 µm (≈62 micro in.).[38] The results for smooth and roughened specimens are shown in Fig. 6. In air, the fatigue life of a roughened A106–Gr B specimen is a factor of ≈3 lower than that of smooth specimens. Another study of the effect of surface finish on the fatigue life of carbon steel in room–temperature air showed a factor of 2 decrease in life when R_a was increased from 0.3 to 5.3 µm.[90] These results are consistent with Eq. 12. Thus, a factor of 2–3 on cycles may be used to account for the effects of surface finish on the fatigue life of carbon and low-alloy steels.
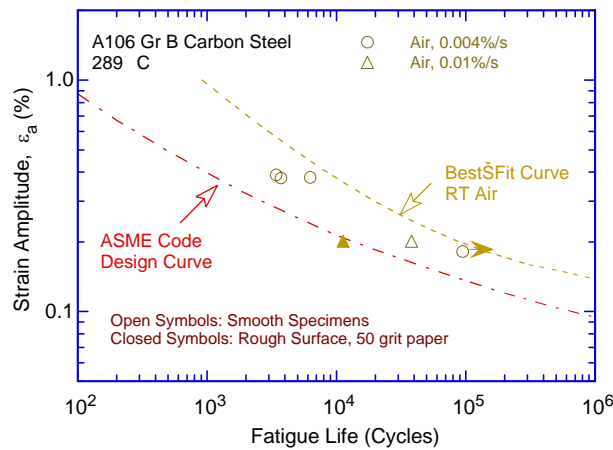
Figure 6.
Effect of surface finish on the fatigue life of A106–Gr B carbon steel in air at 289°C.

- *The effect of surface finish was not investigated in the mean data curve used to develop the Code fatigue design curves; it is included as part of the subfactor that is applied to the mean data curve to account for "surface finish and environment."*

4.1.7   Heat-to-Heat Variability

Several factors, such as small differences in the material composition and structure, can change the tensile and fatigue properties of the material. The effect of interstitial element content on dynamic strain aging and the effect of sulfide morphology on fatigue life have been discussed in Sections 4.1.3 and 4.1.4, respectively. The effect of tensile strength on the fatigue life has been included in the expression for the mean data curve described in the Section III criteria document, i.e., constant A_f in Eq. 2. Also, the fatigue limit of a material has been correlated with its tensile strength, e.g., the fatigue limit increases with increasing tensile yield stress.[91]

The effects of material variability and data scatter must be included to ensure that the design curves not only describe the available test data well, but also adequately describe the fatigue lives of the much larger number of heats of material that are found in the field. The effects of material variability and data scatter are often evaluated by comparing the experimental data to a specific model for fatigue crack initiation, e.g., the best-fit (in some sense) to the data. The adequacy of the evaluation will then depend on the sample of data used in the analysis. For example, if most of the data have been obtained from a heat of material that has poor resistance to fatigue damage or under loading conditions that show significant environmental effects, the results may be conservative for most of the materials or service conditions of interest. Conversely, if most data are from a heat of material with a high resistance to fatigue damage, the results could be nonconservative for many heats in service.

Another method to assess the effect of material variability and data scatter is by considering the best–fit curves determined from tests on individual heats of materials or loading conditions as samples of the much larger population of heats of materials and service conditions of interest. The fatigue behavior of each of the heats or loading conditions is characterized by the value of the constant A in Eq. 6. The values of A for the various data sets are ordered, and median ranks are used to estimate the cumulative distribution of A for the population.[92,93] The distributions were fit to lognormal curves. No rigorous statistical evaluation was performed, but the fits seem reasonable and describe the observed variability adequately. Results for carbon and low–alloy steels in air are shown in Fig. 7. The data were normalized to room-temperature values using Eqs. 13 and 14 (section 4.1.8). The median value of the constant A is 6.583 and 6.449, respectively, for the fatigue life of carbon steels and low-alloy steels in room-temperature air. Note that the two heats of A106–Gr B carbon steel are in the 10–25 percentile of the data, i.e., the fatigue lives of these heats are much lower than the average value for carbon steels.

The A values that describe the 5th percentile of these distributions give fatigue ε–N curves that are expected to bound the fatigue lives of 95% of the heats of the material. The cumulative distributions in Fig. 7 contain two potential sources of error. The mean and standard deviation of the population must be estimated from the mean and standard deviation of the sample,[94] and confidence bounds can then be obtained on the population mean and standard deviation in terms of the sample mean and standard deviation. Secondly, even this condition does not fully address the uncertainty in the distribution because of the large uncertainties in the sample values themselves, i.e., the "horizontal" uncertainty in the actual value of A for a heat of material, as indicated by the error bars in Fig. 7. A Monte Carlo analysis was performed to address both sources of uncertainty. The results for the median value and standard deviation of the constant A did not differ significantly from the experimental values.
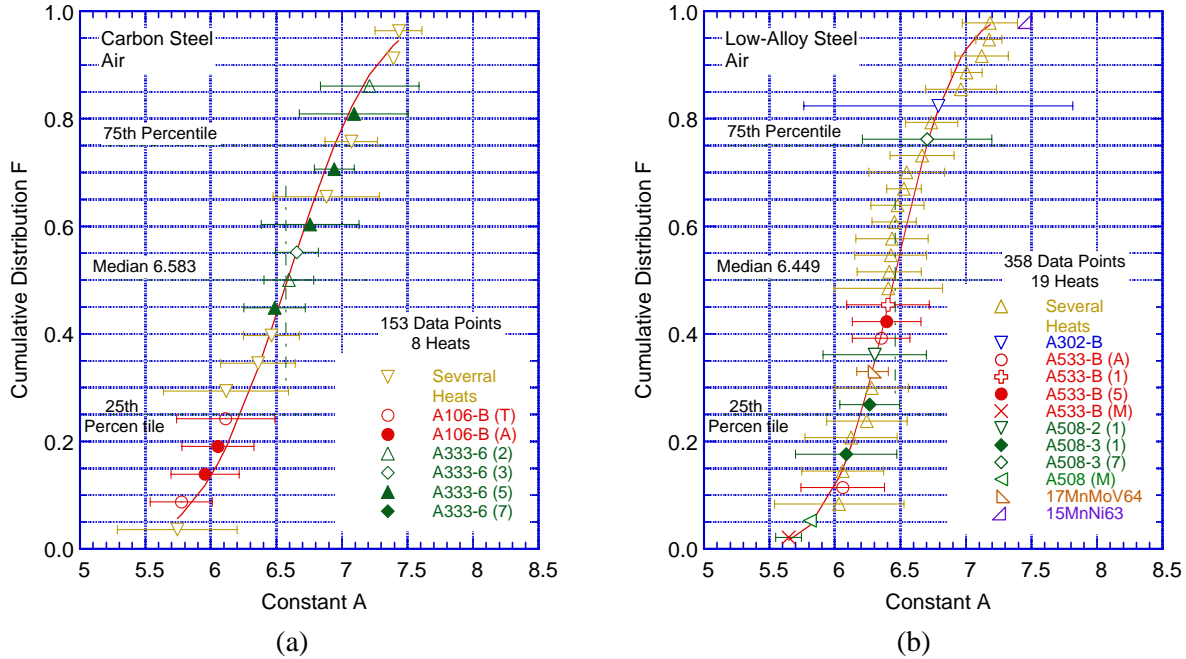
Figure 7. Estimated cumulative distribution of constant A in statistical models for fatigue life with heats of (a) carbon steels and (b) low–alloy steels in air.

The results for carbon and low-alloy steels are summarized in Tables 2 and 3, respectively, in terms of values for A that provide bounds for the portion of the population and the confidence that is desired in the estimates of the bounds. In air, the 5th percentile value of Parameter A at a 95% confidence level is 5.559 for carbon steels and 5.689 for low-alloy steels. From Fig. 7, the median value of A for the sample is 6.583 for carbon steels and 6.449 for low-alloy steels. Thus, the 95/95 value of the margin to account for material variability and data scatter is 2.8 and 2.1 on life for carbon steels and low-alloy steels, respectively. These margins are needed to provide 95% confidence that the resultant life will be greater than that observed for 95% of the materials of interest. The margin is higher for carbon steels because the analysis is based on a smaller number of data sets, i.e., 19 for carbon steels and 32 for low-alloy steels.

• *The mean data curve used to develop the Code fatigue design curves represents the average behavior; heat-to-heat variability is included in the subfactor that is applied to the mean data curve to account for "data scatter and material variability."*

Table 2. Values of parameter A in statistical model for carbon steels in air and the margins on life as a function of confidence level and percentage of population bounded.

Confidence Level	Percentage of Population Bounded (Percentile Distribution of A)				
	95 (5)	90 (10)	75 (25)	67 (33)	50 (50)
	Values of Parameter A				
50	5.798	5.971	6.261	6.373	6.583
75	5.700	5.883	6.183	6.295	6.500
95	5.559	5.756	6.069	6.183	6.381
	Margins on Life				
50	2.2	1.8	1.4	1.2	1.0
75	2.4	2.0	1.5	1.3	1.1
95	2.8	2.3	1.7	1.5	1.2

16

Table 3. Values of parameter A in statistical model for low–alloy steels in air and the margins on life as a function of confidence level and percentage of population bounded.

Confidence Level	Percentage of Population Bounded (Percentile Distribution of A)				
	95 (5)	90 (10)	75 (25)	67 (33)	50 (50)
	Values of Parameter A				
50	5.832	5.968	6.196	6.284	6.449
75	5.774	5.916	6.150	6.239	6.403
95	5.689	5.840	6.085	6.175	6.337
	Margins on Life				
50	1.9	1.6	1.3	1.2	1.0
75	2.0	1.7	1.3	1.2	1.0
95	2.1	1.8	1.4	1.3	1.1

4.1.8 Statistical Model

Statistical models based on the existing fatigue ε–N data have been developed at ANL for estimating the fatigue lives of these steels in air.[4,38] The fatigue life, N, of carbon steels is represented by

$$\ln(N) = 6.614 - 0.00124\ T - 1.975\ \ln(\varepsilon_a - 0.113), \tag{13}$$

and that of low–alloy steels, by

$$\ln(N) = 6.480 - 0.00124\ T - 1.808\ \ln(\varepsilon_a - 0.151), \tag{14}$$

where ε_a is applied strain amplitude (%), and T is the test temperature (°C). Thus, in room-temperature air, the fatigue life of carbon steels is expressed as

$$\ln(N) = 6.583 - 1.975\ \ln(\varepsilon_a - 0.113), \tag{15}$$

and that of low–alloy steels, by

$$\ln(N) = 6.449 - 1.808\ \ln(\varepsilon_a - 0.151). \tag{16}$$

Note that these equations have been updated based on the analysis presented in Section 4.1.7; constant A in the equations is different from the value reported earlier in NUREG/CR-6583 and 6815. Relative to the earlier model, the fatigue lives predicted by the updated model are ≈2% higher for carbon steel and ≈16% lower for low–alloy steels. The experimental values of fatigue life and those predicted by Eqs. 15 and 16 for carbon and low-alloy steels in air are plotted in Fig. 8. The predicted fatigue lives show good agreement with the experimental values; the experimental and predicted values are within a factor of 3.

• *The statistical models represent mean values of fatigue life. The effects of parameters (such as mean stress, surface finish, size and geometry, and loading history) that are known to influence fatigue life are not explicitly considered in the model; such effects are accounted for in the several subfactors that are applied to the mean data curve to obtain the Code fatigue design curve.*
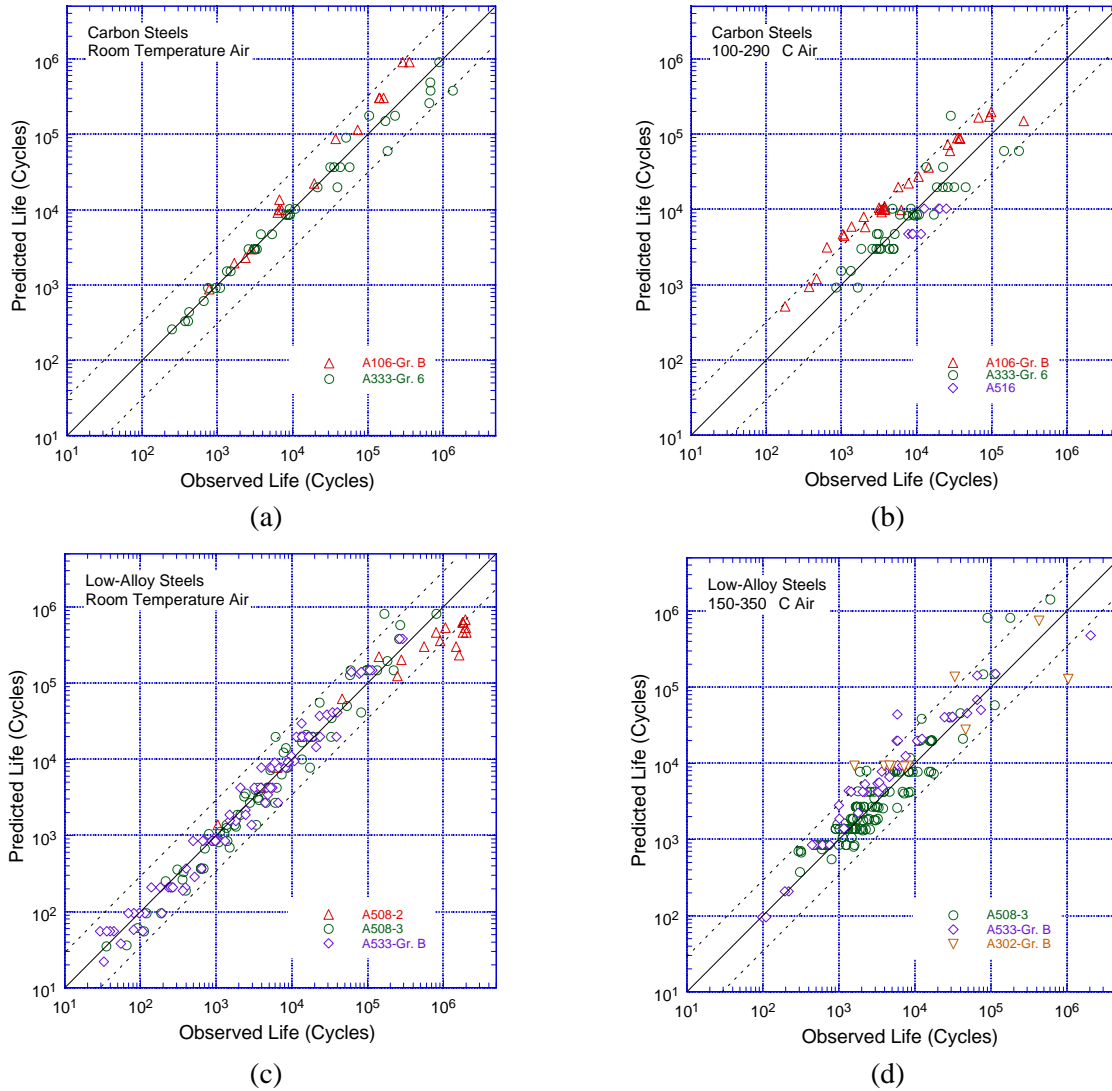
Figure 8.   Experimental and predicted fatigue lives of (a, b) carbon steels and (c, d) low-alloy steels in air.

4.1.9   Fatigue Design Curve

Note that for the current Code design curve, although the two mean curves for carbon and low–alloy steels (i.e., Eqs. 7 and 9) are significantly different, because the mean stress correction is much larger for the low-alloy steels, both curves yield approximately the same design curve up to 10^6 cycles. Thus, the ASME Code provides a common curve for both carbon and low-alloy steels. The fatigue design curves for carbon steels and low-alloy steels based on the ANL statistical model can be obtained from Eqs. 15 and 16, respectively. The best-fit curves are first corrected for mean stress effects using the modified Goodman relationship, and the mean-stress adjusted curve is reduced by a factor of 2 on stress or 20 on cycles, whichever is more conservative. The results indicate that for the low–alloy steels, the current Code design curve is consistent with the existing fatigue ε–N data at stress amplitudes above ≈200 MPa (≈29 ksi) and is somewhat conservative at lower stress amplitudes. However, for the carbon steels, the current Code design curve is consistent with the existing fatigue ε–N data at stress amplitudes above ≈600 MPa (≈87 ksi) and is quite conservative at lower stress amplitudes, e.g., at stress amplitudes less than ≈120 MPa fatigue lives predicted by the Code curve are more than an order of magnitude greater than those observed experimentally.

18

The discussions presented later in Section 6.5 indicate that the current Code requirement of a factor of 20 on cycles, to account for the effects of material variability and data scatter, specimen size, surface finish, and loading history, is conservative by at least a factor of 1.7. Thus, to reduce this conservatism, fatigue design curves based on the ANL model for carbon and low-alloy steels (i.e., Eqs. 15 and 16) have been developed using factors of 12 on life and 2 on stress; these design curves and the current Code design curve for carbon and low–alloy steels with ultimate tensile strength (UTS) ≤552 MPa (≤80 ksi) are shown in Figs. 9 and 10, respectively. The values of stress amplitude (S_a) vs. cycles for the various curves are listed in Table 4. Also, the proposed extension of the design curve to 10^{11} cycles (that has been approved by ASME Section III, Subgroup Fatigue Strength) is also included in the figures.
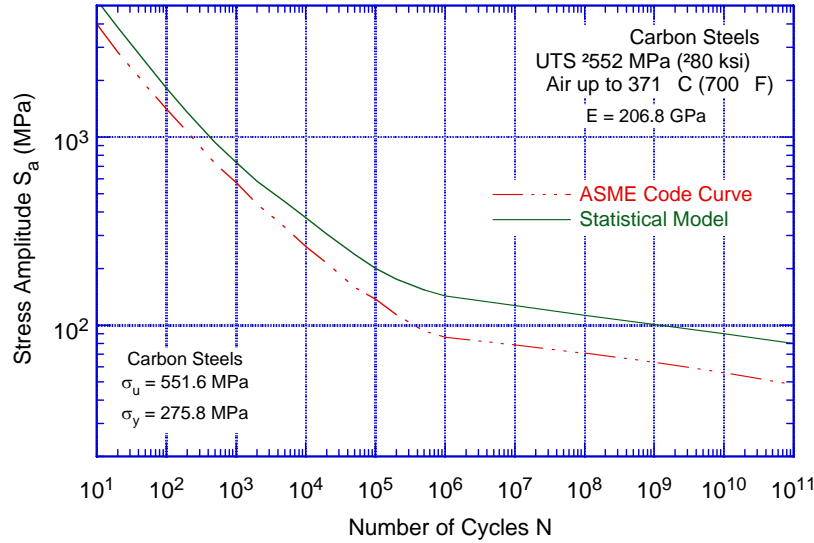
Figure 9.
Fatigue design curve for carbon steels in air. The curve developed from the statistical model is based on factors of 12 on life and 2 on stress.
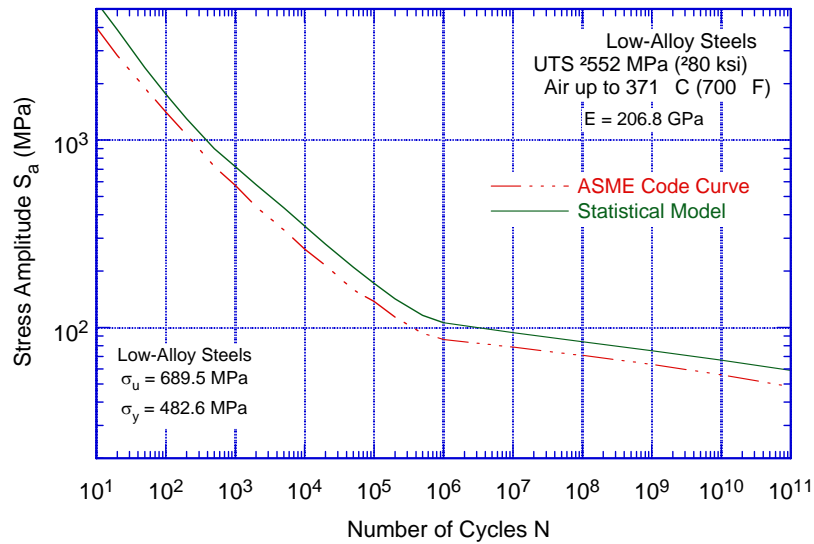
Figure 10.
Fatigue design curve for low-alloy steels in air. The curve developed from the statistical model is based on factors of 12 on life and 2 on stress.

- *For low–alloy steels, the current Code fatigue design curve for carbon and low-alloy steels with ultimate tensile strength <552 MPa (<80 ksi) is either consistent or conservative with respect to the existing fatigue ε–N data. Also, discussions presented in Section 6.5 indicate that current Code requirement of a factor of 20 on life is conservative by at least a factor of 1.7. Fatigue design curves have been developed from the ANL statistical model using factors of 12 on life and 2 on stress.*

19

Table 4.   Fatigue design curves for carbon and low-alloy steels and proposed extension to 10^{11} cycles.

Cycles	Stress Amplitude (MPa/ksi)			Cycles	Stress Amplitude (MPa/ksi)		
	ASME Code Curve	ANL Model Carbon Steel	ANL Model Low-Alloy Steel		ASME Code Curve	ANL Model Carbon Steel	ANL Model Low-Alloy Steel
1 E+01	3999 (580)	5355 (777)	5467 (793)	5 E+04	159 (23)	238 (34.5)	210 (30.5)
2 E+01	2827 (410)	3830 (556)	3880 (563)	1 E+05	138 (20)	201 (29.2)	172 (24.9)
5 E+01	1896 (275)	2510 (364)	2438 (354)	2 E+05	114 (16.5)	176 (25.5)	142 (20.6)
1 E+02	1413 (205)	1820 (264)	1760 (255)	5 E+05	93 (13.5)	154 (22.3)	116 (16.8)
2 E+02	1069 (155)	1355 (197)	1300 (189)	1 E+06	86 (12.5)	143 (20.7)	106 (15.4)
5 E+02	724 (105)	935 (136)	900 (131)	1 E+07	76.5 (11.1)	127 (18.5)	94 (13.7)
1 E+03	572 (83)	733 (106)	720 (104)	1 E+08	68.3 (9.9)	113 (16.5)	84 (12.2)
2 E+03	441 (64)	584 (84.7)	578 (83.8)	1 E+09	60.7 (8.8)	101 (14.7)	75 (10.9)
5 E+03	331 (48)	453 (65.7)	435 (63.1)	1 E+010	54.5 (7.9)	90 (13.0)	67 (9.7)
1 E+04	262 (38)	373 (54.1)	348 (50.5)	1 E+011	48.3 (7.0)	80 (11.6)	59 (8.6)
2 E+04	214 (31)	305 (44.2)	278 (40.3)				

4.2 LWR Environments

4.2.1 Experimental Data

Fatigue ε–N data on carbon and low–alloy steels in air and high–DO water at 288°C are shown in Fig. 11. The curves based on the ANL statistical models (Eqs. 18 and 19 in Section 4.2.12) are also included in the figures. The fatigue data in LWR environments indicate a significant decrease in fatigue life of carbon and low–alloy steels when four key threshold conditions are satisfied simultaneously, viz., applied strain range, service temperature, and DO in the water are above a minimum threshold level, and the loading strain rate is below a threshold value. The S content of the steel is also an important parameter for environmental effects on fatigue life. Although the microstructures and cyclic–hardening behavior of carbon steels and low–alloy steels are significantly different, environmental degradation of fatigue life of these steels is identical. For both steels, environmental effects on fatigue life are moderate (i.e., it is a factor of ≈2 lower) if any one of the key threshold conditions is not satisfied.

The existing fatigue data indicate that a slow strain rate applied during the tensile–loading cycle is primarily responsible for environmentally assisted reduction in fatigue life of these steels.[4]   The mechanism of environmentally assisted reduction in fatigue life of carbon and low-alloy steels has been termed strain–induced corrosion cracking (SICC).[47,54,55]   A slow strain rate applied during both the

(a)   (b)
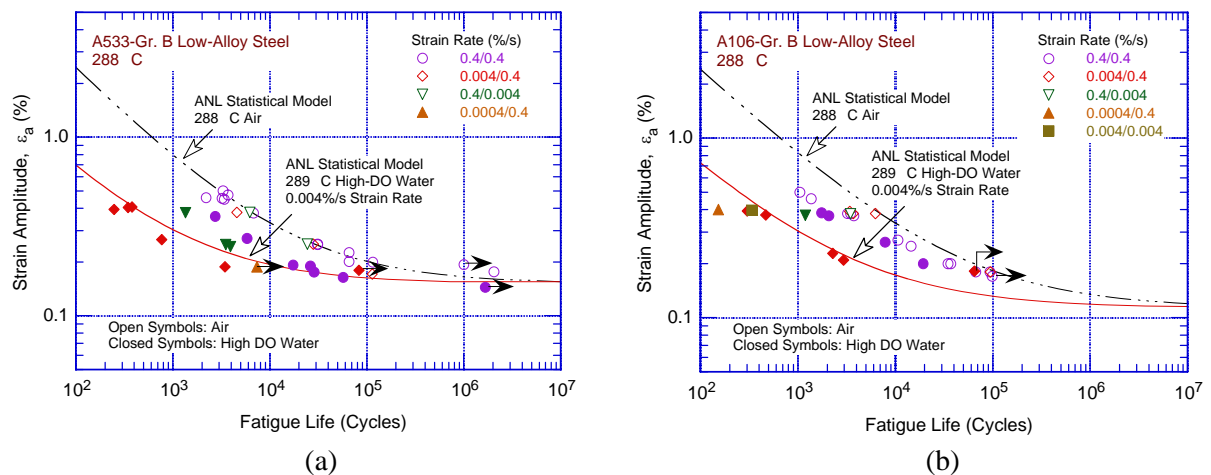
Figure 11.   Strain amplitude vs. fatigue life data for (a) A533–Gr B and (b) A106–Gr B steels in air and high–dissolved–oxygen water at 288°C (Ref. 4).

tensile–load and compressive–load portion of the cycle (i.e., slow/slow strain rate test) does not further decrease the fatigue life, e.g., see solid diamonds and square in Fig. 11b for A106–Gr B carbon steel. Limited data from fast/slow tests indicate that a slow strain rate during the compressive load cycle also decreases fatigue life. However, the decrease in life is relatively small; for fast/slow strain rate tests, the major contribution of environment most likely occurs during slow compressive loading near peak tensile load. For example, the fatigue life of A533–Gr B low-alloy steel at 288°C, 0.7 ppm DO, and ≈0.5% strain range decreased by factors of 5, 8, and 35 for the fast/fast, fast/slow, and slow/fast tests, respectively, i.e., see solid circles, diamonds, and inverted triangles in Fig. 11a. Similar results have been observed for A333–Gr 6 carbon steel;[17] relative to the fast/fast test, fatigue life for slow/fast and fast/slow tests at 288°C, 8 ppm DO, and 1.2% strain range decreased by factors of 7.4 and 3.4, respectively.

The environmental effects on the fatigue life of carbon and low-alloy steels are consistent with the slip oxidation/dissolution mechanism for crack propagation.[95,96] A critical concentration of sulfide (S^{2-}) or hydrosulfide (HS^-) ions, which is produced by the dissolution of sulfide inclusions in the steel, is required at the crack tip for environmental effects to occur. The requirements of this mechanism are that a protective oxide film is thermodynamically stable to ensure that the crack will propagate with a high aspect ratio without degrading into a blunt pit, and that a strain increment occurs to rupture that oxide film and thereby expose the underlying matrix to the environment. Once the passive oxide film is ruptured, crack extension is controlled by dissolution of freshly exposed surface and by the oxidation characteristics. The effect of the environment increases with decreasing strain rate. The mechanism assumes that environmental effects do not occur during the compressive load cycle, because during that period water does not have access to the crack tip.

A model for the initiation or cessation of environmentally assisted cracking (EAC) of these steels in low-DO PWR environments has also been proposed.[97] Initiation of EAC requires a critical concentration of sulfide ions at the crack tip, which is supplied with the sulfide ions as the advancing crack intersects the sulfide inclusions, and the inclusions dissolve in the high-temperature water. Sulfide ions are removed from the crack tip by one or more of the following processes: (a) diffusion due to the concentration gradient, (b) ion transport due to differences in the electrochemical potential (ECP), and (c) fluid flow induced within the crack due to flow of coolant outside the crack. Thus, environmentally enhanced CGRs are controlled by the synergistic effects of S content, environmental conditions, and flow rate. The EAC initiation/cessation model has been used to determine the minimum crack extension and CGRs that are required to maintain the critical sulfide ion concentration at the crack tip and sustained environmental enhancement of growth rates.

- *A LWR environment has a significant effect on the fatigue life of carbon and low-alloy steels; such effects are not considered in the current Code design curve. Environmental effects may be incorporated into the Code fatigue evaluation using the F_{en} approach described in Section 4.2.13.*

4.2.2   Strain Rate

The effects of strain rate on fatigue life of carbon and low-alloy steels in LWR environments are significant when other key threshold conditions, e.g., strain amplitude, temperature, and DO content, are satisfied. When any one of the threshold conditions is not satisfied, e.g., low–DO PWR environment or temperature <150°C, the effects of strain rate are consistent with those observed in air.

When all threshold conditions are satisfied, the fatigue life of carbon and low-alloy steels decreases logarithmically with decreasing strain rate below 1%/s. The fatigue lives of A106–Gr B and A333–Gr 6 carbon steels and A533–Gr B low–alloy steel[4,17] are plotted as a function of strain rate in Fig. 12. Only a moderate decrease in fatigue life is observed in simulated (low–DO) PWR water, e.g., at DO levels of

≤0.05 ppm. For the heats of A106–Gr B carbon steel and A533–Gr B low–alloy steel, the effect of strain rate on fatigue life saturates at ≈0.001%/s strain rate. Although the data for A333–Gr 6 carbon steel at 250°C and 8 ppm DO do not show an apparent saturation at ≈0.001%/s strain rate, the results are comparable to those for the other two steels.

- *In LWR environments, the effect of strain rate on the fatigue life of carbon and low-alloy steels is explicitly considered in F_{en} given in Eqs. 25 and 26 (Section 4.2.13). Also, guidance is provided for defining the strain rate for a specific stress cycle or load set pair.*

(a)

(b)

(c)
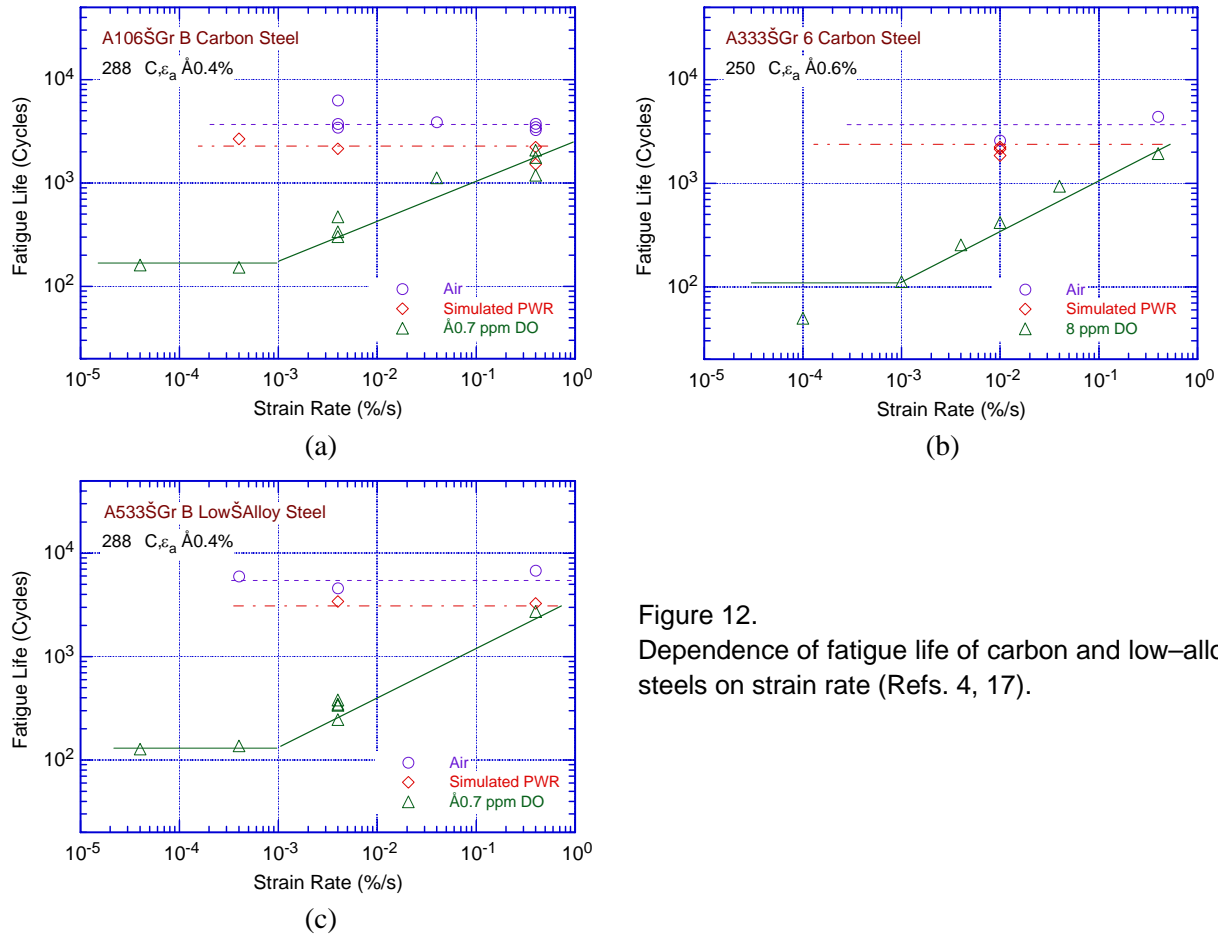
Figure 12.
Dependence of fatigue life of carbon and low–alloy steels on strain rate (Refs. 4, 17).

4.2.3 Strain Amplitude

A minimum threshold strain is required for environmentally assisted decrease in fatigue life, i.e., the LWR coolant environments have no effect on the fatigue life of these steels at strain amplitudes below the threshold value. The fatigue lives of A533–Gr B and A106–Gr B steels in high–DO water at 288°C and various strain rates[4] are shown in Fig. 11. Fatigue tests at low strain amplitudes are rather limited. Because environmental effects on fatigue life increase with decreasing strain rate, fatigue tests at low strain amplitudes and strain rates that would result in significant environmental effects are restrictively time consuming. For the limited data that are available, the threshold strain amplitude appears to be slightly above the fatigue limit of these steels.

Exploratory fatigue tests with changing strain rate have been conducted to determine the threshold strain beyond which environmental effects are significant during a fatigue cycle. The tests are performed

22

with waveforms in which the slow strain rate is applied during only a fraction of the tensile loading cycle.[4,18] The results for A106–Gr B steel tested in air and low– and high–DO environments at 288°C and ≈0.78% strain range are summarized in Fig. 13. The waveforms consist of segments of loading and unloading at fast and slow strain rates. The variation in fatigue life of two heats of carbon steel and one heat of low–alloy steel[4,18] is plotted as a function of the fraction of loading strain at slow strain rate in Fig. 14. Open symbols indicate tests where the slow portions occurred near the maximum tensile strain, and closed symbols indicate tests where the slow portions occurred near the maximum compressive strain. In Fig. 14, if the relative damage were independent of strain amplitude, fatigue life should decrease linearly from A to C along the chain–dot line. Instead, the results indicate that during a strain cycle, the relative damage due to slow strain rate occurs only after the strain amplitude exceeds a threshold value. The threshold strain range for these steels is 0.32–0.36%.

Loading histories with slow strain rate applied near the maximum tensile strain (i.e., waveforms C, D, E, or F in Fig. 13) show continuous decreases in life (line AB in Fig. 14) and then saturation when a portion of the slow strain rate occurs at amplitudes below the threshold value (line BC in Fig. 14). In contrast, loading histories with slow strain rate applied near maximum compressive strain (i.e., waveforms G, H, or I in Fig. 13) produce no damage (line AD in Fig. 14a) until the fraction of the strain is sufficiently large that slow strain rates are occurring for strain amplitudes greater than the threshold. However, tests with such loading histories often show lower fatigue lives than the predicted values, e.g., solid inverted triangle or solid diamond in Fig. 14a.

A
Air:	3,253; 3,753
PWR:	2,230; 1,525
Hi DO:	2,077; 1,756

B
Air:	3,721; 3,424; 6,275
PWR:	2,141
Hi DO:	303; 469

C
Air:	4,122
PWR:	–
Hi DO:	888

D
Air:	5,139
PWR:	–
Hi DO:	615; 553

E
Air:	5,261
PWR:	–
Hi DO:	545

F
Air:	3,893
PWR:	–
Hi DO:	340

G
Air:	4,087
PWR:	–
Hi DO:	1,649; 2,080

H
Air:	–
PWR:	–
Hi DO:	1,935

I
Air:	4,356
PWR:	–
Hi DO:	615
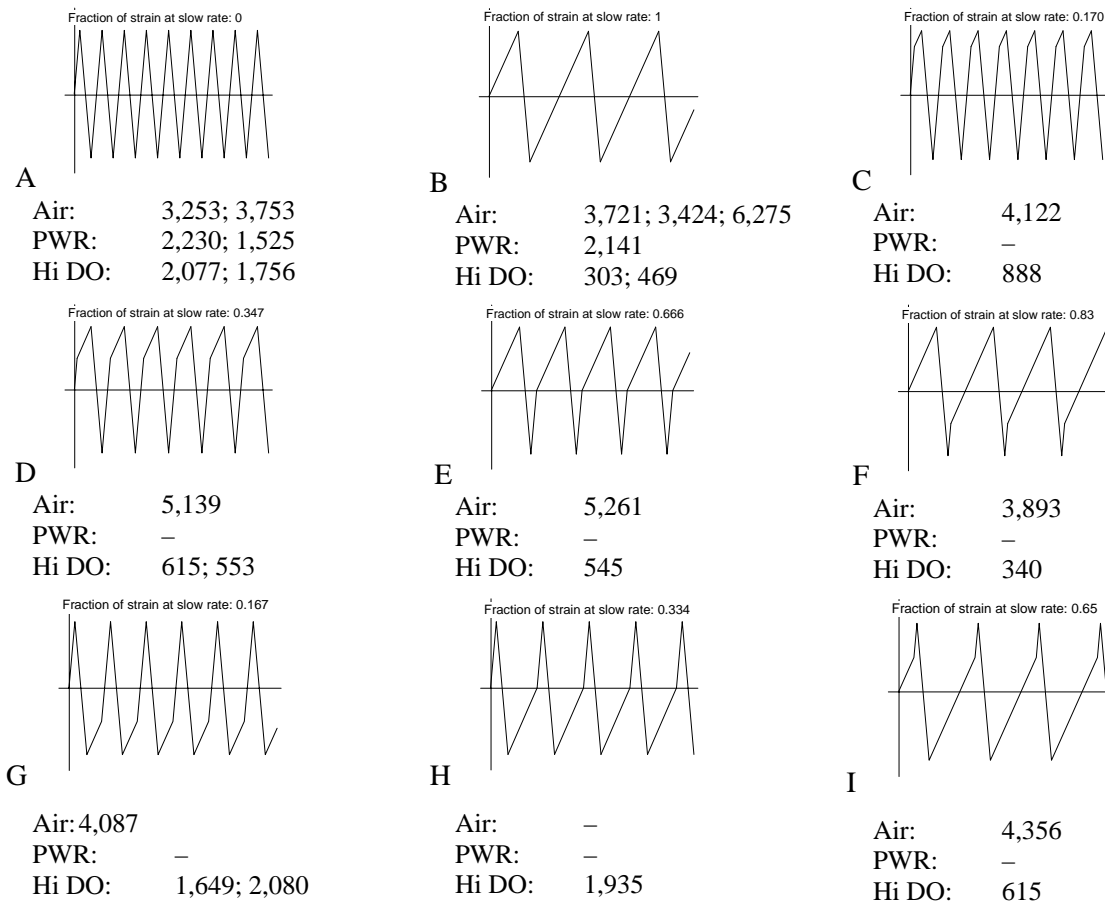
Figure 13.   Fatigue life of A106–Gr B carbon steel at 288°C and 0.75% strain range in air and water environments under different loading waveforms (Ref. 4).

23

(a)

(b)

(c)
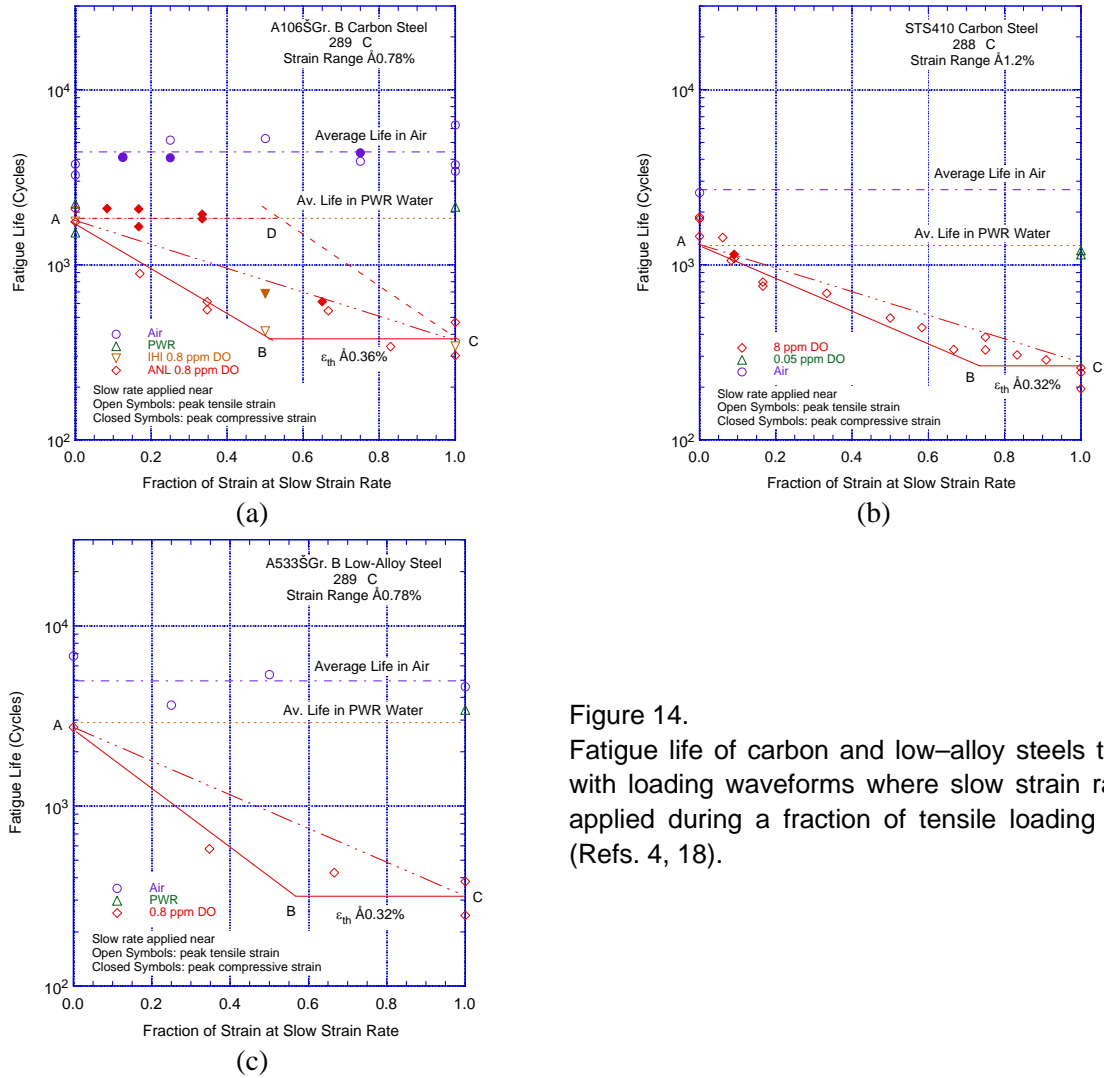
Figure 14.
Fatigue life of carbon and low–alloy steels tested with loading waveforms where slow strain rate is applied during a fraction of tensile loading cycle (Refs. 4, 18).

Similar strain–rate–change tests on austenitic SSs in PWR environments have also showed the existence of a strain threshold below which the material is insensitive to environmental effects.[29] The threshold strain $\Delta\varepsilon_{th}$ appears to be independent of material type (weld metal or base metal) and temperature in the range of 250–325°C, but it tends to decrease as the strain amplitude is decreased. The threshold strain has been expressed in terms of the applied strain range $\Delta\varepsilon$ by the equation

$$\Delta\varepsilon_{th}/\Delta\varepsilon = -0.22\ \Delta\varepsilon + 0.65. \tag{17}$$

This expression may also be used for carbon and low-alloy steels.

The modified rate approach, described in Section 4.2.14, has been used to predict the results from tests on four heats of carbon and low-alloy steels conducted with changing strain rate in low- and high-DO water at 289°C.[18] The results indicate that the modified rate approach, without the consideration of a strain threshold, gives the best estimates of life (Fig. 15). Most of the scatter in the data is due to heat-to-heat variation rather than any inaccuracy in estimation of fatigue life; for the same loading conditions, the fatigue lives of Heat #2 of STS410 steel are a factor of ≈5 lower than those of Heat #1. The estimated fatigue lives are within a factor of 3 of the experimental values.

24
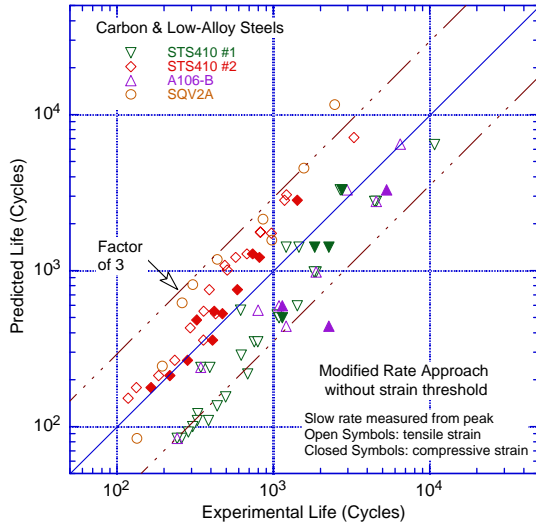
Figure 15.
Experimental values of fatigue life and those predicted from the modified rate approach without consideration of a threshold strain (Ref. 18).

- *In LWR coolant environments, the procedure for calculating F_{en}, defined in Eqs. 25 and 26 (Section 4.2.13), includes a threshold strain amplitude below which environment has no effect on fatigue life, i.e., $F_{en} = 1$. However, while using the damage rate approach to determine F_{en} for a stress cycle or load set pair including a threshold strain (Eq. 29 in Section 4.2.14) may yield nonconservative estimates of life.*

4.2.4   Temperature

The change in fatigue life of two heats of A333–Gr 6 carbon steel[12,13,16] with test temperature at different levels of DO is shown in Fig. 16. Other parameters, e.g., strain amplitude and strain rate, were kept constant; the applied strain amplitude was above and strain rate was below the critical threshold. In air, the two heats have a fatigue life of ≈3300 cycles. The results indicate a threshold temperature of 150°C, above which environment decreases fatigue life if DO in water is also above the critical level. In the temperature range of 150–320°C, the logarithm of fatigue life decreases linearly with temperature; the decrease in life is greater at high temperatures and DO levels. Only a moderate decrease in fatigue life is observed in water at temperatures below the threshold value of 150°C or at DO levels ≤0.05 ppm. Under these conditions, fatigue life in water is a factor of ≈2 lower than in air; Fig. 16 shows an average life of ≈2000 cycles for the heat with 0.015 wt.% S, and ≈1200 cycles for the 0.012 wt.% S steel.
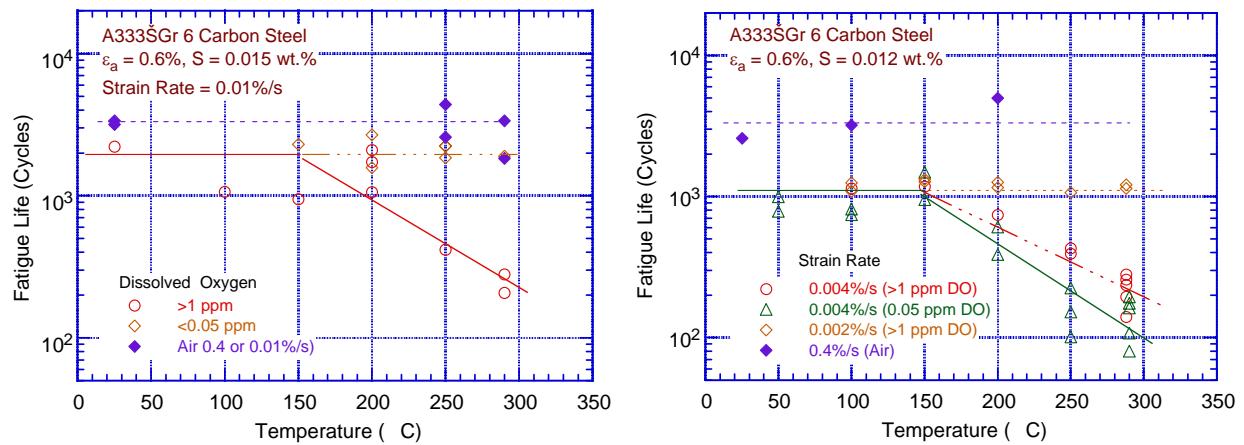
Figure 16.   Change in fatigue life of A333–Gr 6 carbon steel with temperature and DO.

An artificial neural network (ANN) has also been used to find patterns and identify the threshold temperature below which environmental effects are moderate.[98] The main benefits of the ANN approach are that estimates of life are based purely on the data and not on preconceptions, and that the network can interpolate effects where data are not present by learning trends. The factors that affect fatigue life can have synergistic effects on one another. A neural network can detect and utilize these effects in its predictions. A neural network, consisting of two hidden layers with the first containing ten nodes and the second containing six nodes, was trained six times; each training was based on the same data set, but the order in which the data were presented to the ANN for training was varied, and the initial ANN weights were randomized to guard against overtraining and to ensure that the network did not arrive at a solution that was a local minimum. The effect of temperature on the fatigue life of carbon steels and low–alloy steels estimated from ANN is shown in Fig. 17 as dashed or dotted lines. The solid line represents estimates based on the statistical model, and the open circles represent the experimental data. The results indicate that at high strain rate (0.4%/s), fatigue life is relatively insensitive to temperature. At low strain rate (0.004%/s), fatigue life decreases with an increase in temperature beyond a threshold value of ≈150°C. The precision of the data indicates that this trend is present in the data used to train the ANN.

Nearly all of the fatigue ε–N data have been obtained under loading histories with constant strain rate, temperature, and strain amplitude. The actual loading histories encountered during service of nuclear power plants involve variable loading and environmental conditions. Fatigue tests have been conducted in Japan on tube specimens (1– or 3–mm wall thickness) of A333–Gr 6 carbon steel in oxygenated water under combined mechanical and thermal cycling.[15] Triangular waveforms were used for both strain and temperature cycling. Two sequences were selected for temperature cycling (Fig. 18):
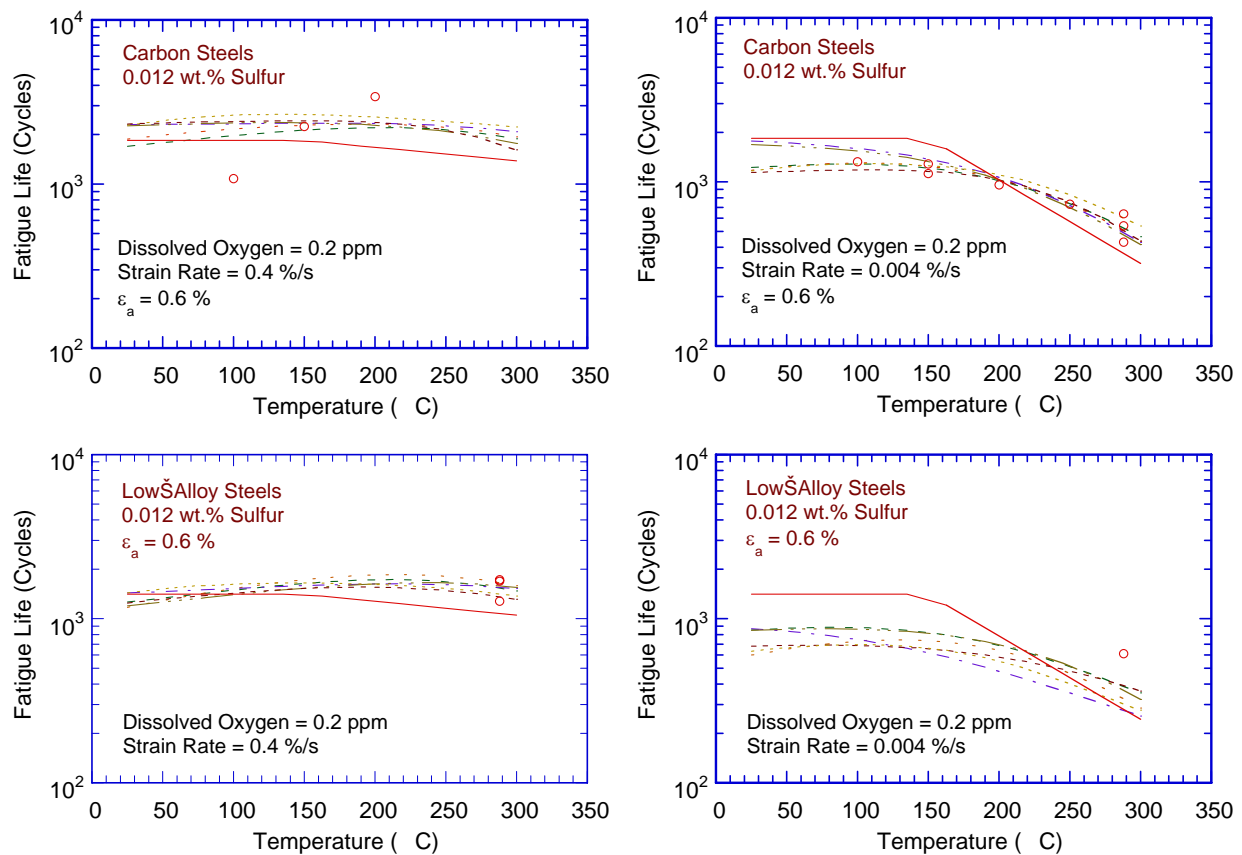
Figure 17.   Dependence of fatigue life on temperature for carbon and low-alloy steels in water.

an in–phase sequence in which temperature cycling was synchronized with mechanical strain cycling, and another sequence in which temperature and strain were out of phase, i.e., maximum temperature occurred at minimum strain level and vice versa. Three temperature ranges, 50–290°C, 50–200°C, and 200–290°C, were selected for the tests. The results are shown in Fig. 19; an average temperature is used to plot the thermal cycling tests. Because environmental effects on fatigue life are moderate and independent of temperature below 150°C, the temperature for tests cycled in the range of 50–290°C or 50–200°C was determined from the average of 150°C and the maximum temperature. The results in Fig. 19 indicate that load cycles involving variable temperature conditions may be represented by an average temperature, e.g., the fatigue lives from variable–temperature tests are comparable with those from constant–temperature tests.
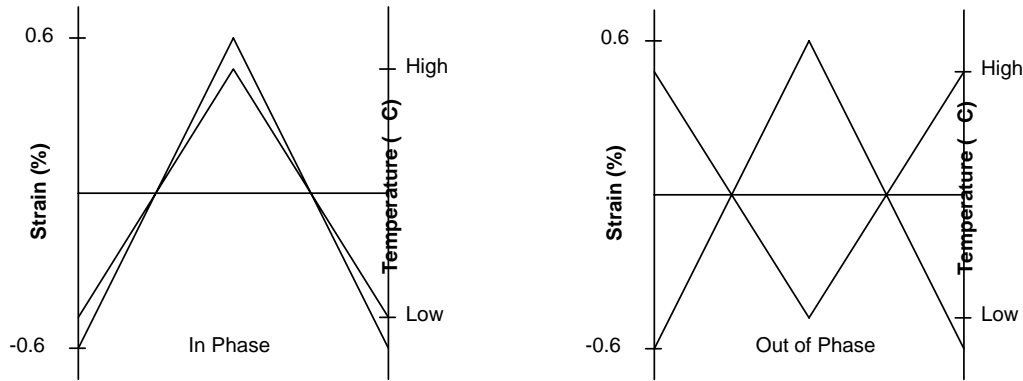
Figure 18. Waveforms for change in temperature during exploratory fatigue tests.
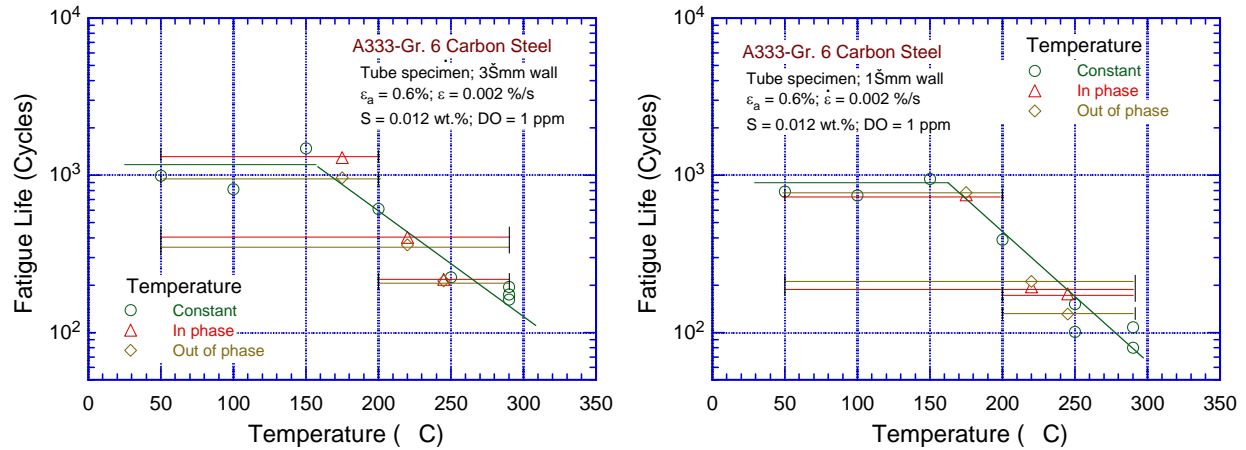
Figure 19. Fatigue life of A333–Gr 6 carbon steel tube specimens under varying temperature, indicated by horizontal bars.

However, the nearly identical fatigue lives of the in–phase and out–of–phase tests are somewhat surprising. If we consider that the tensile–load cycle is primarily responsible for environmentally assisted reduction in fatigue life, and that the applied strain and temperature must be above a minimum threshold value for environmental effects to occur, then fatigue life for the out–of–phase tests should be longer than for the in–phase tests, because applied strains above the threshold strain occur at temperatures above 150°C for in–phase tests, whereas they occur at temperatures below 150°C for the out–of–phase tests. If environmental effects on fatigue life are considered to be minimal below the threshold values of 150°C for temperature and <0.25 % for strain range, the average temperatures for the out–of–phase tests at 50–

27

290°C, 50–200°C, and 200–290°C should be 195, 160, and 236°C, respectively, instead of 220, 175, and 245°C, as plotted in Fig. 19. Thus, the fatigue lives of out–of–phase tests should be at least 50% higher than those of the in–phase tests. Most likely, difference in the cyclic hardening behavior of the material is affecting fatigue life of the out–of–phase tests.

- *In LWR environments, the effect of temperature on the fatigue life of carbon and low-alloy steels is explicitly considered in F_{en} defined in Eqs. 25 and 26 (Section 4.2.13). Also, an average temperature may be used to calculate F_{en} for a specific stress cycle or load set pair.*

4.2.5   Dissolved Oxygen

The dependence of fatigue life of carbon steel on DO content in water[12,13,16] is shown in Fig. 20. The test temperature, applied strain amplitude, and S content in steel were above, and strain rate was below, the critical threshold value. The results indicate a minimum DO level of 0.04 ppm above which environment decreases the fatigue life of the steel. The effect of DO content on fatigue life saturates at 0.5 ppm, i.e., increases in DO levels above 0.5 ppm do not cause further decreases in life. In Fig. 20, for DO levels between 0.04 and 0.5 ppm, fatigue life appears to decrease logarithmically with DO. Estimates of fatigue life from a trained ANN also show a similar effect of DO on the fatigue life of carbon steels and low–alloy steels.
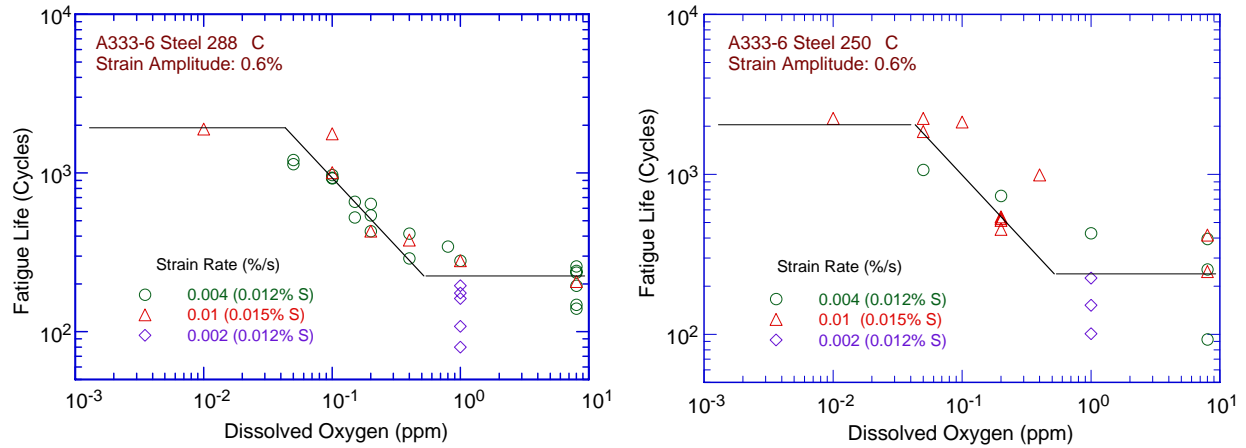
Figure 20.   Dependence on DO of fatigue life of carbon steel in high-purity water.

Environmental effects on the fatigue life of carbon and low-alloy steels are minimal at DO levels below 0.04 ppm, i.e., in low-DO PWR or hydrogen–chemistry BWR environments. In contrast, environmental enhancement of CGRs has been observed in low–alloy steels even in low–DO water.[97] This apparent inconsistency of fatigue ε–N data with the CGR data may be attributed to differences in the environment at the crack tip. The initiation of environmentally assisted enhancement of CGRs in low–alloy steels requires a critical level of sulfides at the crack tip.[97] The development of this critical sulfide concentration requires a minimum crack extension of 0.33 mm and CGRs in the range of 1.3×10^{-4} to 4.2×10^{-7} mm/s. These conditions are not achieved under typical ε-N tests. Thus, environmental effects on fatigue life are expected to be insignificant in low–DO environments.

- *In LWR environments, effect of DO level on the fatigue life of carbon and low-alloy steels is explicitly considered in F_{en}, defined in Eqs. 25 and 26 (Section 4.2.13).*

4.2.6   Water Conductivity

In most studies the DO level in water has generally been considered the key environmental parameter that affects the fatigue life of materials in LWR environments. Studies on the effect of the concentration of anionic impurities in water (expressed as the overall conductivity of water), are somewhat limited. The limited data indicate that the fatigue life of WB36 low–alloy steel at 177°C in water with ≈8 ppm DO decreased by a factor of ≈6 when the conductivity of water was increased from 0.06 to 0.5 μS/cm.[47,99] A similar behavior has also been observed in another study of the effect of conductivity on the initiation of short cracks.[100]

• *Normally, plants are unlikely to accumulate many fatigue cycles under off–normal conditions. Thus, effects of water conductivity on fatigue life have not been considered in the determination of F_{en}.*

4.2.7   Sulfur Content in Steel

It is well known that S content and morphology are the most important material–related parameters that determine susceptibility of low–alloy steels to environmentally enhanced fatigue CGRs.[101–104] A critical concentration of S^{2-} or HS^- ions is required at the crack tip for environmental effects to occur. Both the corrosion fatigue CGRs and threshold stress intensity factor ΔK_{th} are a function of the S content in the range 0.003–0.019 wt.%.[103] The probability of environmental enhancement of fatigue CGRs in precracked specimens of low–alloy steels appears to diminish markedly for S contents <0.005 wt.%.

The fatigue ε–N data for low–alloy steels also indicate a dependence of fatigue life on S content. When all the threshold conditions are satisfied, environmental effects on the fatigue life increase with increased S content. The fatigue lives of A508–Cl 3 steel with 0.003 wt.% S and A533–Gr B steel with 0.010 wt.% S are plotted as a function of strain rate in Fig. 21. However, the available data sets are too sparse to establish a functional form for dependence of fatigue life on S content and to define either a threshold for S content below which environmental effects are unimportant or an upper limit above which the effect of S on fatigue life may saturate. A linear dependence of fatigue life on S content has been assumed in correlations for estimating fatigue life of carbon steels and low–alloy steels in LWR environments.[4,73] The limited data suggest that environmental effects on fatigue life saturate at S contents above 0.015 wt.%.[4]

The existing fatigue ε-N data also indicate significant reductions in fatigue life of some heats of carbon steel with S levels as low as 0.002 wt.%. The fatigue lives of several heats of A333–Gr 6 carbon
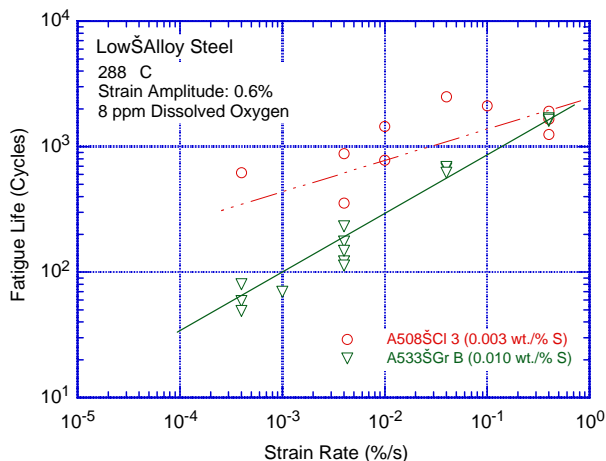
Figure 21.
Effect of strain rate on fatigue life of low–alloy steels with different S contents (JNUFAD database and Ref. 4).

steel with S contents of 0.002–0.015 wt.% in high-DO water at 288°C and 0.6% strain amplitude are plotted as a function of strain rate in Fig. 22.[4] Environmental effects on the fatigue life of these steels seem to be independent of S content in the range of 0.002–0.015 wt.%. However, these tests were conducted in air-saturated water (≈8 ppm DO). The fatigue life of carbon steels seems to be relatively insensitive to S content in very high DO water, e.g., greater than 1 ppm DO; under these conditions, the effect of DO dominates fatigue life. In other words, the saturation DO level of 0.5 ppm most likely is for medium- and high-S steels (i.e., steels with ≥0.005 wt.% S); it may be higher for low-S steels.
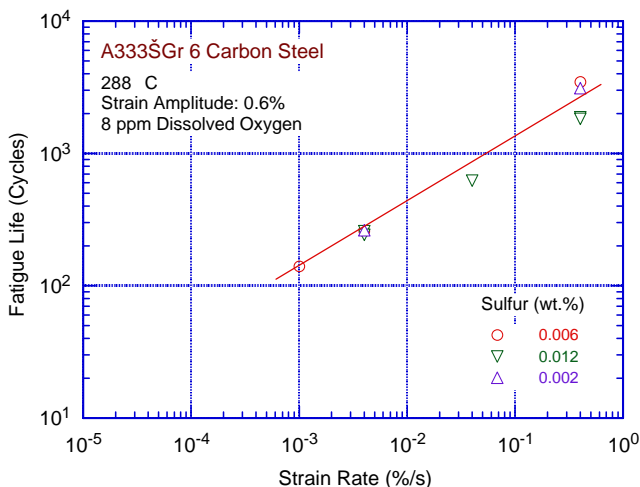
Figure 22.
Effect of strain rate on the fatigue life of A333–Gr 6 carbon steels with different S contents.

- *In LWR environments, the effect of S content on the fatigue life of carbon and low-alloy steels is explicitly considered in F_{en}, defined in Eqs. 25 and 26 (Section 4.2.13). However, evaluation of experimental data on low-S steels (<0.005 wt.% S) in water with ≥1 ppm DO should be done with caution; the effect of S may be larger than that predicted by Eqs. 25 and 26.*

4.2.8   Tensile Hold Period

Fatigue tests conducted using trapezoidal waveforms indicate that a hold period at peak tensile strain decreases the fatigue life of carbon steels in high–DO water at 289°C.[4,18] However, a detailed examination of the data indicated that these results are either due to limitations of the test procedure or caused by a frequency effect. Loading waveforms, hysteresis loops, and fatigue lives for the tests on A106–Gr B carbon steel in air and water environments are shown in Fig. 23.[4] A 300–s hold period is sufficient to reduce fatigue life by ≈50% (≈2000 cycles without and ≈1000 cycles with a hold period); a longer hold period of 1800 s results in only slightly lower fatigue life than that with a 300–s hold period. For example, two 300–s hold tests at 288°C and ≈0.78% strain range in oxygenated water with 0.7 ppm DO gave fatigue lives of 1,007 and 1,092 cycles; life in a 1800–s hold test was 840 cycles. These tests were conducted in stroke–control mode and are somewhat different from the conventional hold–time test in strain–control mode, where the total strain in the sample is held constant during the hold period. However, a portion of the elastic strain is converted to plastic strain because of stress relaxation. In a stroke–control test, there is an additional plastic strain in the sample due to relaxation of elastic strain from the load train (Fig. 23). Consequently, significant strain changes occur during the hold period; the measured plastic strains during the hold period were ≈0.028% from relaxation of the gauge and 0.05– 0.06% from relaxation of the load train. These conditions resulted in strain rates of 0.005–0.02%/s during the hold period. The reduction in life may be attributed to the slow strain rates during the hold period. Also, frequency effects may decrease the fatigue life of hold time tests, e.g., in air, the fatigue life of stroke-control test with hold period is ≈50% lower than that without the hold period.

Hold–time tests have also been conducted on STS410 carbon steel at 289°C in water with 1 ppm DO. The results are given in Table 5.[18] The most significant observation is that a reduction in fatigue life occurs only for those hold–time tests that were conducted at fast strain rates, e.g., at 0.4%/s. At lower strain rates, fatigue life is essentially the same for the tests with or without hold periods. Based on these results, Higuchi et al.[18] conclude that the procedures for calculating F_{en} need not be revised. Also, as discussed in Section 4.2.11, the differences in fatigue life of these tests are within the data scatter for the fatigue ε–N data in LWR environments.

• *The existing data do not demonstrate that hold periods at peak tensile strain affect the fatigue life of carbon and low-alloy steels in LWR environments. Thus, any revision/modification of the method to determine F_{en} is not warranted.*
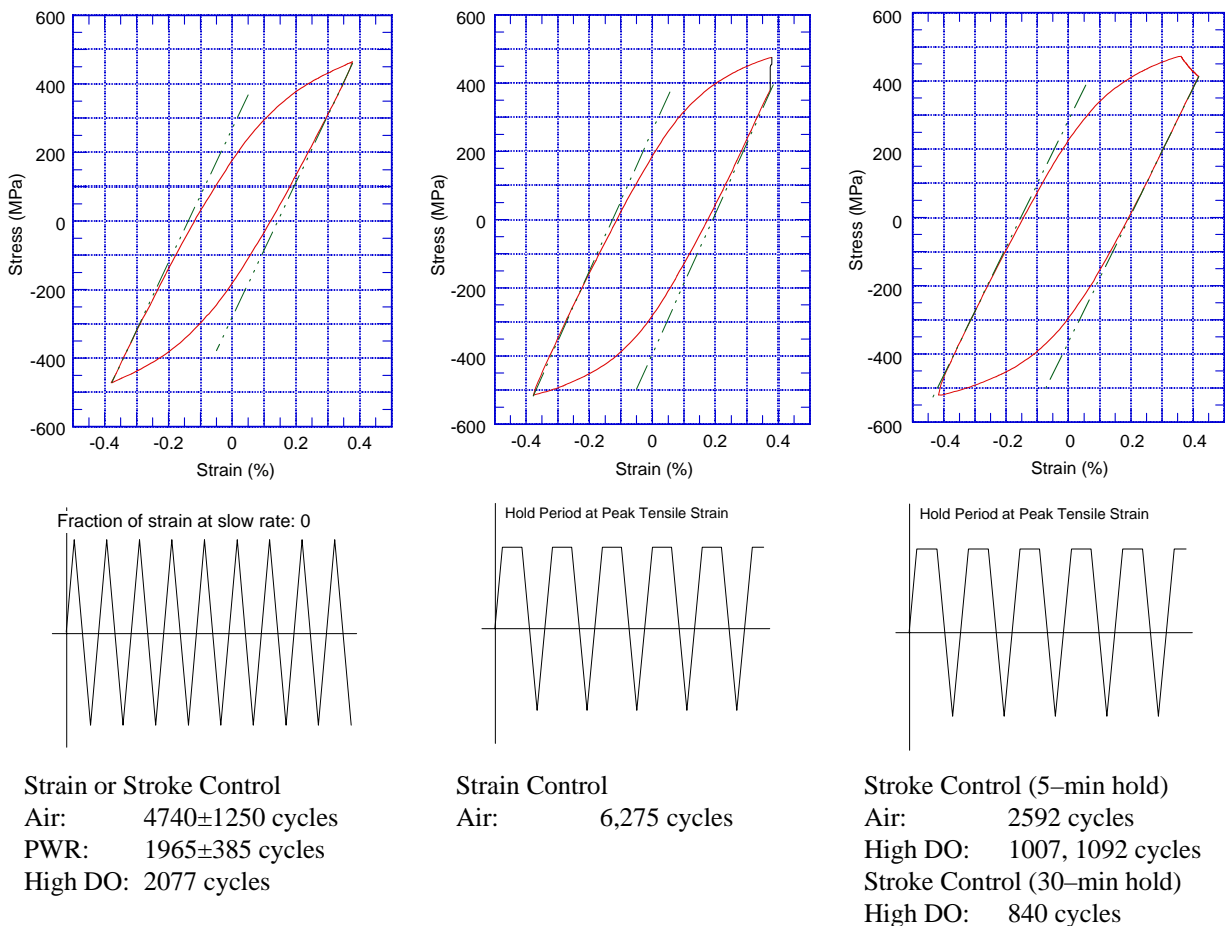
Figure 23. Fatigue life of A106–Gr B steel in air and water environments at 288°C, 0.78% strain range, and hold period at peak tensile strain (Ref. 4). Hysteresis loops are for tests in air.

Table 5. Fatigue data for STS410 steel at 289°C in water with 1 ppm DO and trapezoidal waveform.

Strain Ampl. (%)	Hold Period at Peak Tensile Strain (s)	Tensile / Compressive Strain Rate (%/s)			
		0.4 / 0.4	0.04 / 0.4	0.01 / 0.4	0.004 / 0.4
0.6	0	489	240	-	118
0.6	60	328, 405	238	-	138
0.6	600	173, 217	-	-	-
0.3	0	3270	1290	737	508
0.3	60	1840, 1760	1495	875	587
0.3	600	436, 625	-	-	-

4.2.9   Flow Rate

Nearly all of the fatigue ε–N data for LWR environments have been obtained at very low water flow rates. Recent data indicate that, under the environmental conditions typical of operating BWRs, environmental effects on the fatigue life of carbon steels are at least a factor of 2 lower at high flow rates (7 m/s) than at 0.3 m/s or lower.[19,20,43] The beneficial effects of increased flow rate are greater for high–S steels and at low strain rates.[19,20] The effect of water flow rate on the fatigue life of high–S (0.016 wt.%) A333–Gr 6 carbon steel in high–purity water at 289°C is shown in Fig. 24. At 0.3% strain amplitude, 0.01%/s strain rate, and all DO levels, fatigue life is increased by a factor of ≈2 when the flow rate is increased from ≈10^{-5} to 7 m/s. At 0.6% strain amplitude and 0.001%/s strain rate, fatigue life is increased by a factor of ≈6 in water with 0.2 ppm DO and by a factor of ≈3 in water with 1.0 or 0.05 ppm DO. Under similar loading conditions, i.e., 0.6% strain amplitude and 0.001%/s strain rate, a low–S (0.008 wt.%) heat of A333–Gr 6 carbon steel showed only a factor of ≈2 increase in fatigue life with increased flow rates. Note that the beneficial effects of flow rate are determined from a single test on each material at very low flow rates; data scatter in LWR environments is typically a factor of ≈2.

A factor of 2 increase in fatigue life was observed (Fig. 25) at KWU during component tests with 180° bends of carbon steel tubing (0.025 wt.% S) when internal flow rates of up to 0.6 m/s were established.[43] The tests were conducted at 240°C in water that contained 0.2 ppm DO.

• *Because of the uncertainties in the flow conditions at or near the locations of crack initiation, the beneficial effect of flow rate on the fatigue life is presently not included in fatigue evaluations.*
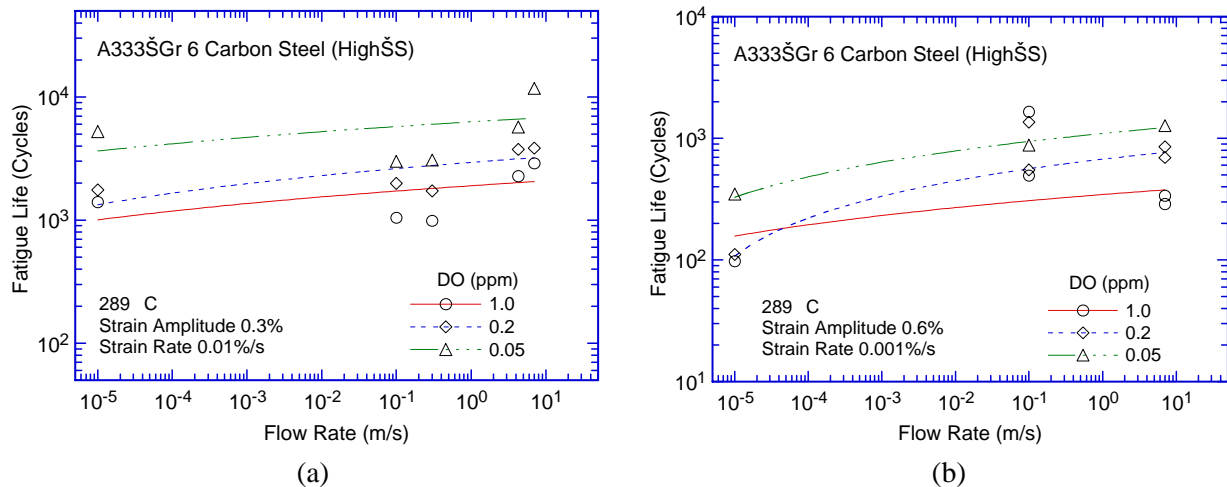
Figure 24.   Effect of water flow rate on fatigue life of A333–Gr 6 carbon steel at 289°C and strain amplitude and strain rates of (a) 0.3% and 0.01%/s and (b) 0.6% and 0.001%/s.
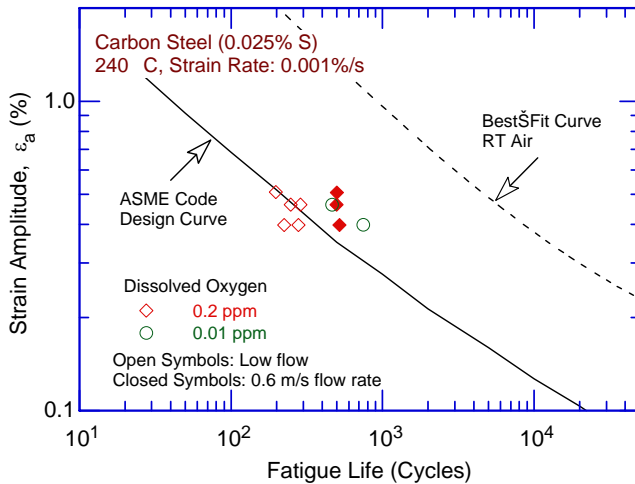
Figure 25.
Effect of flow rate on low–cycle fatigue of carbon steel tube bends in high–purity water at 240°C (Ref. 43). RT = room temperature.

4.2.10 Surface Finish

Fatigue testing has been conducted on specimens of carbon and low-alloy steels that were intentionally roughened in a lathe, under controlled conditions, with 50-grit sandpaper to produce circumferential scratches with an average roughness of 1.2 μm and R_q of 1.6 μm (≈62 micro in.).[38] The results for A106–Gr B carbon steel and A533–Gr B low–alloy steel are shown in Fig. 26. In air, the fatigue life of rough A106–Gr B specimens is a factor of 3 lower than that of smooth specimens, and, in high–DO water, it is the same as that of smooth specimens. In low–DO water, the fatigue life of the roughened A106–Gr B specimen is slightly lower than that of smooth specimens. The effect of surface roughness on the fatigue life of A533–Gr B low–alloy steel is similar to that for A106–Gr B carbon steel; in high–DO water, the fatigue lives of both rough and smooth specimens are the same. The results in water are consistent with a mechanism of growth by a slip oxidation/dissolution process, which seems unlikely to be affected by surface finish. Because environmental effects are moderate in low–DO water, surface roughness would be expected to influence fatigue life.
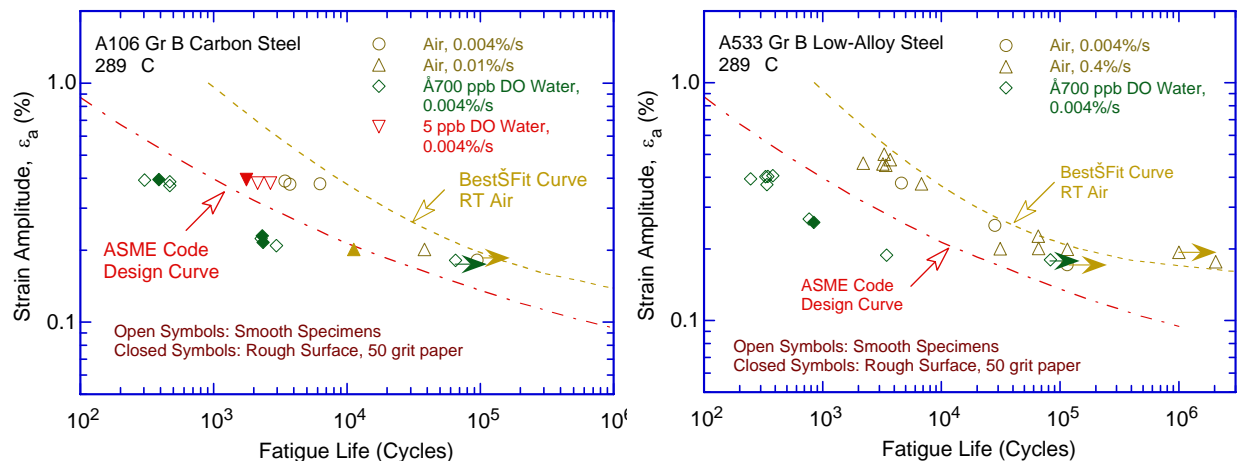
Figure 26. Effect of surface roughness on fatigue life of (a) A106–Gr B carbon steel and (b) A533 low–alloy steel in air and high–purity water at 289°C.

- *The effect of surface finish is not considered in the environmental fatigue correction factor; it is included in the subfactor for "surface finish and environment" that is applied to the mean data curve to develop the Code fatigue design curve in air.*

4.2.11 Heat-to-Heat Variability

The effect of material variability and data scatter on the fatigue life of carbon and low-alloy steels has also been evaluated for LWR environments. The fatigue behavior of each of the heats or loading conditions is characterized by the value of the constant A in the statistical models (e.g., Eq. 6). The values of A for the various data sets are ordered, and median ranks are used to estimate the cumulative distribution of A for the population. Results for carbon and low–alloy steels in water environments are shown in Fig. 27. The median value of A in water is 5.951 for carbon steels and 5.747 for low-alloy steels. The results indicate that environmental effects are approximately the same for the various heats of these steels. For example, the cumulative distribution of data sets for specific heats is approximately the same in air and water environments. The statistical model seem to overestimate the effect of environment for a few heats, e.g., the ranking for A533–Gr B heat 5 is ≈42 percentile in air and ≈95 percentile in water, and for A106–Gr B heat A, it is ≈17 percentile in air and varies from 2 to 60 percentile in water. Monte Carlo analyses were also performed for the fatigue data in LWR environments.
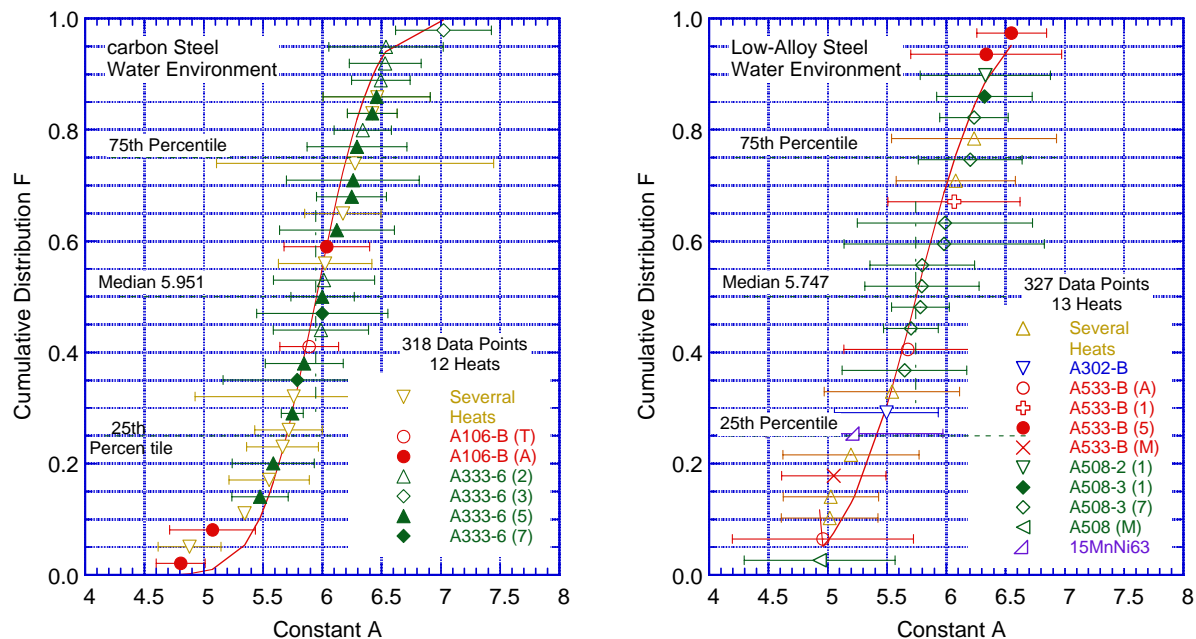
Figure 27.   Estimated cumulative distribution of parameter A in statistical models for fatigue life for heats of carbon and low–alloy steels in LWR environments.

The results for carbon and low-alloy steels in LWR environments are summarized in Tables 6 and 7, respectively, in terms of values for A that provide bounds for the portion of the population and the confidence that is desired in the estimates of the bounds. In LWR environments, the 5th percentile value of parameter A at 95% confidence level is 5.191 for carbon steels and 4.748 for low-alloy steels. From Fig. 27, the median value of A for the sample is 5.951 for carbon steels and 5.747 for low-alloy steels. Thus, the 95/95 value of the margin to account for material variability and data scatter is 2.1 and 2.7 on life for carbon steels and low-alloy steels, respectively. These margins are needed to provide 95% confidence that the resultant life will be greater than that observed for 95% of the materials of interest.

34

Table 6. Values of parameter A in statistical model for carbon steels in water and the margins on life as a function of confidence level and percentage of population bounded.

Confidence Level	Percentage of Population Bounded (Percentile Distribution of A)				
	95 (5)	90 (10)	75 (25)	67 (33)	50 (50)
	Values of Parameter A				
50	5.333	5.469	5.697	5.786	5.951
75	5.275	5.417	5.652	5.742	5.906
95	5.191	5.342	5.587	5.678	5.840
	Margins on Life				
50	1.9	1.6	1.3	1.2	1.0
75	2.0	1.7	1.3	1.2	1.0
95	2.1	1.8	1.4	1.3	1.1

Table 7. Values of parameter A in statistical model for low–alloy steels in water and the margins on life as a function of confidence level and percentage of population bounded.

Confidence Level	Percentage of Population Bounded (Percentile Distribution of A)				
	95 (5)	90 (10)	75 (25)	67 (33)	50 (50)
	Values of Parameter A				
50	4.950	5.126	5.420	5.534	5.747
75	4.867	5.052	5.355	5.470	5.680
95	4.748	4.944	5.261	5.378	5.585
	Margins on Life				
50	2.2	1.9	1.4	1.2	1.0
75	2.4	2.0	1.5	1.3	1.1
95	2.7	2.2	1.6	1.4	1.2

- *The effect of heat-to-heat variability is not considered in the environmental fatigue correction factor; it is included in the subfactor for "data scatter and material variability" that is applied to the mean data curve to develop the Code fatigue design curve in air.*

4.2.12 Statistical Model

Statistical models based on the existing fatigue ε–N data have been developed at ANL for estimating the fatigue lives of carbon and low–alloy steels in LWR environments.[4,38] The effects of key parameters, such as temperature, strain rate, DO content in water, and S content in the steel, are included in the correlations; the effects of these and other parameters on the fatigue life are discussed in below in detail. The functional forms for the effects of strain rate, temperature, DO level in water, and S content in the steel were based on the data trends. For both carbon and low-alloy steels, the model assumes threshold and saturation values of 1.0 and 0.001%/s, respectively, for strain rate, and 0.04 and 0.5 ppm, respectively, for DO. It also considers a threshold value of 150°C for temperature and a saturation value of 0.015 wt.% for S.

In the present report these statistical models have been updated based on the analysis presented in Section 4.2.11, e.g., constant A in the models differs from the value reported earlier in NUREG/CR–6583 and –6815. Relative to the earlier model, the fatigue lives predicted by the updated model are ≈6% lower for carbon steels and ≈2% higher for low–alloy steels. In LWR environments, the fatigue life, N, of carbon steels is represented by

$$\ln(N) = 5.951 - 1.975 \ln(\varepsilon_a - 0.113) + 0.101\, S^* T^* O^* \dot{\varepsilon}^*, \tag{18}$$
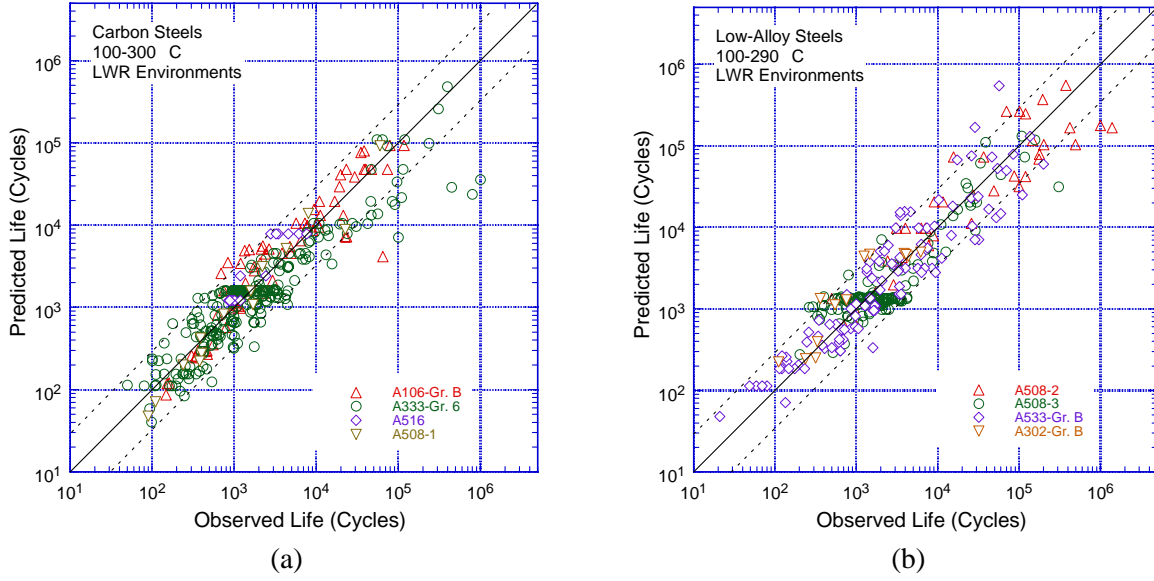
Figure 28. Experimental and predicted fatigue lives of (a) carbon steels and (b) low-alloy steels in LWR environments.

and that of low–alloy steels, by

$$\ln(N) = 5.747 - 1.808 \ln(\varepsilon_a - 0.151) + 0.101\, S^* \, T^* \, O^* \, \dot\varepsilon^*, \tag{19}$$

where S^*, T^*, O^*, and $\dot\varepsilon^*$ are transformed S content, temperature, DO level, and strain rate, respectively, defined as:

$S^* = 0.015$	(DO > 1.0 ppm)
$S^* = S$	(DO $\leq$ 1.0 ppm and S $\leq$ 0.015 wt.%)
$S^* = 0.015$	(DO $\leq$ 1.0 ppm and S > 0.015 wt.%) (20)

$T^* = 0$	(T $\leq$ 150°C)
$T^* = T - 150$	(150 < T $\leq$ 350°C) (21)

$O^* = 0$	(DO $\leq$ 0.04 ppm)
$O^* = \ln(DO/0.04)$	(0.04 ppm < DO $\leq$ 0.5 ppm)
$O^* = \ln(12.5)$	(DO > 0.5 ppm) (22)

$\dot\varepsilon^* = 0$	($\dot\varepsilon$ > 1%/s)
$\dot\varepsilon^* = \ln(\dot\varepsilon)$	(0.001 $\leq \dot\varepsilon \leq$ 1%/s)
$\dot\varepsilon^* = \ln(0.001)$	($\dot\varepsilon$ < 0.001%/s). (23)

These models are recommended for predicted fatigue lives $\leq 10^6$ cycles. Also, as discussed in Section 4.2.7, because the effect of S on the fatigue life of carbon and low–alloy steels appears to depend on the DO level in water, Eqs. 18–23 may yield nonconservative estimates of fatigue life for low–S (<0.007 wt.%) steels in high–temperature water with >1 ppm DO. The experimental values of fatigue life and those predicted by Eqs. 18 and 19 are plotted in Fig. 28. The predicted fatigue lives show good agreement with the experimental values; the experimental and predicted values differ by a factor of 3.

- *The statistical models represent the mean values of fatigue life as a function of applied strain amplitude, temperature, strain rate, DO level in water, and S content of the steel. The effects of parameters (such as mean stress, surface finish, size and geometry, and loading history) that are known to influence fatigue life are not included in the model.*

4.2.13 Environmental Fatigue Correction Factor

The effects of reactor coolant environments on fatigue life have also been expressed in terms of environmental fatigue correction factor, F_{en}, which is defined as the ratio of life in air at room temperature, N_{RTair}, to that in water at the service temperature, N_{water}. Values of F_{en} can be obtained from the statistical model, where

$$\ln(F_{en}) = \ln(N_{RTair}) - \ln(N_{water}). \tag{24}$$

The environmental fatigue correction factor for carbon steels is given by

$$F_{en} = \exp(0.632 - 0.101\ S^*\ T^*\ O^*\ \dot{\varepsilon}^{\,*}), \tag{25}$$

and for low–alloy steels, by

$$F_{en} = \exp(0.702 - 0.101\ S^*\ T^*\ O^*\ \dot{\varepsilon}^{\,*}), \tag{26}$$

where the constants S^*, T^*, $\dot{\varepsilon}^{\,*}$, and O^* are defined in Eqs. 20–23. Note that because the ANL statistical models have been updated in the present report, the constants 0.632 and 0.702 in Eqs. 25 and 26 are different from the values reported earlier in NUREG/CR–6583 and –6815. Relative to the earlier expressions, correction factors determined from Eq. 25 for carbon steels are ≈8% higher, and those determined from Eq. 26 for low–alloy steels are ≈18% lower. A strain threshold is also defined, below which LWR coolant environments have no effect on fatigue life, i.e., $F_{en} = 1$. The strain threshold is 0.07% (145 MPa stress amplitude) for carbon and low–alloy steels. To incorporate environmental effects into a ASME Section III fatigue evaluation, the fatigue usage for a specific stress cycle of load set pair based on the current Code fatigue design curves is multiplied by the correction factor. Further details for incorporating environmental effects into fatigue evaluations are presented in Appendix A.

- *The F_{en} approach may be used to incorporate environmental effects into the Code fatigue evaluations.*

4.2.14 Modified Rate Approach

Nearly all of the existing fatigue ε–N data were obtained under loading histories with constant strain rate, temperature, and strain amplitude. The actual loading histories encountered during service of nuclear power plants are far more complex. Exploratory fatigue tests have been conducted with waveforms in which the test temperature and strain rate were changed.[4,15,18] The results of such tests provide guidance for developing procedures and rules for fatigue evaluation of components under complex loading histories.

The modified rate approach has been proposed to predict fatigue life under changing test conditions.[31,32] It allows calculating F_{en} under conditions where temperature and strain rate are changing. The correction factor, $F_{en}(\dot{\varepsilon}, T)$, is assumed to increase linearly from 1 with increments of strain from a minimum value ε_{min} (%) to a maximum value ε_{max} (%). Increments of F_{en}, dF_{en}, during increments of strain, $d\varepsilon$, are calculated from

$$dF_{en} = (F_{en} - 1) \, d\varepsilon \, /(\, \varepsilon_{max} - \varepsilon_{min}) . \tag{27}$$

Integration of Eq. 27 from ε_{min} to ε_{max} provides the environmental fatigue correction factor under changing temperature and strain rate. The application of the modified rate approach to a strain transient is illustrated in Fig. 29; at each strain increment, $F_{en}(\dot{\varepsilon},T)$ is determined from Eqs. 25 and 26. Thus, F_{en} for the total strain transient is given by

$$F_{en} = \sum_{k=1}^{n} F_{en,k} \left(\dot{\varepsilon}_k, T_k \right) \frac{\Delta\varepsilon_k}{\varepsilon_{max} - \varepsilon_{min}} , \tag{28}$$

where n is the total number of strain increments, and k is the subscript for the k-th incremental segment.

As discussed in Section 4.2.3, a minimum threshold strain, ε_{th}, is required for an environmentally assisted decrease in fatigue life. During a strain cycle, environmental effects are insignificant only after the applied strain level exceeds the threshold value. In application of the modified rate approach when a threshold strain ε_{th} is considered, F_{en} for the total strain transient is given by

$$F_{en} = \sum_{k=1}^{n} F_{en,k} \left(\dot{\varepsilon}_k, T_k \right) \frac{\Delta\varepsilon_k}{\varepsilon_{max} - \left(\varepsilon_{min} + \varepsilon_{th} \right)} . \tag{29}$$
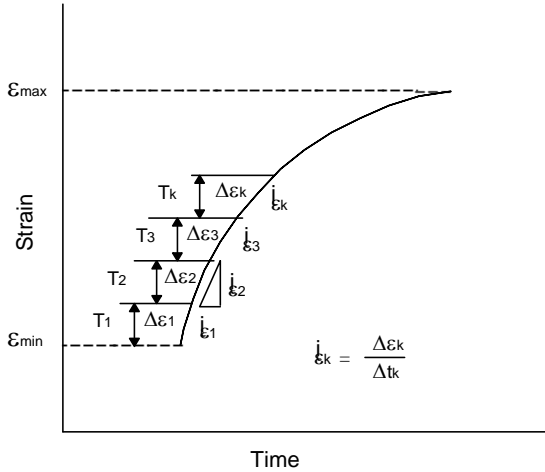
Figure 29.
Application of the modified rate approach to determine the environmental fatigue correction factor F_{en} during a transient.

The modified rate approach has been used to evaluate fatigue life under cyclic loading conditions where both temperature and strain rate were varied during the test.[18,31,32] The studies demonstrate the applicability of the damage rate approach to variable loading conditions such as actual plant transient. Also, the following conclusions may be drawn from these studies.

(a)   The use of a strain threshold, ε_{th}, for calculating F_{en} by the modified rate approach (i.e., Eq. 29) is not necessary because it does not improve the accuracy of estimation.[32] As discussed earlier in Section 4.2.3, application of the modified rate approach, without the consideration of a strain threshold, gives the best estimates of fatigue life.

(b)   Under load cycles that involve variable strain rate, estimates of F_{en} based on an average strain rate [i.e., in Fig. 29, total strain ($\varepsilon_{max} - \varepsilon_{min}$) divided by the total time for the transient] are the most

conservative.[18] Thus, calculations of F_{en} based on an average strain rate for the transient will always yield a conservative estimate of fatigue life.

(c) An average temperature for the transient may be used to estimate F_{en} during a load cycle.

- *Where information is available regarding the transients associated with a specific stress cycle or load set pair, the modified rate approach may be used to determine F_{en}.*

5 Austenitic Stainless Steels

The relevant fatigue ε–N data for austenitic SSs in air include the data compiled by Jaske and O'Donnell[70] for developing fatigue design criteria for pressure vessel alloys, the JNUFAD database from Japan, studies at EdF in France,[67] and the results of Conway et al.[71] and Keller.[72] In water, the existing fatigue ε–N data include the tests performed by GE in a test loop at the Dresden 1 reactor;[8–11] the JNUFAD data base; studies at MHI, IHI, and Hitachi in Japan;[18–30] the work at ANL;[6,7,35–39] and the studies sponsored by EdF.[68–69] Nearly 60% of the tests in air were conducted at room temperature, 20% at 250–325°C, and 20% at 350–450°C. Nearly 90% of the tests in water were conducted at temperatures between 260 and 325°C; the remainder were at lower temperatures. The data on Type 316NG in water have been obtained primarily at DO levels ≥0.2 ppm, and those on Type 316 SS, at ≤0.005 ppm DO; half of the tests on Type 304 SS are at low–DO and the remaining at high–DO levels.

5.1 Air Environment

5.1.1 Experimental Data

The fatigue ε–N data for Types 304, 316, and 316NG SS in air at temperatures between room temperature and 456°C are shown in Fig. 30. The best–fit curve based on the updated ANL statistical model (Eq. 30 in Section 5.1.7) and the ASME Section III mean-data curves are included in the figures. The results indicate that the fatigue life of Type 304 SS is comparable to that of Type 316 SS; the fatigue
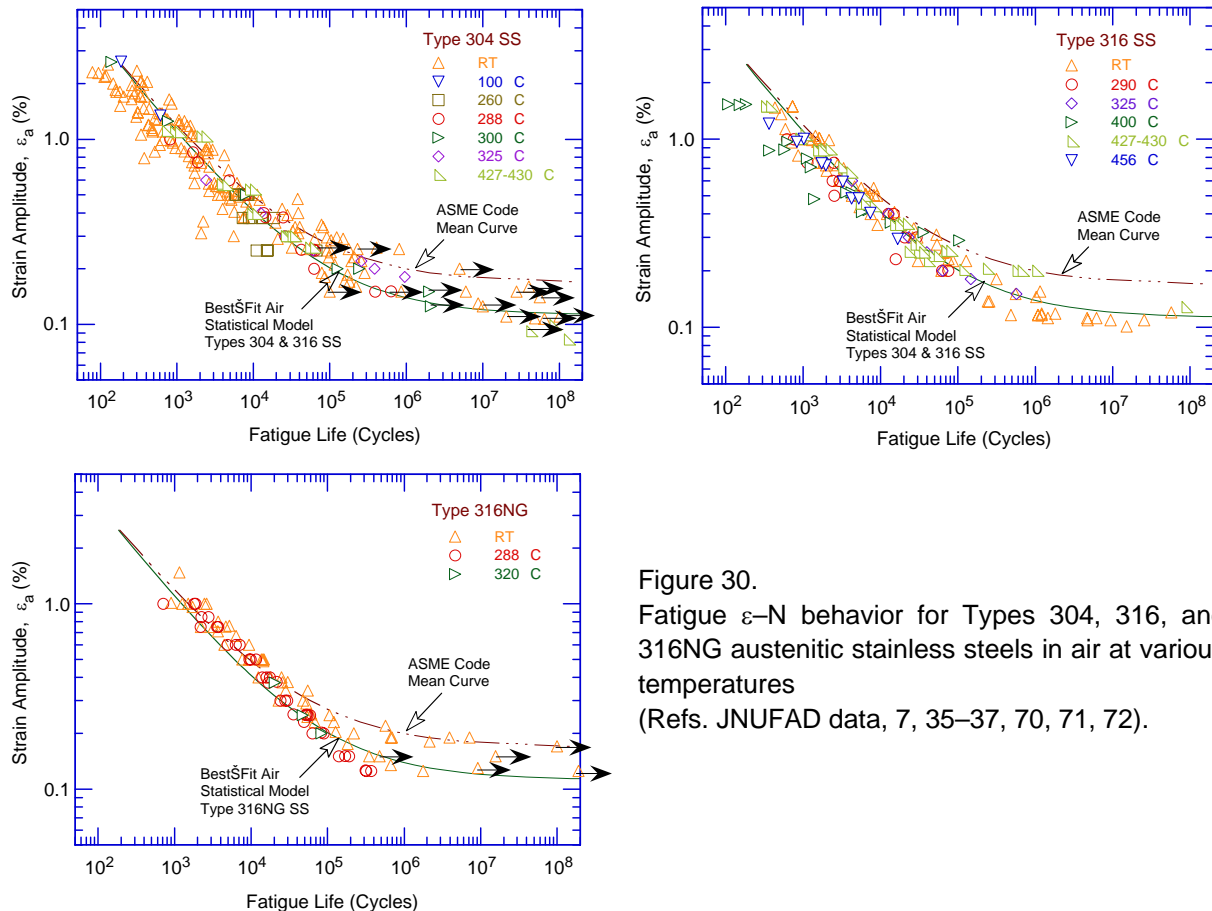
Figure 30.
Fatigue ε–N behavior for Types 304, 316, and 316NG austenitic stainless steels in air at various temperatures
(Refs. JNUFAD data, 7, 35–37, 70, 71, 72).

life of Type 316NG is slightly higher than that of Types 304 and 316 SS at high strain amplitudes. Some of the tests on Type 316 SS in room–temperature air have been conducted in load–control mode at stress levels in the range of 190–230 MPa. The data are shown as triangles in Fig. 30, with strain amplitudes of 0.1–0.12% and fatigue lives of 7 x 10^4–3 x 10^7. For these tests, the strain amplitude was calculated only as elastic strain. Based on cyclic stress–vs.–strain correlations for Type 316 SS,[37] actual strain amplitudes for these tests should be 0.23–0.32%. These results were excluded from the analysis of the fatigue ε–N data to develop the statistical model for estimating the fatigue life of these steels in air.

The results also indicate that the current Code mean-data curve is not consistent with the existing fatigue ε–N data. At strain amplitudes <0.3%, the Code mean curve predicts significantly longer fatigue lives than those observed experimentally. The difference between the Code mean curve and the best–fit of the available experimental data is due most likely to differences in the tensile strength of the steels. The Code mean curve represents SSs with relatively high strength; the fatigue ε–N data obtained during the last 30 years were obtained on SSs with lower tensile strengths.

Furthermore, because, for the current Code mean curve, the value of applied stress at a fatigue life of 10^6 cycles is greater than the monotonic yield strength of austenitic SSs in more common usage, the current Code design curve for austenitic SSs does not include a mean stress correction. Studies on the effect of residual stress on fatigue life indicate that a mean stress correction is needed for austenitic SSs; e.g., an apparent reduction of up to 26% in strain amplitude in the low– and intermediate–cycle regime was observed in fatigue tests with a mean stress of 138 MPa.[105]

- *The current Code mean data curve, and therefore the Code design curve, is nonconservative with respect to the existing fatigue ε–N data for austenitic SSs. A new Code fatigue design curve, which is consistent with the existing fatigue data, has been proposed (see Section 5.1.8 for details).*

5.1.2 Specimen Geometry

The influence of specimen geometry (hourglass vs. gauge length specimens) on the fatigue life of Types 304 and 316 SS is shown in Fig. 31. At temperatures up to 300°C, specimen geometry has little or no effect on the fatigue life of austenitic SSs; the fatigue lives of hourglass specimens are comparable to those of gauge specimens.
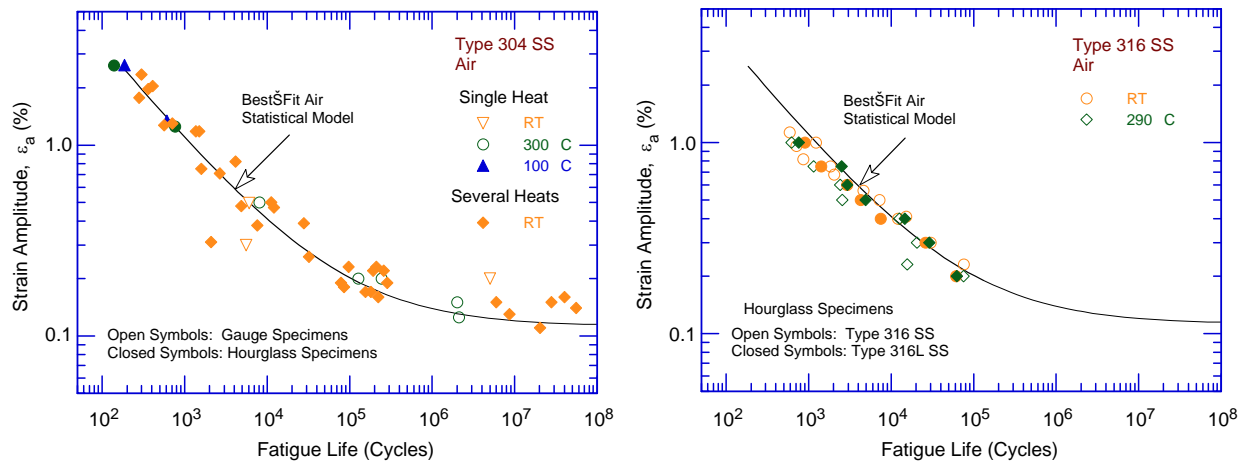
Figure 31. Influence of specimen geometry on fatigue life of Types 304 and 316 stainless steel (JNUFAD data).

- *Fatigue ε–N data obtained either on hourglass or gauge specimens may be used to develop the Code fatigue design curves.*

5.1.3   Temperature

The fatigue life of Types 304 and316 SS in air at temperatures between 100 and 325°C is plotted in Fig. 32; the best-fit curve based on the ANL model (Eq. 30 in Section 5.1.7) and the ASME Code mean curve are also shown in the figures. In air, the fatigue life of austenitic SSs is independent of temperature from room temperature to 400°C. Although the effect of strain rate on fatigue life seems to be significant at temperatures above 400°C, variations in strain rate in the range of 0.4–0.008%/s have no effect on the fatigue lives of SSs at temperatures up to 400°C.[67] In air, the fatigue ε–N data can be represented by a single curve for temperatures from room temperature up to 400°C.
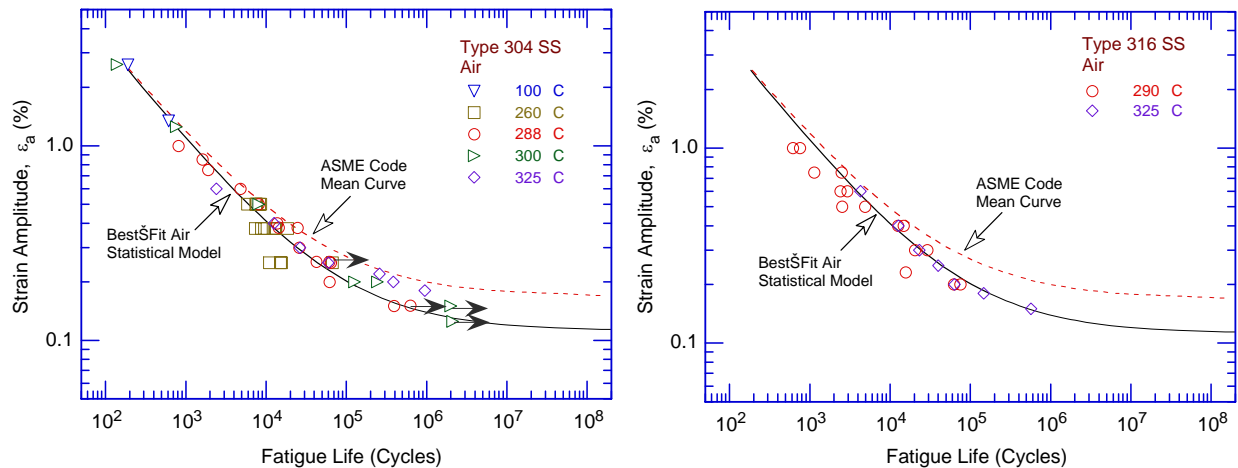
Figure 32.   Influence of temperature on fatigue life of Types 304 and 316 stainless steel in air (Ref. 37, JNUFAD database).

Recent data indicate that temperature can influence the fatigue limit of austenitic SSs because of differences in the secondary hardening behavior of the material due to dynamic strain aging.[69] For a heat of Type 304L SS, the fatigue limit was higher at 300°C than at 150°C because of significant secondary hardening at 300°C.

- *Temperature has no significant effect on the fatigue life of austenitic SSs at temperatures from room temperature to 400°C. Variations in fatigue life due to the effects of secondary hardening behavior are accounted for in the factor applied on stress to obtain the design curve from the mean data curve.*

5.1.4   Cyclic Strain Hardening Behavior

Under cyclic loading, austenitic SSs exhibit rapid hardening during the first 50–100 cycles; the extent of hardening increases with increasing strain amplitude and decreasing temperature and strain rate.[37] The initial hardening is followed by a softening and saturation stage at high temperatures, and by continuous softening at room temperature.

- *The cyclic strain hardening behavior is likely to influence the fatigue limit of the material; variations in fatigue life due to such effects are accounted for in the factor of 2 on stress.*

43
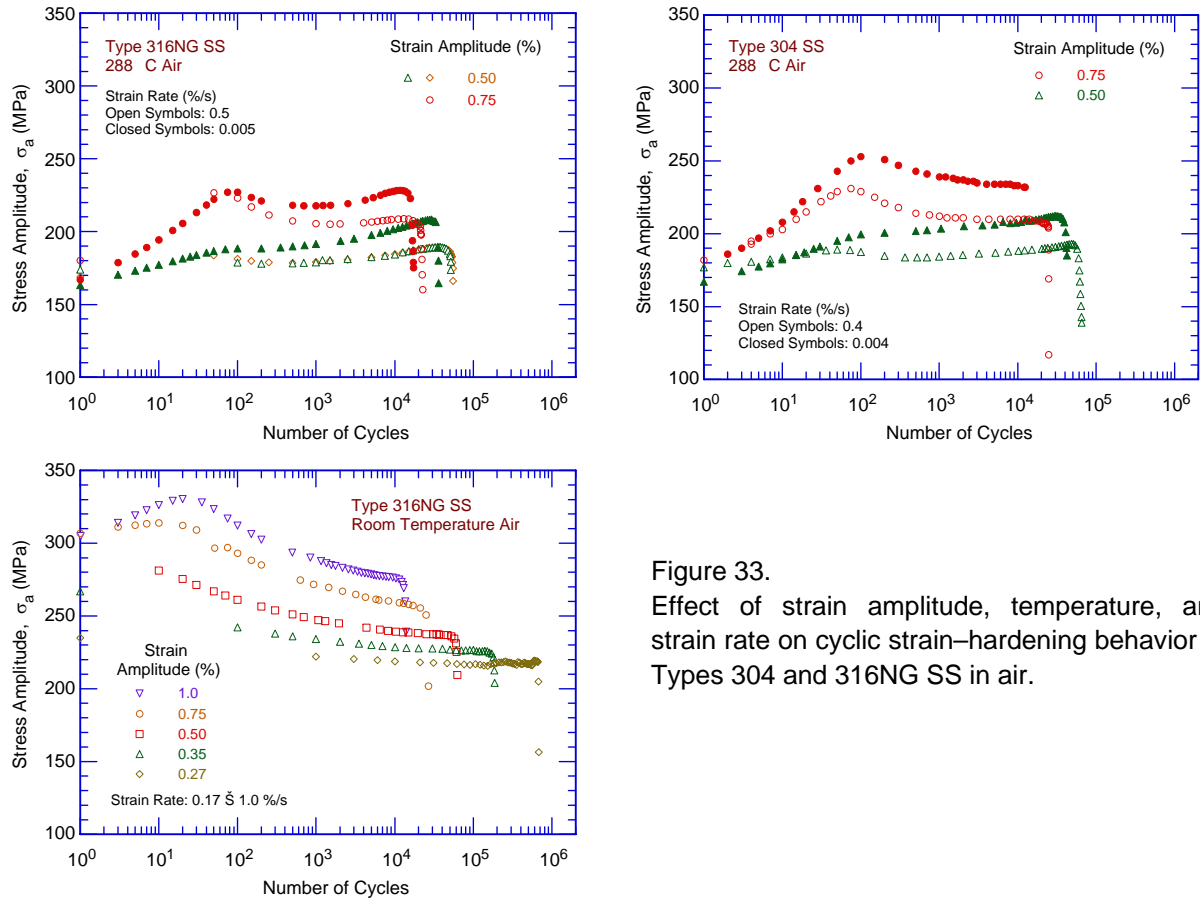
Figure 33.
Effect of strain amplitude, temperature, and strain rate on cyclic strain–hardening behavior of Types 304 and 316NG SS in air.

5.1.5   Surface Finish

Fatigue tests have been conducted on Types 304 and 316NG SS specimens that were intentionally roughened in a lathe, under controlled conditions, with 50-grit sandpaper to produce circumferential cracks with an average surface roughness of 1.2 μm.   The results are shown in Figs. 34a and b,
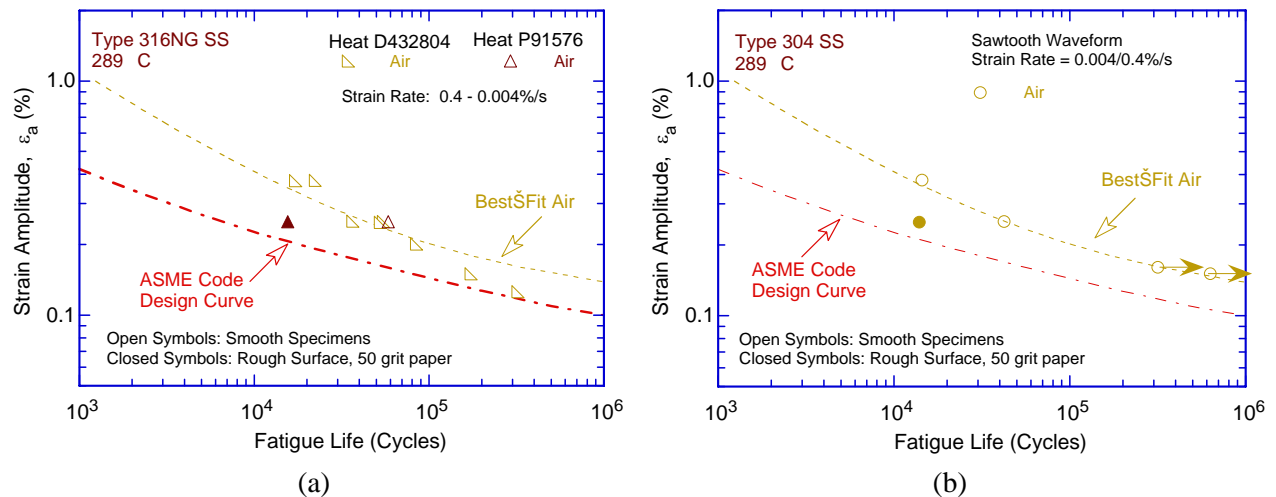
Figure 34.   Effect of surface roughness on fatigue life of (a) Type 316NG and (b) Type 304 SSs in air.

respectively, for Types 316NG and 304 SS. For both steels, the fatigue life of roughened specimens is a factor of ≈3 lower than that of the smooth specimens.

- *The effect of surface finish was not investigated in the mean data curve used to develop the Code fatigue design curves; it is included as part of the subfactor that is applied to the mean data curve to account for "surface finish and environment."*

5.1.6   Heat-to-Heat Variability

The effects of material variability and data scatter must be included to ensure that the design curves not only describe the available test data well, but also adequately describe the fatigue lives of the much larger number of heats of material that are found in the field. As mentioned earlier for carbon and low-alloy steels, material variability and data scatter in the fatigue ε-N data for austenitic SSs are also evaluated by considering the best–fit curves determined from tests on individual heats of materials or loading conditions as samples of the much larger population of heats of materials and service conditions of interest. The fatigue behavior of each of the heats or loading conditions is characterized by the value of the constant A in Eq. 6. The values of A for the various data sets were ordered, and median ranks were used to estimate the cumulative distribution of A for the population. The distributions were fit to lognormal curves. Results for various austenitic SSs in air are shown in Fig. 35. The median value of the constant A is 6.891 for the fatigue life of austenitic SSs in air at temperatures not exceeding 400°C. The values of A that describe the 5th percentile of these distributions give a fatigue ε–N curve that is expected to bound the lives of 95% of the heats of austenitic SSs. A Monte Carlo analysis was performed to address the uncertainties in the median value and standard deviation of the sample used for the analysis.

For austenitic SSs, the values for A that provide bounds for the portion of the population and the confidence that is desired in the estimates of the bounds are summarized in Table 8. From Fig. 35, the median value of A for the sample is 6.891. From Table 8, the 95/95 value of the margin to account for material variability and data scatter is 2.3 on life for austenitic SSs. This margin is needed to provide
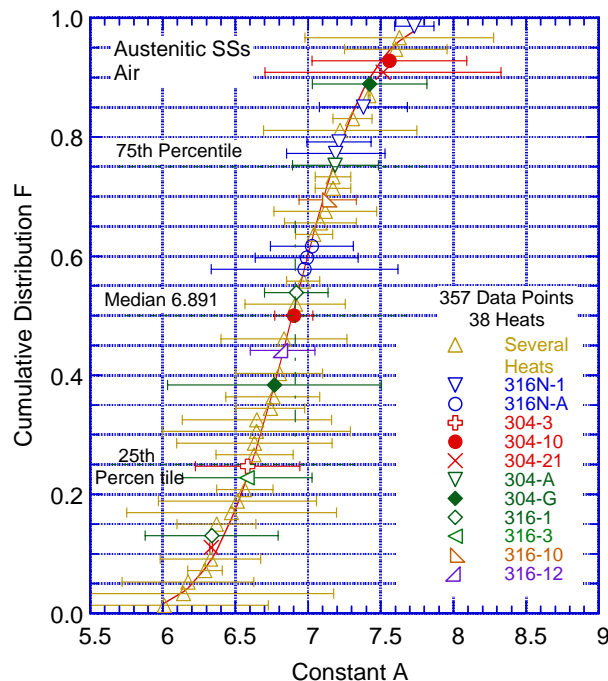
Figure 35.

Estimated cumulative distribution of constant A in statistical model for fatigue life for heats of austenitic SS in air.

45

Table 8. Values of parameter A in statistical model and the margins on life for austenitic SSs in air as a function of confidence level and percentage of population bounded.

Confidence Level	Percentage of Population Bounded (Percentile Distribution of A)				
	95 (5)	90 (10)	75 (25)	67 (33)	50 (50)
	Values of Parameter A				
50	6.205	6.356	6.609	6.707	6.891
75	6.152	6.309	6.569	6.668	6.851
95	6.075	6.241	6.510	6.611	6.793
	Margins on Life				
50	2.0	1.7	1.3	1.2	1.0
75	2.1	1.8	1.4	1.2	1.0
95	2.3	1.9	1.5	1.3	1.1

reasonable confidence that the resultant life will be greater than that observed for 95% of the materials of interest.

- *The mean data curve used to develop the Code fatigue design curves represents the average behavior; heat-to-heat variability is included in the subfactor that is applied to the mean data curve to account for "data scatter and material variability."*

5.1.7 Statistical Model

Statistical models based on the existing fatigue ε–N data have been developed at ANL for estimating the fatigue lives of wrought and cast austenitic SSs in air (NUREG/CR–5704, 6815, and 6878);[37–39] in these earlier reports, separate models were presented for Type 304 or 316 SS and Type 316NG SS. In the present report, the existing data were reanalyzed to develop a single model for the fatigue ε–N behavior of austenitic SSs. The model assumes that the fatigue life in air is independent of temperature and strain rate. Also, to be consistent with the models proposed by Tsutsumi et al.[28] and Jaske and O'Donnell,[70] the value of the constant C in the modified Langer equation (Eq. 6) was lower than that in earlier reports (i.e., 0.112 instead of 0.126). In air, at temperatures up to 400°C, the fatigue data for Types 304, 304L, 316, 316L, and 316NG SS are best represented by the equation:

$$\ln(N) = 6.891 - 1.920 \ln(\varepsilon_a - 0.112) \tag{30}$$

where ε_a is applied strain amplitude (%). The experimental values of fatigue life and those predicted by Eq. 30 for austenitic SSs in air are plotted in Fig. 36. The predicted lives show good agreement with the experimental values; for most tests the difference between the experimental and predicted values is within a factor of 3, and for some, the observed fatigue lives are significantly longer than the predicted values.

- *The statistical models represent mean values of fatigue life. The effects of parameters such as mean stress, surface finish, size and geometry, and loading history, which are known to influence fatigue life, are not explicitly considered in the model; such effects are accounted for in the factors of 20 on life and 2 on stress that are applied to the mean data curve to obtain the Code fatigue design curve.*
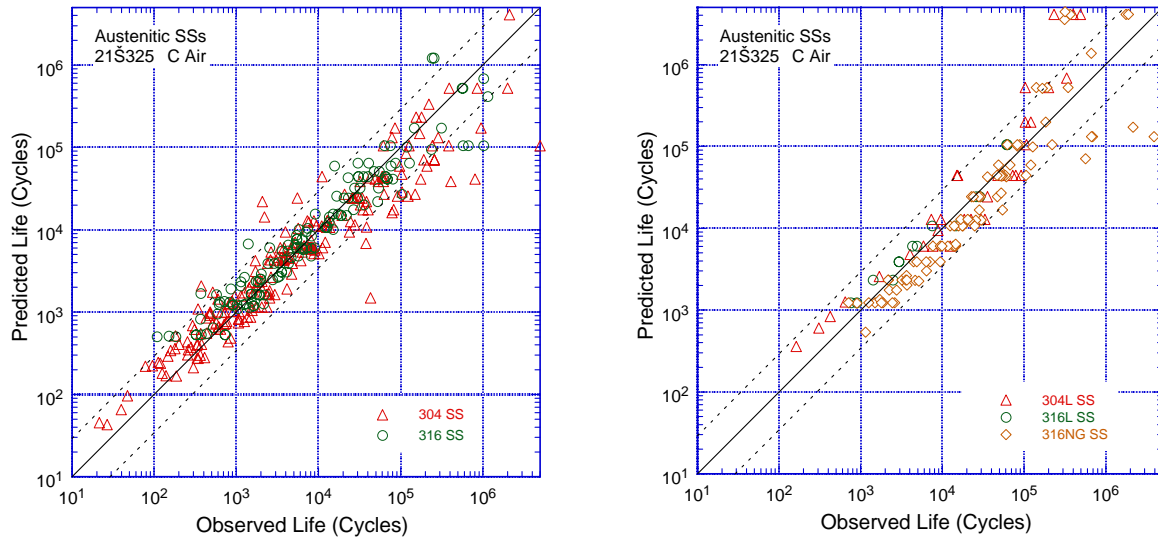
Figure 36. Experimental and predicted fatigue lives of austenitic SSs in air.

5.1.8 New Fatigue Design Curve

As discussed in Section 5.1.1, the current Code mean–data curve that was used to develop the Code fatigue design curve, is not consistent with the existing fatigue ε–N data. A fatigue design curve that is consistent with the existing database may be obtained from the ANL statistical model (Eq. 30) by following the same procedure that was used to develop the current ASME Code fatigue design curve. However, the discussions presented later in Section 6.5 indicate that the current Code requirement of a factor of 20 on cycles, to account for the effects of material variability and data scatter, specimen size, surface finish, and loading history, is conservative by at least a factor of 1.7. Thus, to reduce this conservatism, fatigue design curve based on the ANL model for austenitic SSs (Eq. 30) may be developed by first correcting for mean stress effects using the modified Goodman relationship and then lowering the mean–stress–adjusted curve by a factor of 2 on stress or 20 on cycles, whichever is more conservative. This curve and the current Code design curve are shown in Fig. 37; values of stress amplitude vs. cycles for the current and the proposed design curves are given in Table 9. A fatigue design curve that is consistent with the existing fatigue ε–N data but is not based on the ANL statistical model (Eq. 30) has also been proposed by the ASME Subgroup on Fatigue Strength.[83]

Table 9. The proposed and current Code fatigue design curves for austenitic stainless steels in air.

| | Stress Amplitude (MPa/ksi) | | | Stress Amplitude (MPa/ksi) | |
Cycles	Proposed Design Curve	Current Design Curve	Cycles	Proposed Design Curve	Current Design Curve
1 E+01	6000 (870)	4881 (708)	2 E+05	168 (24.4)	248 (35.9)
2 E+01	4300 (624)	3530 (512)	5 E+05	142 (20.6)	214 (31.0)
5 E+01	2748 (399)	2379 (345)	1 E+06	126 (18.3)	195 (28.3)
1 E+02	1978 (287)	1800 (261)	2 E+06	113 (16.4)	157 (22.8)
2 E+02	1440 (209)	1386 (201)	5 E+06	102 (14.8)	127 (18.4)
5 E+02	974 (141)	1020 (148)	1 E+07	99 (14.4)	113 (16.4)
1 E+03	745 (108)	820 (119)	2 E+07		105 (15.2)
2 E+03	590 (85.6)	669 (97.0)	5 E+07		98.6 (14.3)
5 E+03	450 (65.3)	524 (76.0)	1 E+08	97.1 (14.1)	97.1 (14.1)
1 E+04	368 (53.4)	441 (64.0)	1 E+09	95.8 (13.9)	95.8 (13.9)
2 E+04	300 (43.5)	383 (55.5)	1 E+10	94.4 (13.7)	94.4 (13.7)
5 E+04	235 (34.1)	319 (46.3)	1 E+11	93.7 (13.6)	93.7 (13.6)
1 E+05	196 (28.4)	281 (40.8)	2 E+10		
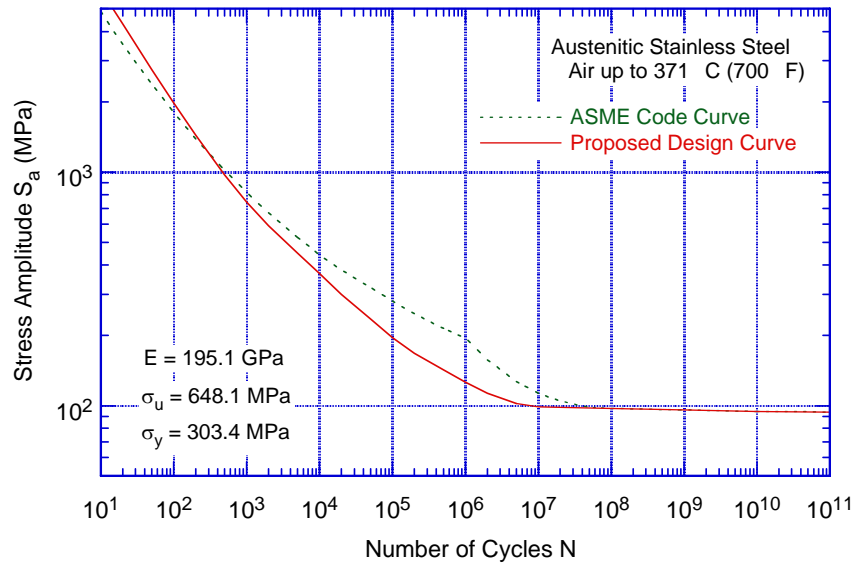
Figure 37.   Fatigue design curve for austenitic stainless steels in air.

The proposed curve extends up to 10^{11} cycles; the two curves are the same beyond 10^8 cycles. Although the curve is based primarily on data for Types 304 and 316 SS, it may be used for wrought Types 304, 310, 316, 347, and 348 SS, and cast CF-3, CF-8, and CF-8M SS for temperatures not exceeding 371°C (700°F). Because the fatigue life of Type 316NG SS is superior to that of Type 304 or 316 SS, the design curve may be somewhat conservative for Type 316NG SSs.

• *The current Code fatigue design curve for austenitic stainless steels is nonconservative with respect to the existing fatigue ε-N data for fatigue lives in the range of 10^3 to 5 x 10^6 cycles. A new design curve, that is consistent with the existing data, has been developed. To reduce the conservatism in the current Code requirement of 20 on life, the new curve was obtained by using factors of 12 on life and 2 on stress.*

5.2   LWR Environment

5.2.1   Experimental Data

The fatigue lives of austenitic SSs are decreased in LWR environments; the fatigue ε-N data for Types 304 and 316NG SS in water at 288°C are shown in Fig. 38. The ε–N curves based on the ANL statistical model (Eq. 30 in Section 5.1.7 and Eq. 32 in Section 5.2.13) are also included in the figures. The fatigue life is decreased significantly when three threshold conditions are satisfied simultaneously, viz., applied strain range and service temperature are above a minimum threshold level, and the loading strain rate is below a threshold value. The DO level in the water and, possibly, the composition and heat treatment of the steel are also important parameters for environmental effects on fatigue life. For some steels, fatigue life is longer in high-DO water than in low-DO PWR environments. Although, in air, the fatigue life of Type 316NG SS is slightly longer than that of Types 304 and 316 SS, the effects of LWR environments are comparable for wrought Types 304, 316, and 316NG. Also, limited data indicate that the fatigue life of cast austenitic SSs in both low-DO and high-DO environments are comparable to that of wrought SSs in low-DO environment.

The existing fatigue data indicate that a slow strain rate applied during the tensile–loading cycle (i.e., up–ramp with increasing strain) is primarily responsible for the environmentally assisted reduction in fatigue life. Slow rates applied during both tensile– and compressive–loading cycles (i.e., up– and
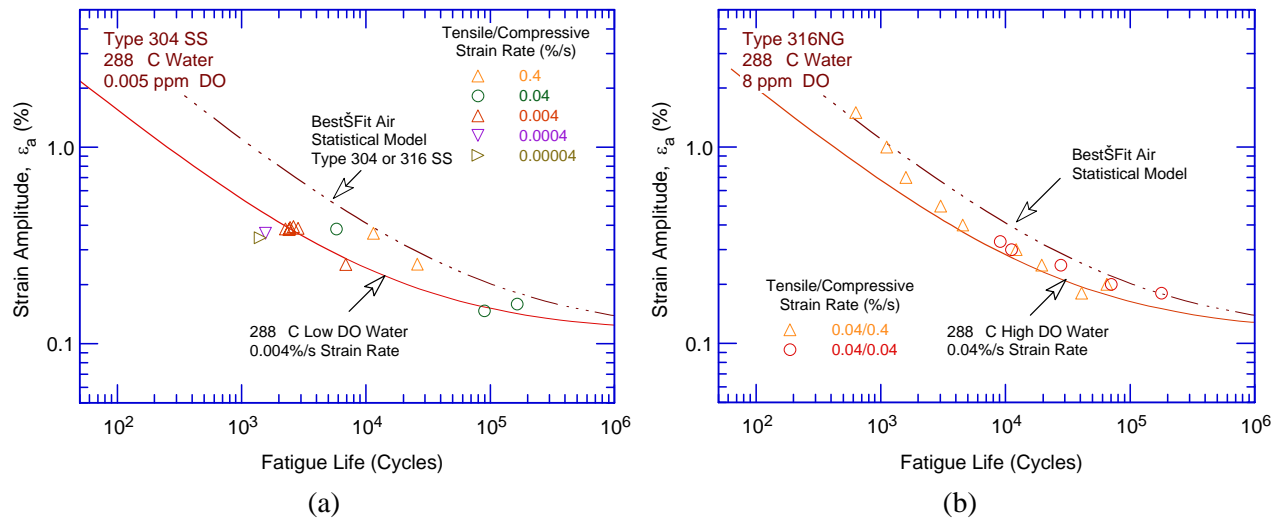
Figure 38. Strain amplitude vs. fatigue life data for (a) Type 304 and (b) Type 316NG SS in water at 288°C (JNUFAD and Refs. 7,37).

down–ramps) do not further decrease fatigue life compared with that observed for tests with only a slow tensile–loading cycle (Fig. 38b). Consequently, loading and environmental conditions during the tensile–loading cycle (strain rate, temperature, and DO level) are important for environmentally assisted reduction of the fatigue lives of these steels.

For austenitic SSs, lower fatigue lives in low–DO water than in high–DO water are difficult to reconcile in terms of the slip oxidation/dissolution mechanism; which assumes that crack growth rates increase with increasing DO in the water. The characteristics of the surface oxide films that form on austenitic SSs in LWR coolant environments can influence the mechanism and kinetics of corrosion processes and thereby influence the initiation stage, i.e., the growth of MSCs. Also, the reduction of fatigue life in high–temperature water has often been attributed to the presence of surface micropits that may act as stress raisers and provide preferred sites for the formation of fatigue cracks. Photomicrographs of the gauge surfaces of Type 316NG specimens tested in simulated PWR water and high–DO water are shown in Fig. 39. Austenitic SSs exposed to LWR environments develop an oxide film that consists of two layers: a fine–grained, tightly–adherent, chromium–rich inner layer, and a
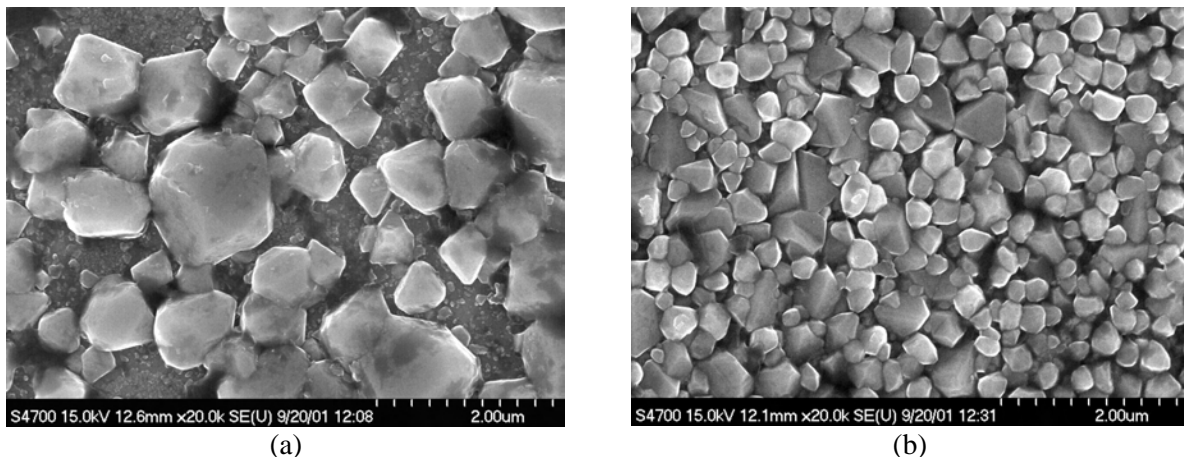
Figure 39. Higher–magnification photomicrographs of oxide films that formed on Type 316NG stainless steel in (a) simulated PWR water and (b) high–DO water.

49
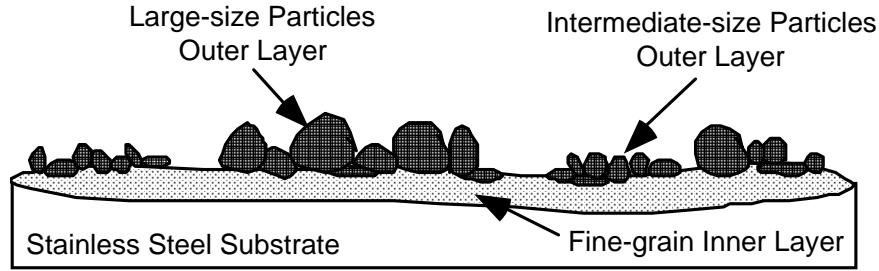
Figure 40. Schematic of the corrosion oxide film formed on austenitic stainless steels in LWR environments.

crystalline, nickel–rich outer layer composed of large and intermediate–size particles. The inner layer forms by solid–state growth, whereas the crystalline outer layer forms by precipitation or deposition from the solution. A schematic representation of the surface oxide film is shown in Fig. 40. The structure and composition of the inner and outer layers and their variation with the water chemistry have been identified.[106,107]

Experimental data indicate that surface micropits or minor differences in the composition or structure of the surface oxide film have no effect on the formation of fatigue cracks. Fatigue tests were conducted on Type 316NG (Heat P91576) specimens that were preexposed to either low–DO or high–DO water and then tested in air or water environments. The results of these tests, as well as data obtained earlier on this heat and Heat D432804 of Type 316NG SS in air and low–DO water at 288°C, are plotted in Fig. 41. The fatigue life of a specimen preoxidized in high–DO water and then tested in low–DO water is identical to that of specimens tested without preoxidation. Also, fatigue lives of specimens preoxidized at 288°C in low–DO water and then tested in air are identical to those of unoxidized specimens (Fig. 41). If micropits were responsible for the reduction in life, the preexposed specimens should show a decrease in life. Also, the fatigue limit of these steels should be lower in water than in air, but the data indicate this limit is the same in water and air environments. Metallographic examination of the test specimens indicated that environmentally assisted reduction in fatigue lives of austenitic SSs most likely is not caused by slip oxidation/dissolution but some other process, such as hydrogen–induced cracking.[7,35,36]

- *A LWR environment has a significant effect on the fatigue life of austenitic SSs; such effects are not considered in the current Code design curve. Environmental effects may be incorporated into the Code*
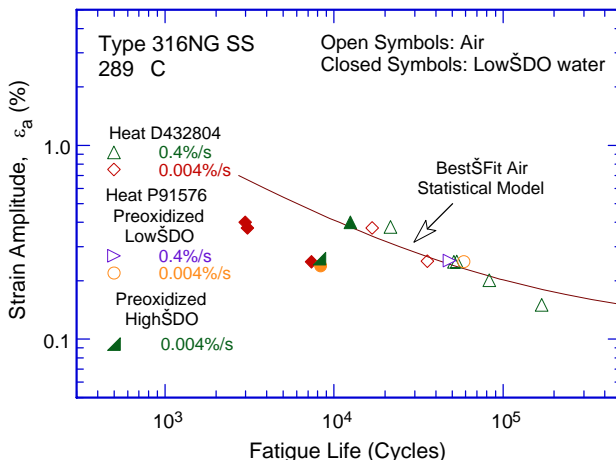
Figure 41.
Effects of environment on formation of fatigue cracks in Type 316NG SS in air and low–DO water at 288°C. Preoxidized specimens were exposed for 10 days at 288°C in water that contained either <5 ppb DO and ≈23 cm^3/kg dissolved H_2 or ≈500 ppb DO and no dissolved H_2 (Ref. 7).

fatigue evaluation using the F_{en} approach described in Section 5.2.14.

5.2.2   Strain Amplitude

As in the case of the carbon and low–alloy steels, a minimum threshold strain is required for the environmentally induced decrease in fatigue lives of SS to occur. Exploratory fatigue tests have also been conducted on austenitic SSs to determine the threshold strain beyond which environmental effects are significant during a fatigue cycle.[24,29] The tests were performed with waveforms in which the slow strain rate is applied during only a fraction of the tensile loading cycle. The results indicate that a minimum threshold strain is required for an environmentally assisted decrease in the fatigue lives of SSs (Fig. 42). The threshold strain $\Delta\varepsilon_{th}$ appears to be independent of material type (weld or base metal) and temperature in the range of 250–325°C, but it tends to decrease as the strain amplitude is decreased.[24,29] The threshold strain may be expressed in terms of the applied strain range $\Delta\varepsilon$ by the equation

$$\Delta\varepsilon_{th}/\Delta\varepsilon = -0.22\,\Delta\varepsilon + 0.65. \tag{31}$$

The results suggest that $\Delta\varepsilon_{th}$ is related to the elastic strain range of the test and does not correspond to the strain at which the crack closes.
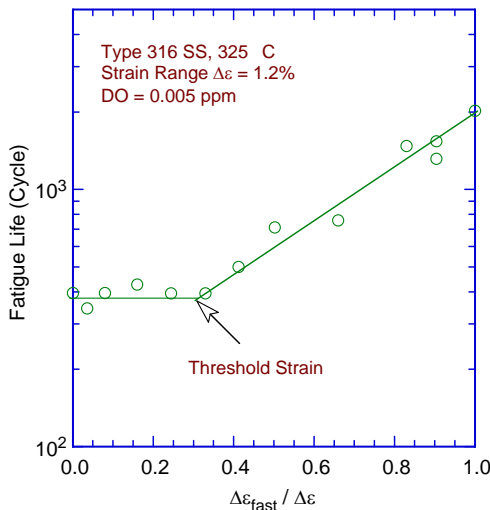
Figure 42.
Results of strain rate change tests on Type 316 SS in low–DO water at 325°C. Low strain rate was applied during only a fraction of tensile loading cycle. Fatigue life is plotted as a function of fraction of strain at high strain rate (Refs. 24,29).

- *In LWR environments, the procedure for calculating F_{en}, defined in Eq. 36 (Section 5.2.14), includes a threshold strain below which LWR coolant environments have no effect on fatigue life, i.e., $F_{en} = 1$. However, a threshold strain should not be considered when the damage rate approach is used to determine F_{en} for a stress cycle or load set pair.*

5.2.3   Hold-Time Effects

Environmental effects on fatigue life occur primarily during the tensile–loading cycle and at strain levels greater than the threshold value. Information on the effect of hold periods on the fatigue life of austenitic SSs in water is very limited. In high–DO water, the fatigue lives of Type 304 SS tested with a trapezoidal waveform (i.e., hold periods at peak tensile and compressive strain)[8] are comparable to those tested with a triangular waveform,[25] as shown in Fig. 43. As discussed in Section 4.2.8, a similar behavior has been observed for carbon and low–alloy steels: the data show little or no effect of hold periods on fatigue lives of the steels in high–DO water.

51
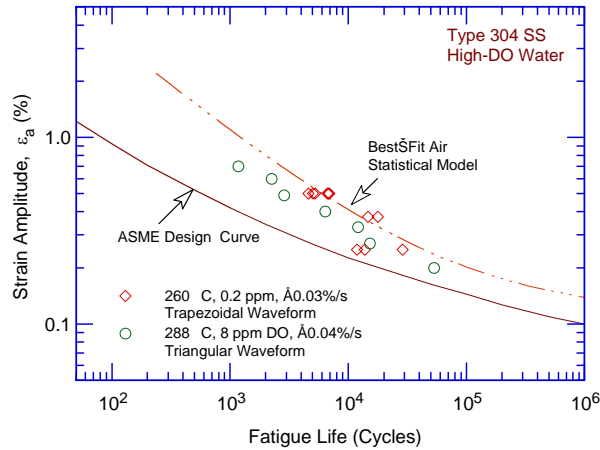
Figure 43.
Fatigue life of Type 304 stainless steel tested in high–DO water at 260–288°C with trapezoidal or triangular waveform (Refs. 8,25).

• *The existing data do not demonstrate that hold periods at peak tensile strain affect the fatigue life of austenitic SSs in LWR environments. Thus, any revision/modification of the method to determine F_{en} is not warranted.*

5.2.4   Strain Rate

The fatigue life of Types 304L and 316 SSs in low-DO water is plotted as a function of tensile strain rate in Fig. 44. In low–DO PWR environment, the fatigue life of austenitic SSs decreases with decreasing strain rate below ≈0.4%/s; the effect of environment on fatigue life saturates at ≈0.0004%/s (Fig. 44).[7,18,21-25,28,29,37-39] Only a moderate decrease in life is observed at strain rates greater than 0.4%/s. A decrease in strain rate from 0.4 to 0.0004%/s decreases the fatigue life by a factor of ≈10.
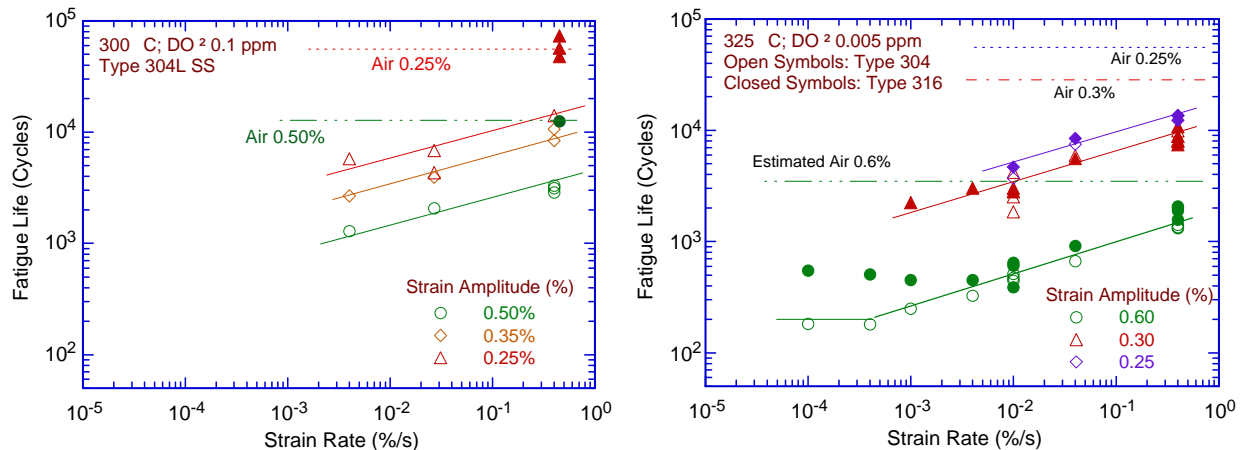
Figure 44.   Dependence of fatigue lives of austenitic stainless steels on strain rate in low–DO water (Refs. 7,37,39,69).

In high-DO water, the effect of strain rate may be less pronounced than in low–DO water (Fig. 45). For example, for Heat 30956 of Type 304 SS, strain rate has no effect on fatigue life in high–DO water, whereas life decreases linearly with strain rate in low–DO water (Fig. 45a). For Heat D432804 of Type 316NG, some effect of strain rate is observed in high–DO water, although it is smaller than that in low–DO water (Fig. 45b).
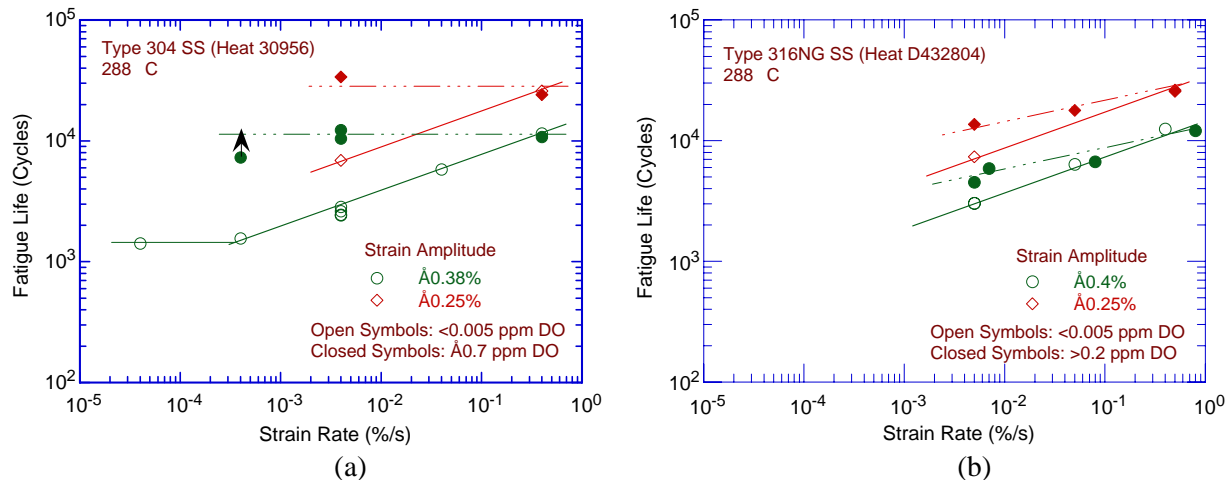
Figure 45. Dependence of fatigue life of Types (a) 304 and (b) 316NG stainless steel on strain rate in high– and low–DO water at 288°C (Ref. 7,37,39).

- *In LWR environments, the effect of strain rate on the fatigue life of austenitic SSs is explicitly considered in F_{en} defined in Eq. 36 (Section 5.2.14). Also, guidance is provided to define the strain rate to be used to calculate F_{en} for a specific stress cycle or load set pair.*

5.2.5 Dissolved Oxygen

In contrast to the behavior of carbon and low–alloy steels, the fatigue lives of austenitic SSs decrease significantly in low–DO (i.e., <0.05 ppm DO) water. In low–DO water, the fatigue life is not influenced by the composition or heat treatment condition of the steel. The fatigue life, however, continues to decrease with decreasing strain rate and increasing temperature.[7,18,23–25,28,29,37–39]

In high–DO water, the fatigue lives of austenitic SSs are either comparable to[23,28] or, in some cases, higher[7,37,39] than those in low–DO water, i.e., for some SSs, environmental effects may be lower in high–DO than in low–DO water. The results presented in Figs. 45a and 45b indicate that, in high–DO water, environmental effects on the fatigue lives of austenitic SSs are influenced by the composition and heat treatment of the steel. For example, for high–carbon Type 304 SS, environmental effects are insignificant for the mill–annealed (MA) material (Fig. 45a), whereas as discussed in Section 5.2.8, for sensitized material the effect of environment is the same in high– and low–DO water. For the low–C Type 316NG SS, some effect of strain rate is apparent in high–DO water, although it is smaller than that in low–DO water (Fig. 45b). The effect of material heat treatment on the fatigue life of Type 304 SS is discussed in Section 5.2.8; in high–DO water, material heat treatment affects the fatigue life of SSs.

- *In LWR environments, the effect of DO on the fatigue life of austenitic SSs is explicitly considered in F_{en}, defined in Eq. 36. Also, guidance is provided to define the DO content to be used to calculate F_{en} for a specific stress cycle or load set pair.*

5.2.6 Water Conductivity

The studies at ANL indicate that, for fatigue tests in high–DO water, the conductivity of water and the ECP of steel are important parameters that must be held constant.[7,37,39] During laboratory tests, the time to reach stable environmental conditions depends on the autoclave volume, DO level, flow rate, etc. In the ANL test facility, fatigue tests on austenitic SSs in high–DO water required a soaking period of

5–6 days for the ECP of the steel to stabilize. The steel ECP increased from zero or a negative value to above 150 mV during this period. The results shown in Fig. 45a for MA Heat 30956 of Type 304 SS in high–DO water (closed circles) were obtained for specimens that were soaked for 5–6 days before the test. The same material tested in high–DO water after soaking for only 24 h showed a significant reduction in fatigue life, as indicated by Fig. 46.

The effect of the conductivity of water and the ECP of the steel on the fatigue life of austenitic SSs is shown in Fig. 46. In high–DO water, fatigue life is decreased by a factor of ≈2 when the conductivity of water is increased from ≈0.07 to 0.4 µS/cm. Note that environmental effects appear more significant for the specimens that were soaked for only 24 h. For these tests, the ECP of steel was initially very low and increased during the test.
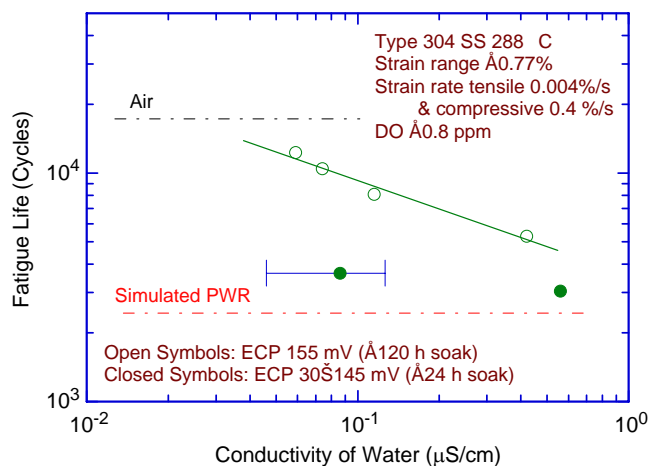
Figure 46.
Effects of conductivity of water and soaking period on fatigue life of Type 304 SS in high–DO water (Ref. 7,37).

• *Effects of water chemistry on fatigue life have not been considered in the determination of F_{en}. Additional guidance may be provided for excursions of off-normal water chemistry conditions.*

5.2.7   Temperature

The change in fatigue lives of austenitic SSs with test temperature at two strain amplitudes and two strain rates is shown in Fig. 47. The results suggest a threshold temperature of 150°C, above which the environment decreases fatigue life in low–DO water if the strain rate is below the threshold of 0.4%/s. In the range of 150–325°C, the logarithm of fatigue life decreases linearly with temperature. Only a moderate decrease in life occurs in water at temperatures below the threshold value of 150°C.

Fatigue tests have been conducted at MHI in Japan on Type 316 SS under combined mechanical and thermal cycling.[23] Triangular waveforms were used for both strain and temperature cycling. Two sequences were selected for temperature cycling: (i) an in–phase sequence, in which temperature cycling was synchronized with mechanical strain cycling, and (ii) a sequence in which temperature and strain were out of phase, i.e., maximum temperature occurred at minimum strain level and vice versa. Two temperature ranges, 100–325°C and 200–325°C, were selected for the tests. The results are shown in Fig. 48, along with data obtained from tests at constant temperature. An average temperature is used in Fig. 48 for the thermal cycling tests. Because environmental effects are considered to be moderate below threshold values of 150°C for temperature and ≈0.25% for strain range, the average temperature for the thermal cycling tests was determined from higher value between 150°C and temperature at threshold strain for in–phase tests, and the lower value between maximum temperature and temperature at threshold strain for out–of–phase tests.

54
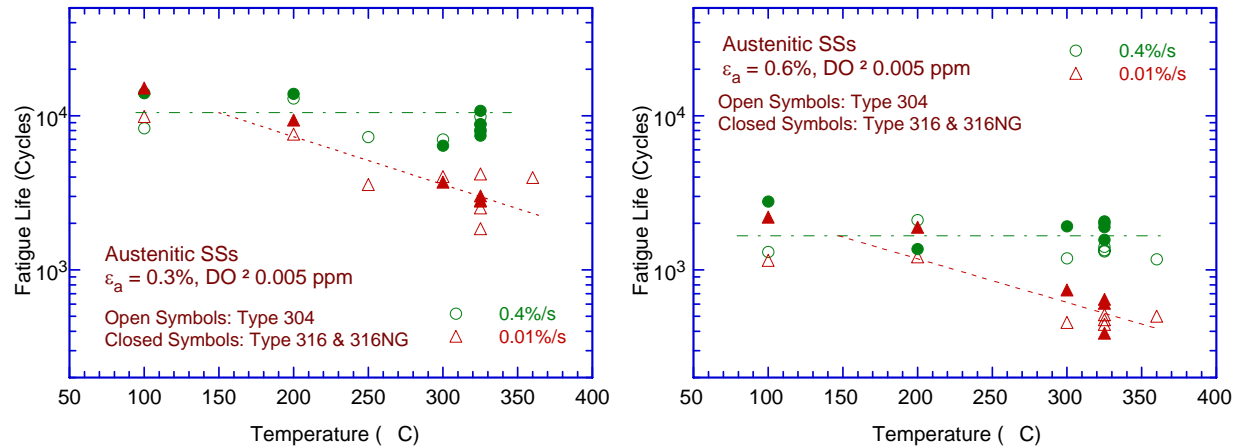
Figure 47. Change in fatigue lives of austenitic stainless steels in low–DO water with temperature (Refs. 7,23–25,28,37–39).

The results in Fig. 48 indicate that for load cycles involving variable temperature, average temperature gives the best estimate of fatigue life. Also, as expected, the fatigue lives of the in–phase tests are shorter than those for the out–of–phase tests. For the thermal cycling tests, fatigue life is longer for out–of–phase tests than for in–phase tests, because applied strains above the threshold strain occur at high temperatures for in–phase tests, whereas they occur at low temperatures for out–of–phase tests. The results from the thermal cycling tests (triangles) agree well with those from the constant–temperature tests (open circles).
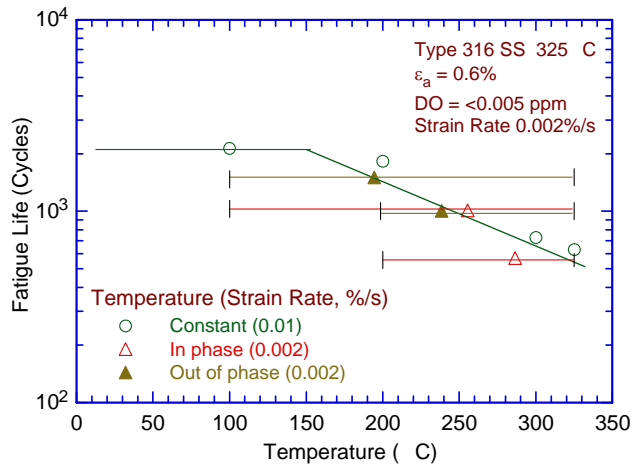
Figure 48.
Fatigue life of Type 316 stainless steel under constant and varying test temperature (Ref. 23).

Another study conducted by the Japan Nuclear Safety Organization on Type 316 SS under combined mechanical and thermal cycling in PWR water showed similar results, e.g., the in–phase tests had lower fatigue lives than the out–of–phase tests.[30,32] These results indicate that load cycles involving variable temperature conditions may be represented by an average temperature.

• *In LWR environments, the effect of temperature on the fatigue life of austenitic SSs is explicitly considered in F_{en}, defined in Eq. 36 (Section 5.2.14). Also, guidance is provided to define the temperature to be used to calculate F_{en} for a specific stress cycle or load set pair.*

55

5.2.8 Material Heat Treatment

Limited data indicate that, although heat treatment has little or no effect on the fatigue life of austenitic SSs in low–DO and air environments, in a high–DO environment, fatigue life may be longer for nonsensitized or slightly sensitized SS.[39] The effect of heat treatment on the fatigue life of Type 304 SS in air, BWR, and PWR environments is shown in Fig. 49. Fatigue life is plotted as a function of the EPR (electrochemical potentiodynamic reactivation) value for the various material conditions. The results indicate that heat treatment has little or no effect on the fatigue life of Type 304 SS in air and PWR environments. In a BWR environment, fatigue life is lower for the sensitized SSs; fatigue life decreases with increasing EPR value.
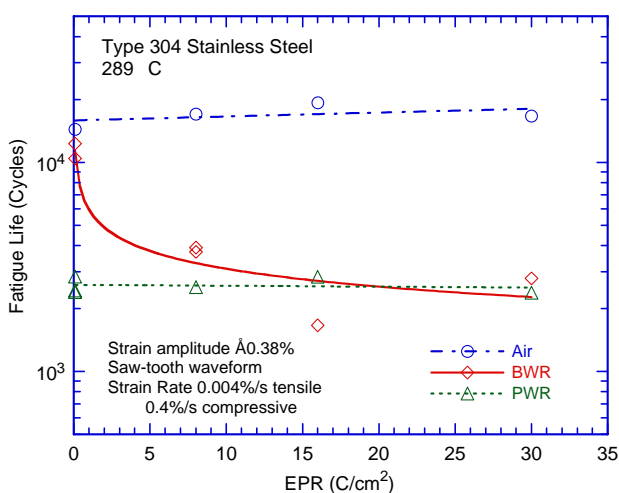
Figure 49.
The effect of material heat treatment on fatigue life of Type 304 stainless steel in air, BWR and PWR environments at 289°C, ≈0.38% strain amplitude, sawtooth waveform, and 0.004%/s tensile strain rate (Ref. 39).

These results are consistent with the data obtained at MHI on solution–annealed and sensitized Types 304 and 316 SS.[21,25] In low–DO (<0.005 ppm) water at 325°C, a sensitization annealing had no effect on the fatigue lives of these steels. In high–DO (8 ppm) water at 300°C, the fatigue life of sensitized Type 304 SS was a factor of ≈2 lower than that of the solution–annealed steel. However, a sensitization anneal had little or no effect on the fatigue life of low-C Type 316NG SS in high–DO water at 288°C, and the lives of solution–annealed and sensitized Type 316NG SS were comparable.

- *The effect of heat treatment is not considered in the environmental fatigue correction factor; estimates of F_{en} based on Eq. 36 (Section 5.2.14) may be conservative for some SSs in high–DO water.*

5.2.9 Flow Rate

It is generally recognized that flow rate most likely affects the fatigue life of LWR materials because it may cause differences in local environmental conditions in the enclaves of the microcracks formed during early stages in the fatigue ε–N test. As discussed in Section 4.2.9, data obtained under typical operating conditions for BWRs indicate that environmental effects on the fatigue life of carbon steels are a factor of ≈2 lower at high flow rates (7 m/s) than at low flow rates (0.3 m/s or lower).[19,20] However, similar tests in both low–DO and high–DO environments indicate that increasing flow rate has no effect or may have a detrimental effect on the fatigue life of austenitic SSs. Figure 50 shows the effect of water flow rate on the fatigue life of Types 316NG and 304 SSs in high-purity water at 289°C. Under all test conditions, the fatigue lives of these steels are slightly lower at high flow rates than those at lower rates or semi–stagnant conditions.
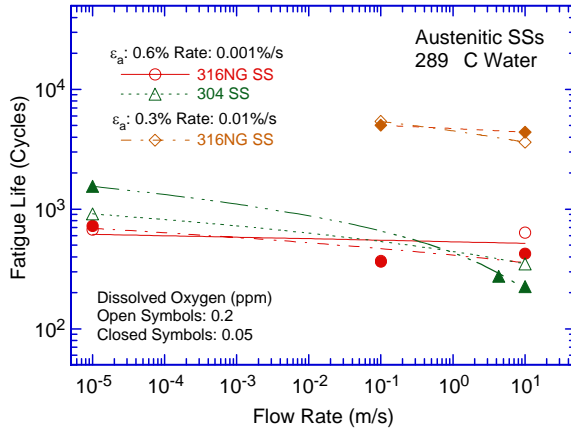
Figure 50.
Effect of water flow rate on the fatigue life of austenitic SSs in high-purity water at 289°C (Ref. 20).

Fatigue tests conducted on SS pipe bend specimens in simulated PWR primary water at 240°C also indicate that water flow rate has no effect on the fatigue life of austenitic SSs.[108] Increasing the flow rate from 0.005 m/s to 2.2 m/s had no effect on fatigue crack initiation in ≈26.5–mm diameter tube specimens. These results appear to be consistent with the notion that, in LWR environments, the mechanism of fatigue crack initiation in austenitic SSs may differ from that in carbon and low–alloy steels.

- *Because of the uncertainties in the flow conditions at or near the locations of crack initiation and the insignificant effect of flow rate, flow rate effects on the fatigue life of austenitic SSs in LWR environments are presently not considered in the fatigue evaluations.*

5.2.10 Surface Finish

Fatigue tests have been conducted on Types 304 and 316NG SS specimens that were intentionally roughened in a lathe, under controlled conditions, with 5-grit sandpaper to produce circumferential cracks with an average surface roughness of 1.2 μm. The results are shown in Figs. 51a and b, respectively, for Types 316NG and 304 SS. For both steels, the fatigue life of roughened specimens is lower than that of the smooth specimens in air and low–DO water environments. In high–DO water, the fatigue life of Heat P91576 of Type 316NG is the same for rough and smooth specimens.

(a)

(b)
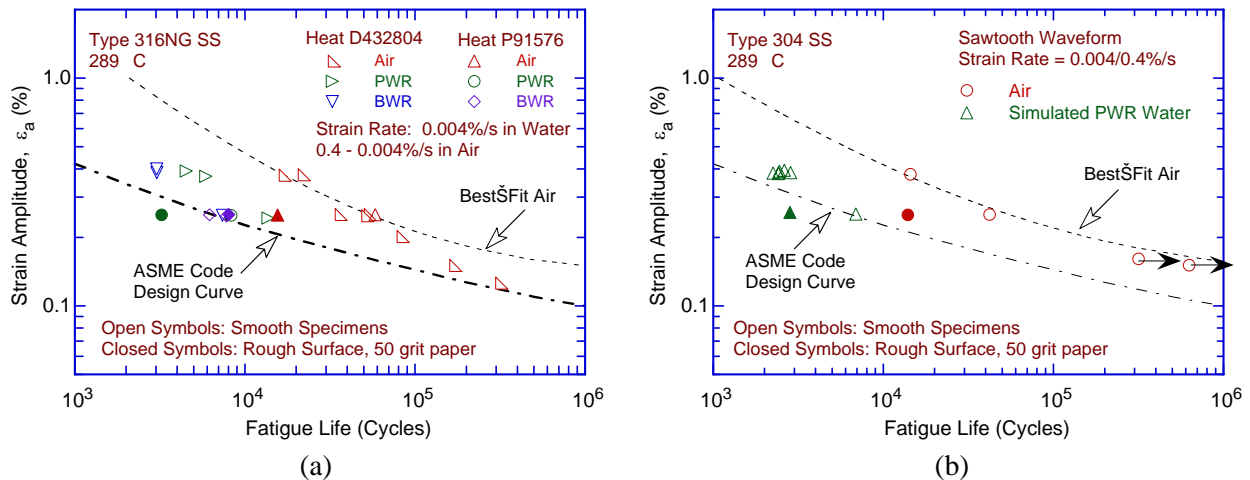
Figure 51. Effect of surface roughness on fatigue life of (a) Type 316NG and (b) Type 304 stainless steels in air and high–purity water at 289°C.

- *The effect of surface finish is not considered in the environmental fatigue correction factor; it is included in the subfactor for "surface finish and environment," which is applied to the mean data curve to develop the Code fatigue design curve in air.*

5.2.11 Heat-to-Heat Variability

The effect of material variability and data scatter on the fatigue life of austenitic SSs has been evaluated for the data in LWR environments. The fatigue behavior of each of the heats or loading conditions is characterized by the value of the constant A in the statistical models (e.g., Eq. 6). The values of A for the various data sets are ordered, and median ranks are used to estimate the cumulative distribution of A for the population. The results in water environments are shown in Fig. 52. The median value of A in water is 6.157. The results indicate that environmental effects are approximately the same for the various heats of these steels. For example, the cumulative distribution of data sets for specific heats is approximately the same in air and water environments. The statistical model seems to over–estimate the effect of environment for a few heats, e.g., the ranking for Type 304 SS heat 3 is ≈25 percentile in air (Fig. 35) and ≈85 percentile in water (Fig. 52).

The values for constant A that provide bounds for the portion of the population and the confidence that is desired in the estimates of the bounds for austenitic SSs in LWR environments are summarized in Table 10. In LWR environments, the 5th percentile value of Parameter A at a 95% confidence level is 5.401. Thus, for the median value of 6.157 for the sample (Table 10), the 95/95 value of the margin to account for material variability and data scatter is 2.3 on life. This margin is needed to provide 95% confidence that the resultant life will be greater than that observed for 95% of the materials of interest.

- *The heat-to-heat variability is included in the Code fatigue design curves as part of the subfactor that is applied to the room-temperature mean data curve to account for "data scatter and material variability."*
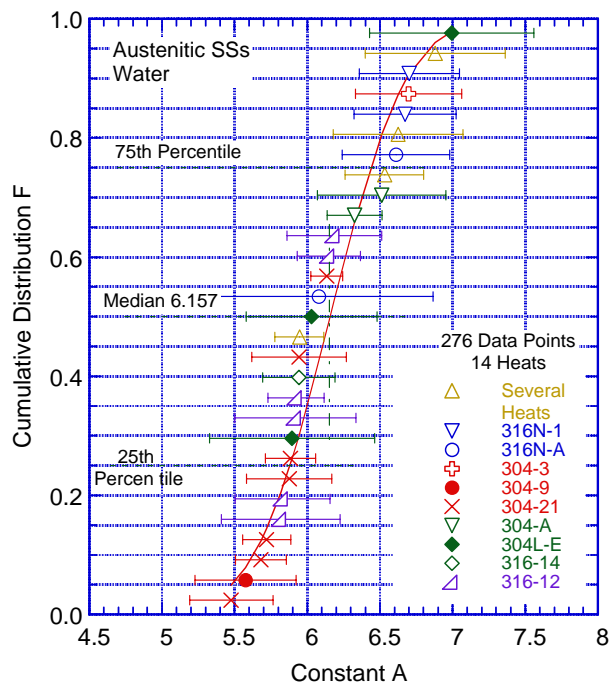
Figure 52.

Estimated cumulative distribution of constant A in statistical model for fatigue life for heats of austenitic SSs in water.

Table 10. Values of parameter A in statistical model and the margins on life for austenitic SSs in water as a function of confidence level and percentage of population bounded.

| Confidence | Percentage of Population Bounded (Percentile Distribution of A) | | | | |
Level	95 (5)	90 (10)	75 (25)	67 (33)	50 (50)
	Values of Parameter A				
50	5.481	5.630	5.880	5.976	6.157
75	5.414	5.570	5.828	5.925	6.104
95	5.317	5.483	5.752	5.851	6.028
	Margins on Life				
50	2.0	1.7	1.3	1.2	1.0
75	2.1	1.8	1.4	1.3	1.1
95	2.3	2.0	1.5	1.4	1.1

5.2.12 Cast Stainless Steels

Available fatigue ε–N data[23,28,36,37] indicate that, in air, the fatigue lives of cast CF–8 and CF–8M SSs are similar to that of wrought austenitic SSs. The fatigue lives of cast austenitic SSs also decrease in LWR coolant environments. Limited data suggest that the fatigue lives of cast SSs in high–DO water are approximately the same as those in low–DO water. In LWR environments the fatigue lives of cast SSs are comparable to those of wrought SSs in low–DO water. Also, the fatigue lives of these steels are relatively insensitive to changes in ferrite content in the range of 12–28%.[23,28] Also, existing data are inadequate to establish the dependence of fatigue life on temperature in LWR environments.

The effect of thermal aging at 250–400°C on the fracture toughness properties of cast SSs are well established, fracture toughness is decreased significantly after thermal aging because of the spinodal decomposition of the ferrite phase to form Cr–rich α' phase.[109,110] The cyclic–hardening behavior of cast austenitic SSs is also influenced by thermal aging.[37] At 288°C, cyclic stresses of cast SSs aged for 10,000 h at 400°C are higher than those for unaged material or wrought SSs. Also, strain rate effects on cyclic stress are greater for aged than for unaged steel, i.e., cyclic stresses increase significantly with decreasing strain rate. The existing data are too sparse to establish the effects of thermal aging on strain–rate effects on the fatigue life of cast SSs in air. Limited data in low–DO water at 288°C indicate that thermal aging for 10,000 h at 400°C decreases the fatigue life of CF–8M steels, Fig. 53b.[37] Note that thermal aging of another heat of CF–8M steel for 25,200 h at 465°C, Fig. 53a, had little or no effect on fatigue life. The different behavior for the two steels may be attributed to differences in the microstructure produced after thermal aging at 400°C as apposed to 465°C. Thermal aging at 400°C results in spinodal decomposition of the ferrite phase which strengthens the ferrite phase and increases cyclic hardening. Thermal aging at 465°C results in the nucleation and growth of large α' particles and other phases such as sigma phase, which do not change the tensile or cyclic hardening properties of the material.

The decrease in fatigue life with decreasing strain rate for three heats of CF–8M cast SS in low–DO water at 325 and 288°C is shown in Fig. 53; the effects of strain rate on the fatigue life of cast SSs are similar to those for wrought SSs. However, for a unaged heat of CF–8M steel with ≈20% ferrite, environmental effects on life do not appear to saturate even at strain rates as low as 0.00001%/s.[23,28] Similar results have also been reported for unaged CF–8M steels in low–DO water at 325°C.[111] Based on these results, the saturation strain rate of 0.0004%/s, recommended for wrought SSs (Eq. 34 in Section 5.2.13), has been decreased to 0.00004%/s for cast SS. However, thermal aging may have influenced the results at very low strain rates. All of the tests at low strain rates were obtained on unaged material; as discussed above, available data indicate that thermal aging decreases the fatigue life of CF–8M steel (Fig. 53b). Limited data indicate that the effects of strain rate are the same in low– and high–DO water.
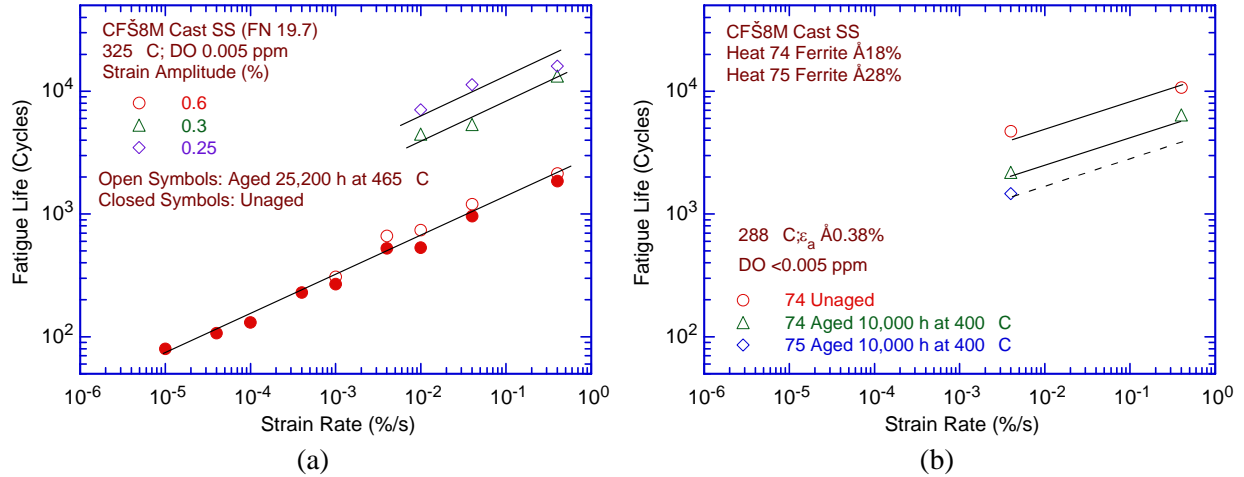
Figure 53. Dependence of fatigue lives of CF–8M cast SSs on strain rate in low–DO water at various strain amplitudes (Refs. 23,28,36,37).

Also, such low strain rates (i.e., less than 0.0004%/s) are not likely to occur in the field. In the present report the effects of strain rate and temperature on the fatigue life of cast austenitic SSs are assumed to be similar to those for wrought SSs.

The estimated cumulative distribution of constant A in statistical model for fatigue life for austenitic SSs, including several heats of cast SSs, in air and water environments are shown in Fig. 54. The results for cast SSs are evenly distributed and have insignificant effect on the median value of the constant A, e.g., the values with and without the cast SS data are 6.878 and 6.891, respectively, in air, and 6.147 and 6.157, respectively, in water. Thus, the statistical models for austenitic SSs adequately represent both wrought and cast SSs.
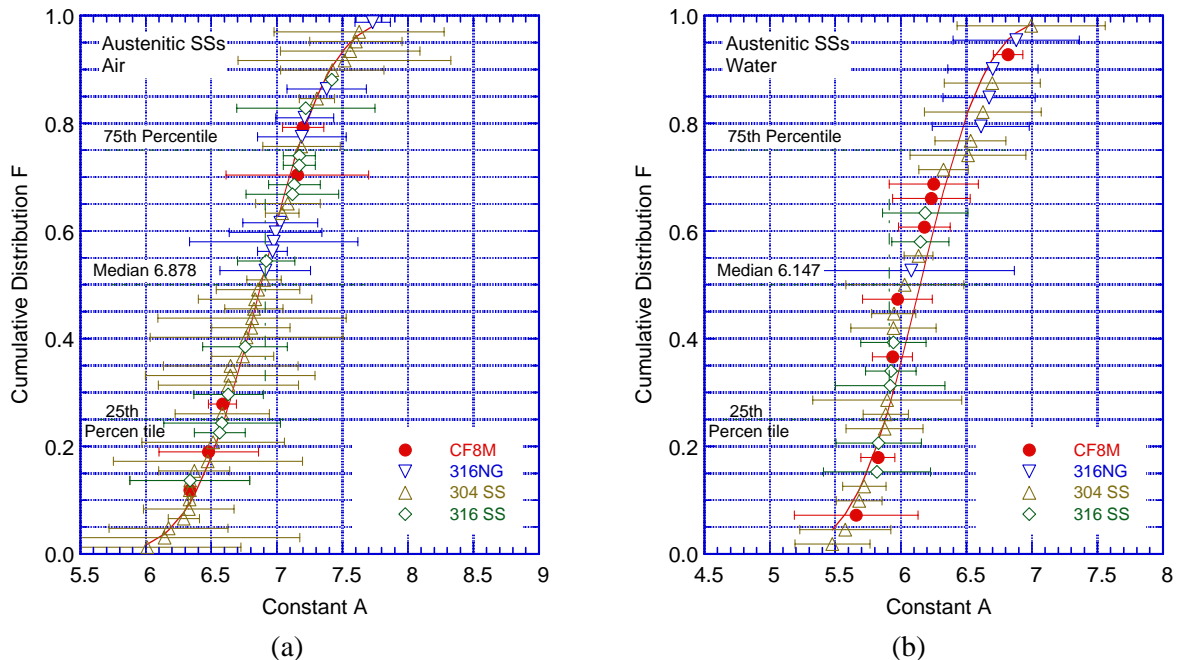
Figure 54. Estimated cumulative distribution of constant A in statistical models for fatigue life of wrought and cast austenitic stainless steels in (a) air and (b) water environments.

60

5.2.13 Statistical Model

In LWR environments, the fatigue life of austenitic SSs depends on strain rate, DO level, and temperature; the effects of these and other parameters on the fatigue life of austenitic SSs are discussed in detail below. The functional forms for the effects of strain rate and temperature are based on the data trends. For both wrought and cast austenitic SSs, the model assumes threshold and saturation values of 0.4 and 0.0004%/s, respectively, for strain rate and a threshold value of 150°C for temperature.

The influence of DO level on the fatigue life of austenitic SSs is not well understood. As discussed in Section 5.2.5, the fatigue lives of austenitic SSs are decreased significantly in low–DO water, whereas in high–DO water they are either comparable or, for some steels, higher than those in low–DO water. In high–DO water, the composition and heat treatment of the steel influence the magnitude of environmental effects on austenitic SSs. Until more data are available to clearly establish the effects of DO level on fatigue life, the effect of DO level on fatigue life is assumed to be the same in low– and high–DO water and for wrought and cast austenitic SSs.

The least–squares fit of the experimental data in water yields a steeper slope for the ε–N curve than the slope of the curve obtained in air.[37,76] These results indicate that environmental effect may be more pronounced at low than at high strain amplitudes. Differing slopes for the ε–N curves in air and water environments would add complexity to the determination of the environmental fatigue correction factor F_{en}, discussed in the next section. In the ANL statistical model, the slope of the ε–N curve is assumed to be the same in LWR and air environments. In LWR environments, fatigue data for austenitic SSs are best represented by the equation:

$$\ln(N) = 6.157 - 1.920 \ln(\varepsilon_a - 0.112) + T' \, \dot{\varepsilon}' \, O', \tag{32}$$

where T', $\dot{\varepsilon}'$, and O' are transformed temperature, strain rate, and DO, respectively, defined as follows:

$$
\begin{aligned}
T' &= 0 & &(T < 150°C) \\
T' &= (T - 150)/175 & &(150 \le T < 325°C) \\
T' &= 1 & &(T \ge 325°C)
\end{aligned} \tag{33}
$$

$$
\begin{aligned}
\dot{\varepsilon}' &= 0 & &(\dot{\varepsilon} > 0.4\%/s) \\
\dot{\varepsilon}' &= \ln(\dot{\varepsilon}/0.4) & &(0.0004 \le \dot{\varepsilon} \le 0.4\%/s) \\
\dot{\varepsilon}' &= \ln(0.0004/0.4) & &(\dot{\varepsilon} < 0.0004\%/s)
\end{aligned} \tag{34}
$$

$$O' = 0.281 \qquad\qquad \text{(all DO levels)}. \tag{35}$$

These models are recommended for predicted fatigue lives $\le 10^6$ cycles. Note that Eq. 32 is based on the updated ANL model for austenitic SSs in air (Eq. 30) and the analysis presented in Section 5.2.11. A single expression is used for Types 304, 304L, 316, 316L, and 316NG SSs, and constant A and slope B in the equation are different from the values reported earlier in NUREG/CR–5704, –6815, and –6878. Equations 32–35 can also be used for cast austenitic SSs such as CF-3, CF-8, and CF–8M. Also, because the influence of DO level on the fatigue life of austenitic SSs may be influenced by the material heat treatment, the statistical model may be somewhat conservative for some SSs in high–DO water.

The experimental values of fatigue life and those predicted by Eq. 32 for austenitic SSs in LWR environments are plotted in Fig. 55. The predicted fatigue lives show good agreement with the experimental values. The difference between the experimental and predicted values is within a factor of 3
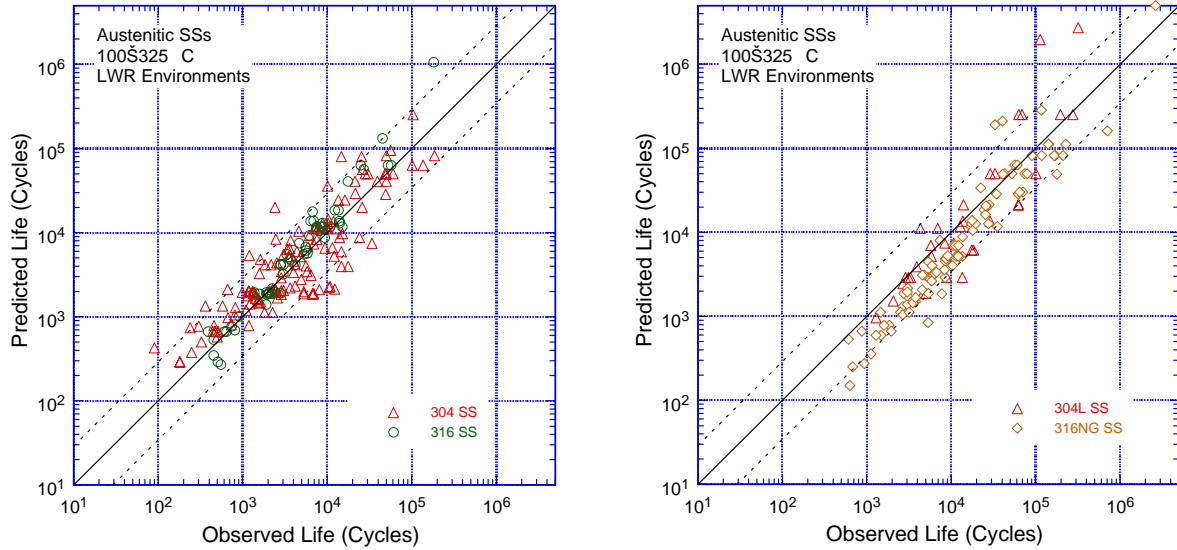
Figure 55.   Experimental and predicted values of fatigue lives of austenitic SSs in LWR environments.

for most tests; the experimental fatigue lives of a few tests on Type 304 SS are up to a factor of ≈4 lower than the predicted values, all of these tests were on tube specimens with 1– or 3–mm wall thickness.

• *The statistical models represent the mean values of fatigue life as a function of applied strain amplitude, temperature, strain rate, and DO level in water. The effects of parameters such as mean stress, surface finish, size and geometry, and loading history, which are known to influence fatigue life, are not included in the model.*

5.2.14 Environmental Correction Factor

The effects of reactor coolant environments on fatigue life have also been expressed in terms of a fatigue life correction factor F_{en}, which is defined as the ratio of life in air at room temperature to that in water at the service temperature. The fatigue life correction factor for austenitic SSs, based on the ANL model, is given by

$$F_{en} = \exp(0.734 - T' \, \varepsilon' \, O'), \tag{36}$$

where the constants T', ε', and O' are defined in Eqs. 33–35. Note that because the ANL statistical model for austenitic SSs has been updated in the present report, the constant 0.734 in Eq. 36 is different from the values reported earlier in NUREG/CR–5704, 6815, and 6878. Relative to the earlier expressions, correction factors determined from Eq. 36 are 45–60% lower. A strain threshold is also defined, below which LWR coolant environments have no effect on fatigue life, i.e., $F_{en} = 1$. The strain threshold is 0.10% (195 MPa stress amplitude) for austenitic SSs. To incorporate environmental effects into a Section III fatigue evaluation, the fatigue usage for a specific stress cycle, based on the proposed new fatigue design curve (Fig. 37 and Table 9 in Section 5.1.8), is multiplied by the correction factor. Further details for incorporating environmental effects into fatigue evaluations are presented in Appendix A.

• *The F_{en} approach may be used to incorporate environmental effects into the Code fatigue evaluations.*

6   Margins in ASME Code Fatigue Design Curves

Conservatism in the ASME Code fatigue evaluations may arise from (a) the fatigue evaluation procedures and/or (b) the fatigue design curves. The overall conservatism in ASME Code fatigue evaluations has been demonstrated in fatigue tests on components. [112,113] Mayfield et al.[112] have shown that, in air, the margins on the number of cycles to failure for elbows and tees were 40–310 and 104–510, respectively, for austenitic SS and 118–2500 and 123–1700, respectively, for carbon steel. The margins for girth butt welds were significantly lower, 6–77 for SS and 14–128 for carbon steel. Data obtained by Heald and Kiss[113] on 26 piping components at room temperature and 288°C showed that the design margin for cracking exceeds 20, and for most of the components, it is >100. In these tests, fatigue life was expressed as the number of cycles for the crack to penetrate through the wall, which ranged in thickness from 6 to 18 mm. Consequently, depending on wall thickness, the actual margins to form a 3–mm crack may be lower by a factor of more than 2.

Deardorff and Smith[114] discussed the types and extent of conservatism present in the ASME Section III fatigue evaluation procedures and the effects of LWR environments on fatigue margins. The sources of conservatism in the procedures include the use of design transients that are significantly more severe than those experienced in service, conservative grouping of transients, and use of simplified elastic–plastic analyses that lead to higher stresses. The authors estimated that the ratio of the CUFs computed with the mean experimental curve for test specimen data in air and more accurate values of the stress to the CUFs computed with the Code fatigue design curve were ≈60 and 90, respectively, for PWR and BWR nozzles. The reductions in these margins due to environmental effects were estimated to be factors of 5.2 and 4.6 for PWR and BWR nozzles, respectively. Thus, Deardorff and Smith[114] argue that, after accounting for environmental effects, factors of 12 and 20 on life for PWR and BWR nozzles, respectively, account for uncertainties due to material variability, surface finish, size, mean stress, and loading sequence.

However, other studies on piping and components indicate that the Code fatigue design procedures do not always ensure large margins of safety.[115,116] Southwest Research Institute performed fatigue tests in room–temperature water on 0.91–m–diameter carbon and low–alloy steel vessels.[115] In the low–cycle regime, ≈5–mm–deep cracks were initiated slightly above (a factor of <2) the number of cycles predicted by the ASME Code design curve (Fig. 56a). Battelle–Columbus conducted tests on 203–mm or 914–mm carbon steel pipe welds at room temperature in an inert environment, and Oak Ridge National Laboratory (ORNL) performed four–point bend tests on 406–mm–diameter Type 304 SS pipe removed from the C–reactor at the Savannah River site.[116] The results showed that the number of cycles to produce a leak was lower, and in some cases significantly lower, than that expected from the ASME Code fatigue design curves (Fig. 56a and b). The most striking results are for the ORNL "tie–in" and flawed "test" weld; these specimens cracked completely through the 12.7–mm–thick wall in a life 6 or 7 times shorter than expected from the Code curve. Note that the Battelle and ORNL results represent a through–wall crack; the number of cycles to initiate a 3–mm crack may be a factor of 2 lower.

Much of the margin in the current evaluations arises from design procedures (e.g., stress analysis rules and cycle counting) that, as discussed by Deardorff and Smith,[114] are quite conservative. However, the ASME Code permits new and improved approaches to fatigue evaluations (e.g., finite–element analyses, fatigue monitoring, and improved K_e factors) that can significantly decrease the conservatism in the current fatigue evaluation procedures.
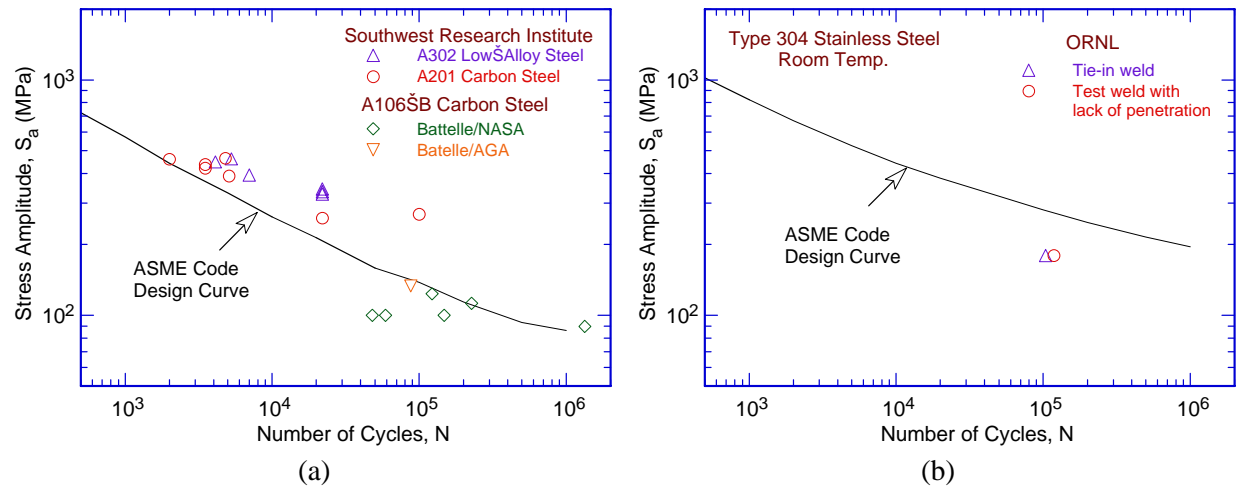
Figure 56.   Fatigue data for (a) carbon and low–alloy steel and (b) Type 304 stainless steel components (Refs. 115,116).

The factors of 2 on stress and 20 on cycles used in the Code were intended to cover the effects of variables that can influence fatigue life but were not investigated in the tests that provided the data for the curves. It is not clear whether the particular values of 2 and 20 include possible conservatism. A study sponsored by the PVRC to assess the margins of 2 and 20 in fatigue design curves concluded that these margins should not be changed.[117]

The variables that can affect fatigue life in air and LWR environments can be broadly classified into three groups:

(a)   Material
    (i)   Composition
    (ii)   Metallurgy: grain size, inclusions, orientation within a forging or plate
    (iii)   Processing: cold work, heat treatment
    (iv)   Size and geometry
    (v)   Surface finish: fabrication surface condition
    (vi)   Surface preparation: surface work hardening

(b)   Loading
    (i)   Strain rate: rise time
    (ii)   Sequence: linear damage summation or Miner's rule
    (iii)   Mean stress
    (iv)   Biaxial effects: constraints

(c)   Environment
    (i)   Water chemistry: DO, lithium hydroxide, boric acid concentrations
    (ii)   Temperature
    (iii)   Flow rate

The existing fatigue ε–N database covers an adequate range of material parameters (i–iii), a loading parameter (i), and the environment parameters (i–ii); therefore, the variability and uncertainty in fatigue life due to these parameters have been incorporated into the model. The existing data are most likely conservative with respect to the effects of surface preparation because the fatigue ε–N data are obtained for specimens that are free of surface cold work. Fabrication procedures for fatigue test specimens

generally follow American Society for Testing and Materials (ASTM) guidelines, which require that the final polishing of the specimens avoid surface work–hardening. Biaxial effects are covered by design procedures and need not be considered in the fatigue design curves.

As discussed earlier, under the conditions typical of operating BWRs, environmental effects on the fatigue life are a factor of ≈2 lower at high flow rates (7 m/s) than those at very low flow rates (0.3 m/s or lower) for carbon and low–alloy steels and are independent of flow rate for austenitic SSs.[19,20] However, because of the uncertainties in the flow conditions at or near the locations of crack initiation, the beneficial effect of flow rate on the fatigue life of carbon and low-alloy steels is presently not included in fatigue evaluations.

Thus, the contributions of four groups of variables, namely, material variability and data scatter, specimen size and geometry, surface finish, and loading sequence (Miner's rule), must be considered in developing fatigue design curves that are applicable to components.

6.1 Material Variability and Data Scatter

The effects of material variability and data scatter must be included to ensure that the design curves not only describe the available test data well, but also adequately describe the fatigue lives of the much larger number of heats of material that are found in the field. The effects of material variability and data scatter have been evaluated for the various materials by considering the best–fit curves determined from tests on individual heats of materials or loading conditions as samples of the much larger population of heats of materials and service conditions of interest. The fatigue behavior of each of the heats or loading conditions is characterized by the value of the constant A in Eq. 6. The values of A for the various data sets are ordered, and median ranks are used to estimate the cumulative distribution of A for the population. The distributions were fit to lognormal curves. The median value of A and standard deviation for each sample, as well as the number of data sets in the sample, are listed in Table 11. The 95/95 value of the margin on the median value to account for material variability and data scatter vary from 2.1 to 2.8 for the various samples. These margins applied to the mean value of life determined from the ANL statistical models provide 95% confidence that the fatigue life of 95 percentile of the materials and loading conditions of interest will be greater than the resultant value.

Table 11.   The median value of A and standard deviation for the various fatigue ε–N data sets used to evaluate material variability and data scatter.

	Air Environment			Water Environment		
	Median Value of A	Standard Deviation	Number of Data Sets	Median Value of A	Standard Deviation	Number of Data Sets
Carbon Steel	6.583	0.477	17	5.951	0.376	33
Low-Alloy Steel	6.449	0.375	32	5.747	0.484	26
Stainless Steel	6.891	0.417	51	6.328	0.462	36

6.2 Size and Geometry

The effect of specimen size on the fatigue life was reviewed in earlier reports.[6,38] Various studies conclude that "size effect" is not a significant parameter in the design curve margins when the fatigue curve is based on data from axial strain control rather than bending tests. No intrinsic size effect has been observed for smooth specimens tested in axial loading or plain bending. However, a size effect does occur in specimens tested in rotating bending; the fatigue endurance limit decreases by ≈25% if the specimen size is increased from 2 to 16 mm but does not decrease further with larger sizes. Also, some effect of size and geometry has been observed on small–scale–vessel tests conducted at the Ecole

65

Polytechnique in conjunction with the large–size–pressure–vessel tests carried out by the Southwest Research Institute.[115] The tests at the Ecole Polytechnique were conducted in room–temperature water on 19–mm–thick shells with ≈305–mm inner diameter nozzles and made of machined bar stock. The results indicate that the fatigue lives determined from tests on the small–scale–vessel are 30–50% lower than those obtained from tests on small, smooth fatigue specimen. However, the difference in fatigue lives in these tests cannot be attributed to specimen size alone, it is due to the effects of both size and surface finish.

During cyclic loading, cracks generally form at surface irregularities either already in existence or produced by slip bands, grain boundaries, second phase particles, etc. In smooth specimens, formation of surface cracks is affected by the specimen size; crack initiation is easier in larger specimens because of the increased surface area and, therefore, increased number of sites for crack initiation. Specimen size is not likely to influence crack initiation in specimens with rough surfaces because cracks initiate at existing irregularities on the rough surface. As discussed in the next section, surface roughness has a large effect on fatigue life. Consequently, for rough surfaces, the effect of specimen size may not be considered in the margin of 20 on life. However, conservatively, a factor of 1.2–1.4 on life may be used to incorporate size effects on fatigue life in the low–cycle regime.

6.3 Surface Finish

The effect of surface finish must be considered to account for the difference in fatigue life expected in actual components with industrial–grade surface finish compared to the smooth polished surface of a test specimen. Fatigue life is sensitive to surface finish; cracks can initiate at surface irregularities that are normal to the stress axis. The height, spacing, shape, and distribution of surface irregularities are important for crack initiation. The effect of surface finish on crack initiation is expressed by Eq. 12 in terms of the RMS value of surface roughness (R_q).

The roughness of machined surfaces or natural finishes can range from ≈0.8 to 6.0 μm. Typical surface finish for various machining processes is in the range of 0.2–1.6 μm for cylindrical grinding, 0.4–3.0 μm for surface grinding, 0.8–3.0 μm for finish turning, and drilling and 1.6–4.0 μm for milling. For fabrication processes, it is in the range of 0.8–3.0 μm for extrusion and 1.6–4.0 μm for cold rolling. Thus, from Eq. 12, the fatigue life of components with such rough surfaces may be a factor of 2–3.5 lower than that of a smooth specimen.

Limited data in LWR environments on specimens that were intentionally roughened indicate that the effects of surface roughness on fatigue life is the same in air and water environments for austenitic SSs, but are insignificant in water for carbon and low-alloy steels. Thus, in LWR environments, a factor of 2.0–3.5 on life may also be used to account for the effects of surface finish on the fatigue life of austenitic SSs, but the factor may be lower for carbon and low-alloy steels, e.g., a factor of 2 may be used for carbon and low-alloy steels.

6.4 Loading Sequence

The effects of variable amplitude loading of smooth specimens were also reviewed in an earlier report.[38] In a variable loading sequence, the presence of a few cycles at high strain amplitude causes the fatigue life at smaller strain amplitude to be significantly lower than that at constant–amplitude loading, i.e., the fatigue limit of the material is lower under variable loading histories.

As discussed in Section 2, fatigue life has conventionally been divided into two stages: initiation, expressed as the cycles required to form microstructurally small cracks (MSCs) on the surface, and propagation, expressed as cycles required to propagate these MSCs to engineering size. The transition from initiation to propagation stage strongly depends on applied stress amplitude; at stress levels above the fatigue limit, the transition from initiation to propagation stage occurs at crack depths in the range of 150 to 250 μm. However, under constant loading at stress levels below the fatigue limit of the material (e.g., $\Delta\sigma_1$ in Fig. 1), although microcracks ≈10 μm can form quite early in life, they do not grow to an engineering size. Under the variable loading conditions encountered during service of power plants, cracks created by growth of MSCs at high stresses ($\Delta\sigma_3$ in Fig. 1) to depths larger than the transition crack depth can then grow to an engineering size even at stress levels below the fatigue limit.

Studies on fatigue damage in Type 304 SS under complex loading histories[118] indicate that the loading sequence of decreasing strain levels (i.e., high strain level followed by low strain level) is more damaging than that of increasing strain levels. The fatigue life of the steel at low strain levels decreased by a factor of 2–4 under a decreasing–strain sequence. In another study, the fatigue limit of medium carbon steels was lowered even after low–stress high–cycle fatigue; the higher the stress, the greater the decrease in fatigue threshold.[119] Because variable loading histories primarily influence fatigue life at low strain levels, the mean fatigue ε–N curves are lowered to account for damaging cycles that occur below the constant–amplitude fatigue limit of the material. However, conservatively, a factor of 1.2–2.0 on life may be used to incorporate the possible effects of load histories on fatigue life in the low–cycle regime.

6.5 Fatigue Design Curve Margins Summarized

The ASME Code fatigue design curves are currently obtained from the mean data curves by first adjusting for the effects of mean stress, and then reducing the life at each point of the adjusted curve by a factor of 2 on strain and 20 on life, whichever is more conservative. The factors on strain are needed primarily to account for the variation in the fatigue limit of the material caused by material variability, component size, surface finish, and load history. Because these variables affect life through their influence on the growth of short cracks (<100 μm), the adjustment on strain to account for such variations is typically not cumulative, i.e., the portion of the life can only be reduced by a finite amount. Thus, it is controlled by the variable that has the largest effect on life. In relating the fatigue lives of laboratory test specimens to those of actual reactor components, the factor of 2 on strain that is currently being used to develop the Code design curves is adequate to account for the uncertainties associated with material variability, component size, surface finish, and load history.

The factors on life are needed to account for variations in fatigue life in the low–cycle regime. Based on the discussions presented above the effects of various material, loading, and environmental parameters on fatigue life may be summarized as follows:

(a)   The results presented in Table 11 may be used to determine the margins that need to be applied to the mean value of life to ensure that the resultant value of life would bound a specific percentile (e.g., 95 percentile) of the materials and loading conditions of interest.

(b)   For rough surfaces, specimen size is not likely to influence fatigue life, and therefore, the effect of specimen size need not be considered in the margin of 20 on life. However, conservatively, a factor of 1.2–1.4 on life may be used to incorporate size effects on fatigue life.

Table 12. Factors on life applied to mean fatigue ε–N curve to account for the effects of various material, loading, and environmental parameters.

Parameter	Section III Criterion Document	Present Report
Material Variability and Data Scatter (minimum to mean)	2.0	2.1–2.8
Size Effect	2.5	1.2–1.4
Surface Finish, etc.	4.0	2.0–3.5[*]
Loading History	–	1.2–2.0
Total Adjustment	20	6.0–27.4

[*]A factor of 2 on life may be used for carbon and low-alloy steels in LWR environments.

(c) Limited data indicate that, for carbon and low-alloy steels, the effects of surface roughness on fatigue life are insignificant in LWR environments. A factor of 2 on life may be used for carbon and low-alloy steels in water environments instead of the 2.0–3.5 used for carbon and low–alloy steels in air and for austenitic SSs in both air and water environments.

(d) Variable loading histories primarily influence fatigue life at low strain levels, i.e., in the high–cycle regime, and the mean fatigue ε–N curves are lowered by a factor of 2 on strain to account for damaging cycles that occur below the constant–strain fatigue limit of the material. Conservatively, a factor of 1.2–2.0 on life may be used to incorporate the possible effects of load histories on fatigue life in the low–cycle regime.

The subfactors that are needed to account for the effects of the various material, loading, and environmental parameters on fatigue life are summarized in Table 12. The total adjustment on life may vary from 6 to 27. Because the maximum value represents a relatively poor heat of material and assumes the maximum effects of size, surface finish, and loading history, the maximum value of 27 is likely to be quite conservative. A value of 20 is currently being used to develop the Code design curves from the mean-data curves.

To determine the most appropriate value for the design margin on life, Monte Carlo simulations were performed using the material variability and data scatter results given in Table 11, and the margins needed to account for the effects of size, surface finish, and loading history listed in Table 12. A lognormal distribution was also assumed for the effects of size, surface finish, and loading history, and the minimum and maximum values of the adjustment factors, e.g., 1.2–1.4 for size, 2.0–3.5 for surface finish, and 1.2–2.0 for loading history, were assumed to represent the 5th and 95th percentile, respectively. The cumulative distribution of the values of A in the fatigue ε–N curve for test specimens and the adjusted curve that represents the behavior of actual components is shown in Fig. 57 for carbon and low–alloy steels and austenitic SSs.

The results indicate that, relative to the specimen curve, the median value of constant A for the component curve decreased by a factor of 5.6 to account for the effects of size, surface finish, and loading history, and the standard deviation of heat-to-heat variation of the component curve increased by 6–10%. The margin that has to be applied to the mean data curve for test specimens to obtain a component curve that would bound 95% of the population, is 11.0–12.7 for the various materials; the values are given in Table 13. An average value of 12 on life may be used for developing fatigue design curves from the mean data curve. The choice of bounding the 95th percentile of the population for a design curve is somewhat arbitrary. It is done with the understanding that the design curve controls fatigue initiation, not failure. The choice also recognizes that there are conservatisms implied in the choice of log normal

distributions, which have an infinite tail, and in the identification of what in many cases are bounding values of the effects as 95th percentile values.

Table 13. Margin applied to the mean values of fatigue life to bound 95% of the population.

Material	Air Environment
Carbon Steels	12.6
Low–Alloy Steels	11.0
Austenitic Stainless Steels	11.6
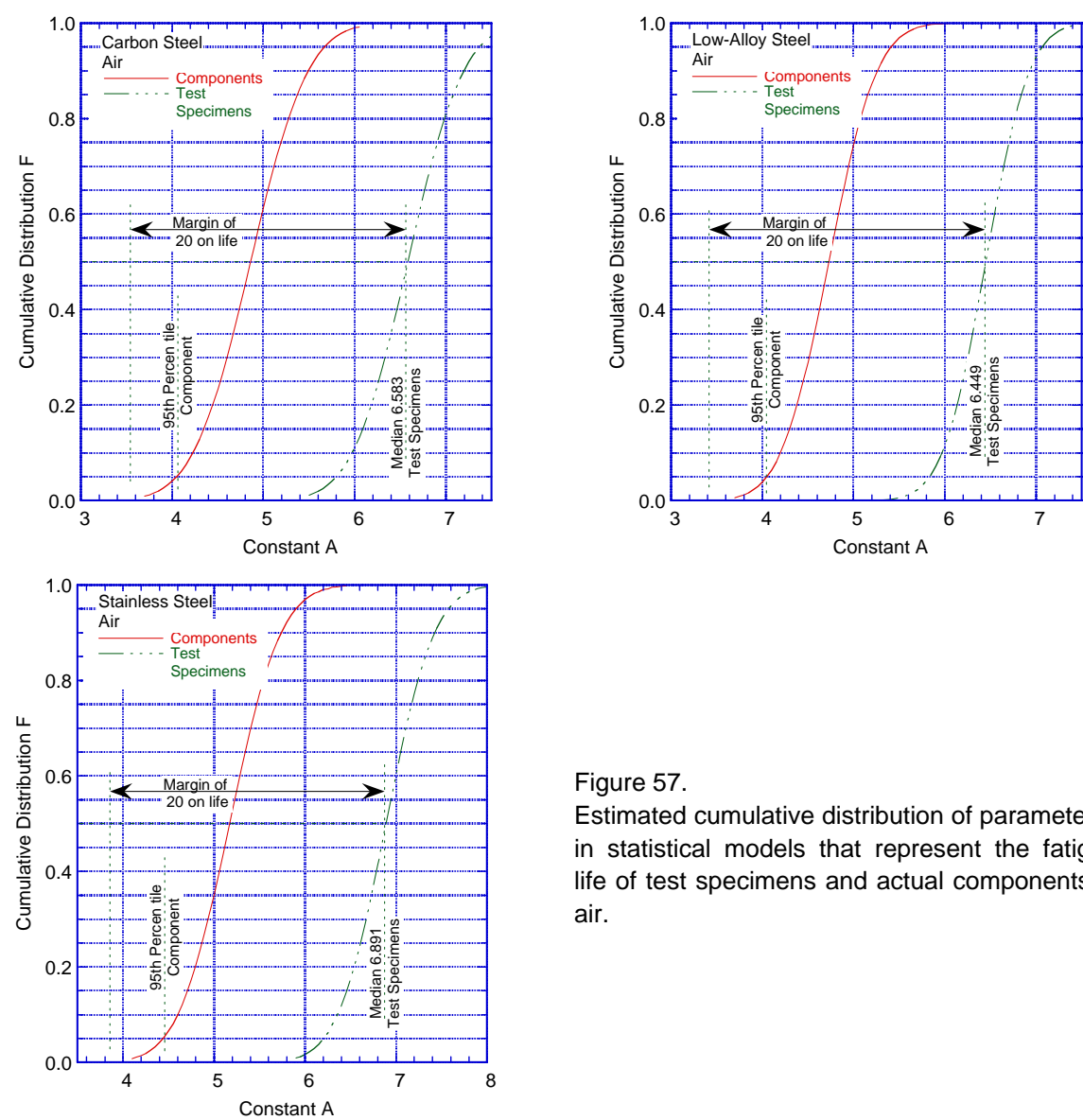
Figure 57.
Estimated cumulative distribution of parameter A in statistical models that represent the fatigue life of test specimens and actual components in air.

These results suggest that for all materials, the current ASME Code requirements of a factor of 20 on cycles to account for the effects of material variability and data scatter, as well as specimen size, surface finish, and loading history, contain at least a factor of 1.7 conservatism (i.e., $20/12 \approx 1.7$). Thus, to reduce this conservatism, fatigue design curves may be obtained from the mean data curve by first correcting for mean stress effects using the modified Goodman relationship, and then reducing the mean-stress adjusted curve by a factor of 2 on stress or 12 on cycles, whichever is more conservative. Fatigue design curves have been developed from the ANL statistical models using this procedure; the curves for carbon and low–alloy steels are presented in Section 4.1.9 and for wrought and cast austenitic SSs in Section 5.1.8.

7   Summary

The existing fatigue ε–N data for carbon and low–alloy steels and wrought and cast austenitic SSs have been evaluated to define the effects of key material, loading, and environmental parameters on the fatigue lives of these steels. The fatigue lives of carbon and low–alloy steels and austenitic SSs are decreased in LWR environments; the magnitude of the reduction depends on temperature, strain rate, DO level in water, and, for carbon and low–alloy steels, the S content of the steel. For all steels, environmental effects on fatigue life are significant only when critical parameters (temperature, strain rate, DO level, and strain amplitude) meet certain threshold values. Environmental effects are moderate, e.g., less than a factor of 2 decrease in life, when any one of the threshold conditions is not satisfied. The threshold values of the critical parameters and the effects of other parameters (such as water conductivity, water flow rate, and material heat treatment) on the fatigue life of the steels are summarized.

In air, the fatigue life of carbon and low–alloy steels depends on steel type, temperature, orientation, and strain rate. The fatigue life of carbon steels is a factor of ≈1.5 lower than that of low–alloy steels. For both steels, fatigue life decreases with increase in temperature. Some heats of carbon and low–alloy steels exhibit effects of strain rate and orientation. For these heats, fatigue life decreases with decreasing strain rate. Also, based on the distribution and morphology of sulfides, the fatigue properties in the transverse orientation may be inferior to those in the rolling orientation. The data indicate significant heat–to–heat variation; at 288°C, the fatigue life of carbon and low–alloy steels may vary by up to a factor of 3 above or below the mean value. Fatigue life is very sensitive to surface finish; the fatigue life of specimens with rough surfaces may be up to a factor of 3 lower than that of smooth specimens. The results also indicate that in room-temperature air, the ASME mean curve for low–alloy steels is in good agreement with the available experimental data, and the curve for carbon steels is somewhat conservative.

The fatigue lives of both carbon and low–alloy steels are decreased in LWR environments; the reduction depends on temperature, strain rate, DO level in water, and S content of the steel. The fatigue life is decreased significantly when four conditions are satisfied simultaneously, viz., the strain amplitude, temperature, and DO in water are above certain minimum levels, and the strain rate is below a threshold value. The S content in the steel is also important; its effect on life depends on the DO level in water.

Although the microstructures and cyclic–hardening behavior of carbon and low–alloy steels differ significantly, environmental degradation of the fatigue life of these steels is very similar. For both steels, only a moderate decrease in life (by a factor of <2) is observed when any one of the threshold conditions is not satisfied, e.g., low–DO PWR environment, temperatures <150°C, or vibratory fatigue. The existing fatigue S–N data have been reviewed to establish the critical parameters that influence fatigue life and define their threshold and limiting values within which environmental effects are significant.

In air, the fatigue lives of Types 304 and 316 SS are comparable; those of Type 316NG are superior to those of Types 304 and 316 SS at high strain amplitudes. The fatigue lives of austenitic SSs in air are independent of temperature in the range from room temperature to 427°C. Also, variation in strain rate in the range of 0.4–0.008%/s has no effect on the fatigue lives of SSs at temperatures up to 400°C. The fatigue ε–N behavior of cast SSs is similar to that of wrought austenitic SSs. The results indicate that the ASME mean-data curve for SSs is not consistent with the experimental data at strain amplitudes <0.5% or stress amplitudes <975 MPa (<141 ksi); the ASME mean curve predicts significantly longer lives than those observed experimentally.

The fatigue lives of cast and wrought austenitic SSs decrease in LWR environments compared to those in air. The decrease depends on strain rate, DO level in water, and temperature. A minimum threshold strain is required for an environmentally assisted decrease in the fatigue life of SSs, and this strain appears to be independent of material type (weld or base metal) and temperature in the range of 250–325°C. Environmental effects on fatigue life occur primarily during the tensile–loading cycle and at strain levels greater than the threshold value. Strain rate and temperature have a strong effect on fatigue life in LWR environments. Fatigue life decreases with decreasing strain rate below 0.4%/s; the effect saturates at 0.0004%/s. Similarly, the fatigue ε–N data suggest a threshold temperature of 150°C; in the range of 150–325°C, the logarithm of life decreases linearly with temperature.

The effect of DO level may be different for different steels. In low–DO water (i.e., <0.01 ppm DO) the fatigue lives of all wrought and cast austenitic SSs are decreased significantly; composition or heat treatment of the steel has little or no effect on fatigue life. However, in high–DO water, the environmental effects on fatigue life are influenced by the composition and heat treatment of the steel. For a high–C Type 304 SS, environmental effects are significant only for sensitized steel. For a low–C Type 316NG SS, some effect of environment was observed even for mill–annealed steel in high–DO water, although the effect was smaller than that observed in low–DO water. Limited fatigue ε–N data indicate that the fatigue lives of cast SSs are approximately the same in low– and high–DO water and are comparable to those observed for wrought SSs in low–DO water.

Statistical models developed earlier to predict fatigue lives of small smooth specimens of carbon and low–alloy steels and wrought and cast austenitic SSs as a function of material, loading, and environmental parameters have been updated/revised using a larger fatigue ε–N database. The functional form and bounding values of these parameters were based on experimental observations and data trends. The models are applicable for predicted fatigue lives $\leq 10^6$ cycles.

An approach, based on the environmental fatigue correction factor, is discussed to incorporate the effects of LWR coolant environments into the ASME Code fatigue evaluations. To incorporate environmental effects into a Section III fatigue evaluation, the fatigue usage for a specific stress cycle of load set pair based on the current Code fatigue design curves is multiplied by the correction factor.

The report also presents a critical review of the ASME Code fatigue design margins of 2 on stress and 20 on life and assesses the possible conservatism in the current choice of design margins. These factors cover the effects of variables that can influence fatigue life but were not investigated in the tests that provided the data for the design curves. Although these factors were intended to be somewhat conservative, they should not be considered safety margins because they were intended to account for variables that are known to affect fatigue life. Data available in the literature have been reviewed to evaluate the margins on cycles and stress that are needed to account for the differences and uncertainties. Monte Carlo simulations were performed to determine the margin on cycles needed to obtain a fatigue design curve that would provide a somewhat conservative estimate of the number of cycles to initiate a fatigue crack in reactor components. The results suggest that for both carbon and low–alloy steels and austenitic SSs, the current ASME Code requirements of a factor of 20 on cycles to account for the effects of material variability and data scatter, as well as size, surface finish, and loading history, contain at least a factor of 1.7 conservatism. Thus, to reduce this conservatism, fatigue design curves have been developed from the ANL statistical model by first correcting for mean stress effects, and then reducing the mean–stress adjusted curve by a factor of 2 on stress and 12 on cycles, whichever is more conservative. A detailed procedure for incorporating environmental effects into fatigue evaluations is also presented in Appendix A.

References

1. Langer, B. F., "Design of Pressure Vessels for Low–Cycle Fatigue," ASME J. Basic Eng. 84, 389–402, 1962.

2. "Criteria of the ASME Boiler and Pressure Vessel Code for Design by Analysis in Sections III and VIII, Division 2," The American Society of Mechanical Engineers, New York, 1969.

3. Cooper, W. E., "The Initial Scope and Intent of the Section III Fatigue Design Procedure," Welding Research Council, Inc., Technical Information from Workshop on Cyclic Life and Environmental Effects in Nuclear Applications, Clearwater, Florida, Jan. 22-21, 1992.

4. Chopra, O. K., and W. J. Shack, "Effects of LWR Coolant Environments on Fatigue Design Curves of Carbon and Low–Alloy Steels," NUREG/CR–6583, ANL–97/18, March 1998.

5. Gavenda, D. J., P. R. Luebbers, and O. K. Chopra, "Crack Initiation and Crack Growth Behavior of Carbon and Low–Alloy Steels," Fatigue and Fracture 1, Vol. 350, S. Rahman, K. K. Yoon, S. Bhandari, R. Warke, and J. M. Bloom, eds., American Society of Mechanical Engineers, New York, pp. 243–255, 1997.

6. Chopra, O. K., and W. J. Shack, "Environmental Effects on Fatigue Crack Initiation in Piping and Pressure Vessel Steels," NUREG/CR–6717, ANL–00/27, May 2001.

7. Chopra, O. K., "Mechanisms and Estimation of Fatigue Crack Initiation in Austenitic Stainless Steels in LWR Environments," NUREG/CR–6787, ANL–01/25, Aug. 2002.

8. Hale, D. A., S. A. Wilson, E. Kiss, and A. J. Gianuzzi, "Low–Cycle Fatigue Evaluation of Primary Piping Materials in a BWR Environment," GEAP–20244, U.S. Nuclear Regulatory Commission, Sept. 1977.

9. Hale, D. A., S. A. Wilson, J. N. Kass, and E. Kiss, "Low Cycle Fatigue Behavior of Commercial Piping Materials in a BWR Environment," J. Eng. Mater. Technol. 103, 15–25, 1981.

10. Ranganath, S., J. N. Kass, and J. D. Heald, "Fatigue Behavior of Carbon Steel Components in High–Temperature Water Environments," BWR Environmental Cracking Margins for Carbon Steel Piping, EPRI NP–2406, Appendix 3, Electric Power Research Institute, Palo Alto, CA, May 1982.

11. Ranganath, S., J. N. Kass, and J. D. Heald, "Fatigue Behavior of Carbon Steel Components in High–Temperature Water Environments," Low–Cycle Fatigue and Life Prediction, ASTM STP 770, C. Amzallag, B. N. Leis, and P. Rabbe, eds., American Society for Testing and Materials, Philadelphia, pp. 436–459, 1982.

12. Nagata, N., S. Sato, and Y. Katada, "Low–Cycle Fatigue Behavior of Pressure Vessel Steels in High–Temperature Pressurized Water," ISIJ Intl. 31 (1), 106–114, 1991.

13. Higuchi, M., and K. Iida, "Fatigue Strength Correction Factors for Carbon and Low–Alloy Steels in Oxygen–Containing High–Temperature Water," Nucl. Eng. Des. 129, 293–306, 1991.

14.   Katada, Y., N. Nagata, and S. Sato, "Effect of Dissolved Oxygen Concentration on Fatigue Crack Growth Behavior of A533 B Steel in High Temperature Water," ISIJ Intl. 33 (8), 877–883, 1993.

15.   Kanasaki, H., M. Hayashi, K. Iida, and Y. Asada, "Effects of Temperature Change on Fatigue Life of Carbon Steel in High Temperature Water," Fatigue and Crack Growth: Environmental Effects, Modeling Studies, and Design Considerations, PVP Vol. 306, S. Yukawa, ed., American Society of Mechanical Engineers, New York, pp. 117–122, 1995.

16.   Nakao, G., H. Kanasaki, M. Higuchi, K. Iida, and Y. Asada, "Effects of Temperature and Dissolved Oxygen Content on Fatigue Life of Carbon and Low–Alloy Steels in LWR Water Environment," Fatigue and Crack Growth: Environmental Effects, Modeling Studies, and Design Considerations, PVP Vol. 306, S. Yukawa, ed., American Society of Mechanical Engineers, New York, pp. 123–128, 1995.

17.   Higuchi, M., K. Iida, and Y. Asada, "Effects of Strain Rate Change on Fatigue Life of Carbon Steel in High–Temperature Water," Fatigue and Crack Growth: Environmental Effects, Modeling Studies, and Design Considerations, PVP Vol. 306, S. Yukawa, ed., American Society of Mechanical Engineers, New York, pp. 111–116, 1995; also Proc. of Symp. on Effects of the Environment on the Initiation of Crack Growth, ASTM STP 1298, American Society for Testing and Materials, Philadelphia, 1997.

18.   Higuchi, M., K. Iida, and K. Sakaguchi, "Effects of Strain Rate Fluctuation and Strain Holding on Fatigue Life Reduction for LWR Structural Steels in Simulated PWR Water," Pressure Vessel and Piping Codes and Standards, PVP Vol. 419, M. D. Rana, ed., American Society of Mechanical Engineers, New York, pp. 143–152, 2001.

19.   Hirano, A., M. Yamamoto, K. Sakaguchi, T. Shoji, and K. Iida, "Effects of Water Flow Rate on Fatigue Life of Ferritic and Austenitic Steels in Simulated LWR Environment," Pressure Vessel and Piping Codes and Standards – 2002, PVP Vol. 439, M. D. Rana, ed., American Society of Mechanical Engineers, New York, pp. 143–150, 2002.

20.   Hirano, A., M. Yamamoto, K. Sakaguchi, and T. Shoji, "Effects of Water Flow Rate on Fatigue Life of Carbon and Stainless Steels in Simulated LWR Environment," Pressure Vessel and Piping Codes and Standards – 2004, PVP Vol. 480, American Society of Mechanical Engineers, New York, pp. 109–119, 2004.

21.   Fujiwara, M., T. Endo, and H. Kanasaki, "Strain Rate Effects on the Low–Cycle Fatigue Strength of 304 Stainless Steel in High–Temperature Water Environment. Fatigue Life: Analysis and Prediction," Proc. Intl. Conf. and Exposition on Fatigue, Corrosion Cracking, Fracture Mechanics, and Failure Analysis, ASM, Metals Park, OH, pp. 309–313, 1986.

22.   Mimaki, H., H. Kanasaki, I. Suzuki, M. Koyama, M. Akiyama, T. Okubo, and Y. Mishima, "Material Aging Research Program for PWR Plants," Aging Management Through Maintenance Management, PVP Vol. 332, I. T. Kisisel, ed., American Society of Mechanical Engineers, New York, pp. 97–105, 1996.

23.   Kanasaki, H., R. Umehara, H. Mizuta, and T. Suyama, "Fatigue Lives of Stainless Steels in PWR Primary Water," Trans. 14th Intl. Conf. on Structural Mechanics in Reactor Technology (SMiRT 14), Lyon, France, pp. 473–483, 1997.

24. Kanasaki, H., R. Umehara, H. Mizuta, and T. Suyama, "Effects of Strain Rate and Temperature Change on the Fatigue Life of Stainless Steel in PWR Primary Water," Trans. 14th Intl. Conf. on Structural Mechanics in Reactor Technology (SMiRT 14), Lyon, France, pp. 485–493, 1997.

25. Higuchi, M., and K. Iida, "Reduction in Low–Cycle Fatigue Life of Austenitic Stainless Steels in High–Temperature Water," Pressure Vessel and Piping Codes and Standards, PVP Vol. 353, D. P. Jones, B. R. Newton, W. J. O'Donnell, R. Vecchio, G. A. Antaki, D. Bhavani, N. G. Cofie, and G. L. Hollinger, eds., American Society of Mechanical Engineers, New York, pp. 79–86, 1997.

26. Hayashi, M., "Thermal Fatigue Strength of Type 304 Stainless Steel in Simulated BWR Environment," Nucl. Eng. Des. 184, 135–144, 1998.

27. Hayashi, M., K. Enomoto, T. Saito, and T. Miyagawa, "Development of Thermal Fatigue Testing with BWR Water Environment and Thermal Fatigue Strength of Austenitic Stainless Steels," Nucl. Eng. Des. 184, 113–122, 1998.

28. Tsutsumi, K., H. Kanasaki, T. Umakoshi, T. Nakamura, S. Urata, H. Mizuta, and S. Nomoto, "Fatigue Life Reduction in PWR Water Environment for Stainless Steels," Assessment Methodologies for Preventing Failure: Service Experience and Environmental Considerations, PVP Vol. 410-2, R. Mohan, ed., American Society of Mechanical Engineers, New York, pp. 23–34, 2000.

29. Tsutsumi, K., T. Dodo, H. Kanasaki, S. Nomoto, Y. Minami, and T. Nakamura, "Fatigue Behavior of Stainless Steel under Conditions of Changing Strain Rate in PWR Primary Water," Pressure Vessel and Piping Codes and Standards, PVP Vol. 419, M. D. Rana, ed., American Society of Mechanical Engineers, New York, pp. 135–141, 2001.

30. Tsutsumi, K., M. Higuchi, K. Iida, and Y. Yamamoto, "The Modified Rate Approach to Evaluate Fatigue Life under Synchronously Changing Temperature and Strain Rate in Elevated Temperature Water," Pressure Vessel and Piping Codes and Standards – 2002, PVP Vol. 439, M. D. Rana, ed., American Society of Mechanical Engineers, New York, pp. 99–107, 2002.

31. Higuchi, M., T. Hirano, and K. Sakaguchi, "Evaluation of Fatigue Damage on Operating Plant Components in LWR Water," Pressure Vessel and Piping Codes and Standards – 2004, PVP Vol. 480, American Society of Mechanical Engineers, New York, pp. 129–138, 2004.

32. Nomura, Y., M. Higuchi, Y. Asada, and K. Sakaguchi, "The Modified Rate Approach Method to Evaluate Fatigue Life under Synchronously Changing Temperature and Strain Rate in Elevated Temperature Water in Austenitic Stainless Steels," Pressure Vessel and Piping Codes and Standards – 2004, PVP Vol. 480, American Society of Mechanical Engineers, New York, pp. 99–108, 2004.

33. Chopra, O. K., and W. J. Shack, "Evaluation of Effects of LWR Coolant Environments on Fatigue Life of Carbon and Low–Alloy Steels," Effects of the Environment on the Initiation of Crack Growth, ASTM STP 1298, W. A. Van Der Sluys, R. S. Piascik, and R. Zawierucha, eds., American Society for Testing and Materials, Philadelphia, pp. 247–266, 1997.

34. Chopra, O. K., and W. J. Shack, "Low–Cycle Fatigue of Piping and Pressure Vessel Steels in LWR Environments," Nucl. Eng. Des. 184, 49–76, 1998.

35. Chopra, O. K., and D. J. Gavenda, "Effects of LWR Coolant Environments on Fatigue Lives of Austenitic Stainless Steels," J. Pressure Vessel Technol. 120, 116–121, 1998.

36. Chopra, O. K., and J. L. Smith, "Estimation of Fatigue Strain–Life Curves for Austenitic Stainless Steels in Light Water Reactor Environments," Fatigue, Environmental Factors, and New Materials, PVP Vol. 374, H. S. Mehta, R. W. Swindeman, J. A. Todd, S. Yukawa, M. Zako, W. H. Bamford, M. Higuchi, E. Jones, H. Nickel, and S. Rahman, eds., American Society of Mechanical Engineers, New York, pp. 249–259, 1998.

37. Chopra, O. K., "Effects of LWR Coolant Environments on Fatigue Design Curves of Austenitic Stainless Steels," NUREG/CR–5704, ANL–98/31, 1999.

38. Chopra, O. K., and W. J. Shack, "Review of the Margins for ASME Code Design Curves – Effects of Surface Roughness and Material Variability," NUREG/CR–6815, ANL–02/39, Sept. 2003.

39. Chopra, O. K., B. Alexandreanu, and W. J. Shack, "Effect of Material Heat Treatment on Fatigue Crack Initiation in Austenitic Stainless Steels in LWR Environments," NUREG/CR–6878, ANL–03/35, July 2005.

40. Terrell, J. B., "Fatigue Life Characterization of Smooth and Notched Piping Steel Specimens in 288°C Air Environments," NUREG/CR–5013, EM–2232 Materials Engineering Associates, Inc., Lanham, MD, May 1988.

41. Terrell, J. B., "Fatigue Strength of Smooth and Notched Specimens of ASME SA 106–B Steel in PWR Environments," NUREG/CR–5136, MEA–2289, Materials Engineering Associates, Inc., Lanham, MD, Sept. 1988.

42. Terrell, J. B., "Effect of Cyclic Frequency on the Fatigue Life of ASME SA–106–B Piping Steel in PWR Environments," J. Mater. Eng. 10, 193–203, 1988.

43. Lenz, E., N. Wieling, and H. Muenster, "Influence of Variation of Flow Rates and Temperature on the Cyclic Crack Growth Rate under BWR Conditions," Environmental Degradation of Materials in Nuclear Power Systems – Water Reactors, The Metallurgical Society, Warrendale, PA, 1988.

44. Garud, Y. S., S. R. Paterson, R, B, Dooley, R. S. Pathania, J. Hickling, and A. Bursik, "Corrosion Fatigue of Water Touched Pressure Retaining Components in Power Plants," EPRI TR–106696, Final Report, Electric Power Research Institute, Palo Alto, Nov. 1997.

45. Faidy, C., T. Le Courtois, E. de Fraguier, J–A Leduff, A. Lefrancois, and J. Dechelotte, "Thermal Fatigue in French RHR System," Int. Conf. on Fatigue of Reactor Components, Napa, CA, July 31–August 2, 2000.

46. Kussmaul, K., R. Rintamaa, J. Jansky, M. Kemppainen, and K. Törrönen, "On the Mechanism of Environmental Cracking Introduced by Cyclic Thermal Loading," in IAEA Specialists Meeting, Corrosion and Stress Corrosion of Steel Pressure Boundary Components and Steam Turbines, VTT Symp. 43, Espoo, Finland, pp. 195–243, 1983.

47. Hickling, J., "Strain Induced Corrosion Cracking of Low-Alloy Reactor Pressure Vessel Steels under BWR Conditions," Proc. 10th Intl. Symp. on Environmental Degradation of Materials in Nuclear Power Systems – Water Reactors, F. P. Ford, S. M. Bruemmer, and G. S. Was, eds., The Minerals, Metals, and Materials Society, Warrendale, PA, CD-ROM, paper 0156, 2001.

48. Hickling, J., "Research and Service Experience with Environmentally Assisted Cracking of Low–Alloy Steel," Power Plant Chem., 7 (1), 4–15, 2005.

49. Iida, K., "A Review of Fatigue Failures in LWR Plants in Japan," Nucl. Eng. Des. 138, 297–312, 1992.

50. NRC IE Bulletin No. 79–13, "Cracking in Feedwater System Piping," U.S. Nuclear Regulatory Commission, Washington, DC, June 25, 1979.

51. NRC Information Notice 93–20, "Thermal Fatigue Cracking of Feedwater Piping to Steam Generators," U.S. Nuclear Regulatory Commission, Washington, DC, March 24, 1993.

52. Kussmaul, K., D. Blind, and J. Jansky, "Formation and Growth of Cracking in Feed Water Pipes and RPV Nozzles," Nucl. Eng. Des. 81, 105–119, 1984.

53. Gordon, B. M., D. E. Delwiche, and G. M. Gordon, "Service Experience of BWR Pressure Vessels," Performance and Evaluation of Light Water Reactor Pressure Vessels, PVP Vol.–119, American Society of Mechanical Engineers, New York, pp. 9–17, 1987.

54. Lenz, E., B. Stellwag, and N. Wieling, "The Influence of Strain–Induced Corrosion Cracking on the Crack Initiation in Low–Alloy Steels in HT–Water – A Relation Between Monotonic and Cyclic Crack Initiation Behavior," in IAEA Specialists Meeting Corrosion and Stress Corrosion of Steel Pressure Boundary Components and Steam Turbines, VTT Symp. 43, Espoo, Finland, pp. 243–267, 1983.

55. Hickling, J., and D. Blind, "Strain–Induced Corrosion Cracking of Low–Alloy Steels in LWR Systems – Case Histories and Identification of Conditions Leading to Susceptibility," Nucl. Eng. Des. 91, 305–330, 1986.

56. Hirschberg, P., A. F. Deardorff, and J. Carey, "Operating Experience Regarding Thermal Fatigue of Unisolable Piping Connected to PWR Reactor Coolant Systems," Int. Conf. on Fatigue of Reactor Components, Napa, CA, July 31–August 2, 2000.

57. NRC Information Notice 88–01, "Safety Injection Pipe Failure," U.S. Nuclear Regulatory Commission, Washington, DC (Jan. 27, 1988).

58. NRC Bulletin No. 88–08, "Thermal Stresses in Piping Connected to Reactor Coolant Systems," U.S. Nuclear Regulatory Commission, Washington, DC, June 22; Suppl. 1, June 24; Suppl. 2, Aug. 4, 1988; Suppl. 3, April 1989.

59. Sakai, T., "Leakage from CVCS Pipe of Regenerative Heat Exchanger Induced by High–Cycle Thermal Fatigue at Tsuruga Nuclear Power Station Unit 2," Int. Conf. on Fatigue of Reactor Components, Napa, CA, July 31–August 2, 2000.

60. Hoshino, T., T. Ueno, T. Aoki, and Y. Kutomi, "Leakage from CVCS Pipe of Regenerative Heat Exchanger Induced by High–Cycle Thermal Fatigue at Tsuruga Nuclear Power Station Unit 2," Proc. 8th Intl. Conf. on Nuclear Engineering, 1.01 Operational Experience/Root Cause Failure Analysis, Paper 8615, American Society of Mechanical Engineers, New York, 2000.

61. Stephan, J.–M., and J. C. Masson, "Auxiliary Feedwater Line Stratification and Coufast Simulation," Int. Conf. on Fatigue of Reactor Components, Napa, CA, July 31–August 2, 2000.

62. NRC Bulletin No. 88–11, "Pressurizer Surge Line Thermal Stratification," U.S. Nuclear Regulatory Commission, Washington, DC, Dec. 20, 1988.

63. Majumdar, S., O. K. Chopra, and W. J. Shack, "Interim Fatigue Design Curves for Carbon, Low–Alloy, and Austenitic Stainless Steels in LWR Environments," NUREG/CR–5999, ANL–93/3, 1993.

64. Keisler, J., O. K. Chopra, and W. J. Shack, "Fatigue Strain–Life Behavior of Carbon and Low–Alloy Steels, Austenitic Stainless Steels, and Alloy 600 in LWR Environments," NUREG/CR–6335, ANL–95/15, 1995.

65. Park, H. B., and O. K. Chopra, "A Fracture Mechanics Approach for Estimating Fatigue Crack Initiation in Carbon and Low-Alloy Steels in LWR Coolant Environment," Assessment Methodologies for Preventing Failure: Service Experience and Environmental Considerations, PVP Vol. 410-2, R. Mohan, ed., American Society of Mechanical Engineers, New York, pp. 3–11, 2000.

66. O'Donnell, T. P., and W. J. O'Donnell, "Stress Intensity Values in Conventional S-N Fatigue Specimens," Pressure Vessels and Piping Codes and Standard: Volume 1 – Current Applications, PVP Vol. 313–1, K. R. Rao and Y. Asada, eds., American Society of Mechanical Engineers, New York, pp. 191–192, 1995.

67. Amzallag, C., P. Rabbe, G. Gallet, and H.–P. Lieurade, "Influence des Conditions de Sollicitation Sur le Comportement en Fatigue Oligocyclique D'aciers Inoxydables Austénitiques," Memoires Scientifiques Revue Metallurgie Mars, pp. 161–173, 1978.

68. Solomon, H. D., C. Amzallag, A. J. Vallee, and R. E. De Lair, "Influence of Mean Stress on the Fatigue Behavior of 304L SS in Air and PWR Water," Proc. Of the 2005 ASME Pressure Vessels and Piping Conf., July 17–21, 2005, Denver, CO, paper # PVP2005–71064.

69. Solomon, H. D., C. Amzallag, R. E. De Lair, and A. J. Vallee, "Strain Controlled Fatigue of Type 304L SS in Air and PWR Water," Proc. Third Intl. Conf. on Fatigue of Reactor Components, Seville, Spain, Oct. 3–6, 2004.

70. Jaske, C. E., and W. J. O'Donnell, "Fatigue Design Criteria for Pressure Vessel Alloys," Trans. ASME J. Pressure Vessel Technol. 99, 584–592, 1977.

71. Conway, J. B., R. H. Stentz, and J. T. Berling, "Fatigue, Tensile, and Relaxation Behavior of Stainless Steels," TID–26135, U.S. Atomic Energy Commission, Washington, DC, 1975.

72. Keller, D. L., "Progress on LMFBR Cladding, Structural, and Component Materials Studies During July, 1971 through June, 1972, Final Report," Task 32, Battelle–Columbus Laboratories, BMI–1928, 1977.

73. Iida, K., T. Bannai, M. Higuchi, K. Tsutsumi, and K. Sakaguchi, "Comparison of Japanese MITI Guideline and Other Methods for Evaluation of Environmental Fatigue Life Reduction," Pressure Vessel and Piping Codes and Standards, PVP Vol. 419, M. D. Rana, ed., American Society of Mechanical Engineers, New York, pp. 73–81, 2001.

74. Chopra, O. K., and W. J. Shack, "Overview of Fatigue Crack Initiation in Carbon and Low–Alloy Steels in Light Water Reactor Environments," J. Pressure Vessel Technol. 121, 49–60, 1999.

75. Higuchi, M., "Revised Proposal of Fatigue Life Correction Factor F_{en} for Carbon and Low Alloy Steels in LWR Water Environments," Assessment Methodologies for Preventing Failure: Service Experience and Environmental Considerations, PVP Vol. 410-2, R. Mohan, ed., American Society of Mechanical Engineers, New York, pp. 35–44, 2000.

76. Leax, T. R., "Statistical Models of Mean Stress and Water Environment Effects on the Fatigue Behavior of 304 Stainless Steel," Probabilistic and Environmental Aspects of Fracture and Fatigues, PVP Vol. 386, S. Rahman, ed., American Society of Mechanical Engineers, New York, pp. 229–239, 1999.

77. Ford, F. P., S. Ranganath, and D. Weinstein, "Environmentally Assisted Fatigue Crack Initiation in Low–Alloy Steels - A Review of the Literature and the ASME Code Design Requirements," EPRI Report TR-102765, Electroic Power Research Institute, Palo Alto, CA, Aug. 1993.

78. Ford, F. P., "Prediction of Corrosion Fatigue Initiation in Low–Alloy and Carbon Steel/Water Systems at 288°C," Proc. 6th Intl. Symp. on Environmental Degradation of Materials in Nuclear Power Systems – Water Reactors, R. E. Gold and E. P. Simonen, eds., The Metallurgical Society, Warrendale, PA, pp. 9–17, 1993.

79. Mehta, H. S., and S. R. Gosselin, "Environmental Factor Approach to Account for Water Effects in Pressure Vessel and Piping Fatigue Evaluations," Nucl. Eng. Des. 181, 175–197, 1998.

80. Mehta, H. S., "An Update on the Consideration of Reactor Water Effects in Code Fatigue Initiation Evaluations for Pressure Vessels and Piping," Assessment Methodologies for Preventing Failure: Service Experience and Environmental Considerations, PVP Vol. 410-2, R. Mohan, ed., American Society of Mechanical Engineers, New York, pp. 45–51, 2000.

81. Van Der Sluys, W. A., and S. Yukawa, "Status of PVRC Evaluation of LWR Coolant Environmental Effects on the S–N Fatigue Properties of Pressure Boundary Materials," Fatigue and Crack Growth: Environmental Effects, Modeling Studies, and Design Considerations, PVP Vol. 306, S. Yukawa, ed., American Society of Mechanical Engineers, New York, pp. 47–58, 1995.

82. Van Der Sluys, W. A., "PVRC's Position on Environmental Effects on Fatigue Life in LWR Applications," Welding Research Council Bulletin 487, Welding Research Council, Inc., New York, Dec. 2003.

83. O'Donnell, W. J., W. J. O'Donnell, and T. P. O'Donnell, "Proposed New Fatigue Design Curves for Austenitic Stainless Steels, Alloy 600, and Alloy 800," Proc. Of the 2005 ASME Pressure Vessels and Piping Conf., July 17–21, 2005, Denver, CO, paper # PVP2005–71409.

84. O'Donnell, W. J., W. J. O'Donnell, and T. P. O'Donnell, "Proposed New Fatigue Design Curves for Carbon and Low–Alloy Steels in High Temperature Water," Proc. Of the 2005 ASME Pressure Vessels and Piping Conf., July 17–21, 2005, Denver, CO, paper # PVP2005–71410.

85. Abdel–Raouf, H., A. Plumtree, and T. H. Topper, "Effects of Temperature and Deformation Rate on Cyclic Strength and Fracture of Low–Carbon Steel," Cyclic Stress–Strain Behavior – Analysis, Experimentation, and Failure Prediction, ASTM STP 519, American Society for Testing and Materials, Philadelphia, pp. 28–57, 1973.

86. Lee, B. H., and I. S. Kim, "Dynamic Strain Aging in the High–Temperature Low–Cycle Fatigue of SA 508 Cl. 3 Forging Steel," J. Nucl. Mater. 226, 216–225, 1995.

87. Maiya, P. S., and D. E. Busch, "Effect of Surface Roughness on Low–Cycle Fatigue Behavior of Type 304 Stainless Steel," Met. Trans. 6A, 1761–1766, 1975.

88. Maiya, P. S., "Effect of Surface Roughness and Strain Range on Low–Cycle Fatigue Behavior of Type 304 Stainless Steel," Scripta Metall. 9, 1277–1282, 1975.

89. Stout, K. J., "Surface Roughness – Measurement, Interpretation, and Significance of Data," Mater. Eng. 2, 287–295, 1981.

90. Iida, K., "A Study of Surface Finish Effect Factor in ASME B & PV Code Section III," Pressure Vessel Technology, Vol. 2, L. Cengdian and R. W. Nichols, eds., Pergamon Press, New York, pp. 727–734, 1989.

91. Manjoine, M. J., and R. L. Johnson, "Fatigue Design Curves for Carbon and Low Alloy Steels up to 700°F (371°C)," Material Durability/Life Prediction Modeling: Materials for the 21st Century, PVP–Vol. 290, American Society of Mechanical Engineers, New York, 1994.

92. Johnson, L. G., "The Median Ranks of Sample Values in Their Population with an Application to Certain Fatigue Studies," Ind. Math. 2, 1–9, 1951.

93. Lipson, C., and N. J. Sheth, Statistical Design and Analysis of Engineering Experiments, McGraw Hill, New York, 1973.

94. Beck, J., and K. Arnold, Parameter Estimation in Engineering and Science, J. Wiley, New York, 1977.

95. Ford, F. P., and P. L. Andresen, "Stress Corrosion Cracking of Low–Alloy Pressure Vessel Steel in 288°C Water," Proc. 3rd Int. Atomic Energy Agency Specialists' Meeting on Subcritical Crack Growth, NUREG/CP–0112, Vol. 1, pp. 37–56, Aug. 1990.

96. Ford, F. P., "Overview of Collaborative Research into the Mechanisms of Environmentally Controlled Cracking in the Low Alloy Pressure Vessel Steel/Water System," Proc. 2nd Int. Atomic Energy Agency Specialists' Meeting on Subcritical Crack Growth, NUREG/CP–0067, MEA–2090, Vol. 2, pp. 3–71, April 1986.

97. Wire, G. L., and Y. Y. Li, "Initiation of Environmentally–Assisted Cracking in Low–Alloy Steels," Fatigue and Fracture Volume 1, PVP Vol. 323, H. S. Mehta, ed., American Society of Mechanical Engineers, New York, pp. 269–289, 1996.

98. Pleune, T. T., and O. K. Chopra, "Artificial Neural Networks and Effects of Loading Conditions on Fatigue Life of Carbon and Low–Alloy Steels," Fatigue and Fracture Vol. 1, PVP Vol. 350, S. Rahman, K. K. Yoon, S. Bhandari, R. Warke, and J. M. Bloom, eds., American Society of Mechanical Engineers, New York, pp. 413–423, 1997.

99. Solomon, H. D., R. E. DeLair, and A. D. Unruh, "Crack Initiation in Low-Alloy Steel in High-Purity Water," Effects of the Environment on the Initiation of Crack Growth, ASTM STP 1298, W. A. Van Der Sluys, R. S. Piascik, and R. Zawierucha, eds., American Society for Testing and Materials, Philadelphia, pp. 135–149, 1997.

100. Solomon, H. D., R. E. DeLair, and E. Tolksdorf, "LCF Crack Initiation in WB36 in High-Temperature Water," Proc. 9th Intl. Symp. on Environmental Degradation of Materials in Nuclear Power Systems – Water Reactors, F. P. Ford, S. M. Bruemmer, and G. S. Was, eds., The Minerals, Metals, and Materials Society, Warrendale, PA, pp. 865–872, 1999.

101. Cullen, W. H., M. Kemppainen, H. Hänninen, and K. Törrönen, "The Effects of Sulfur Chemistry and Flow Rate on Fatigue Crack Growth Rates in LWR Environments," NUREG/CR–4121, 1985.

102. Van Der Sluys, W. A., and R. H. Emanuelson, "Environmental Acceleration of Fatigue Crack Growth in Reactor Pressure Vessel Materials and Environments," Environmentally Assisted Cracking: Science and Engineering, ASTM STP 1049, W. B. Lisagor, T. W. Crooker, and B. N. Leis, eds., American Society for Testing and Materials, Philadelphia, PA, pp. 117–135, 1990.

103. Atkinson, J. D., J. Yu, and Z.–Y. Chen, "An Analysis of the Effects of Sulfur Content and Potential on Corrosion Fatigue Crack Growth in Reactor Pressure Vessel Steels," Corros. Sci. 38 (5), 755–765, 1996.

104. Auten, T. A., S. Z. Hayden, and R. H. Emanuelson, "Fatigue Crack Growth Rate Studies of Medium Sulfur Low Alloy Steels Tested in High Temperature Water," Proc. 6th Int. Symp. on Environmental Degradation of Materials in Nuclear Power Systems – Water Reactors, R. E. Gold and E. P. Simonen, eds., The Metallurgical Society, Warrendale, PA, pp. 35–40, 1993.

105. Wire, G. L., T. R. Leax, and J. T. Kandra, "Mean Stress and Environmental Effects on Fatigue in Type 304 Stainless Steel," in Probabilistic and Environmental Aspects of Fracture and Fatigues, PVP Vol. 386, S. Rahman, ed., American Society of Mechanical Engineers, New York, pp. 213–228, 1999.

106. Kim, Y. J., "Characterization of the Oxide Film Formed on Type 316 Stainless Steel in 288°C Water in Cyclic Normal and Hydrogen Water Chemistries," Corrosion 51 (11), 849–860, 1995.

107. Kim, Y. J., "Analysis of Oxide Film Formed on Type 304 Stainless Steel in 288°C Water Containing Oxygen, Hydrogen, and Hydrogen Peroxide," Corrosion 55 (1), 81–88, 1999.

108. Kilian, R., J. Hickling, and R. Nickell, "Environmental Fatigue Testing of Stainless Steel Pipe Bends in Flowing, Simulated PWR Primary Water at 240°C," Third Intl. Conf. Fatigue of Reactor Components, MRP-151, Electric Power Research Institute, Palo Alto, CA, Aug. 2005.

109. Chopra, O. K., "Estimation of Fracture Toughness of Cast Stainless Steels During Thermal Aging in LWR Systems," NUREG/CR–4513, ANL–93/22, Aug. 1994.

110. Chopra, O. K., "Effect of Thermal Aging on Mechanical Properties of Cast Stainless Steels," in Proc. of the 2nd Int. Conf. on Heat–Resistant Materials, K. Natesan, P. Ganesan, and G. Lai, eds., ASM International, Materials Park, OH, pp. 479–485, 1995.

111. Higuchi, M., "Review and Consideration of Unsettled Problems on Evaluation of Fatigue Damage in LWR Water," Proc. Of the 2005 ASME Pressure Vessels and Piping Conf., July 17–21, 2005, Denver, CO, paper # PVP2005–71306.

112. Mayfield, M. E., E. C. Rodabaugh, and R. J. Eiber, "A Comparison of Fatigue Test Data on Piping with the ASME Code Fatigue Evaluation Procedure," ASME Paper 79–PVP–92, American Society of Mechanical Engineers, New York, 1979.

113. Heald, J. D., and E. Kiss, "Low Cycle Fatigue of Nuclear Pipe Components," J. Pressure Vessel Technol. 74, PVP–5, 1–6, 1974.

114. Deardorff, A. F., and J. K. Smith, "Evaluation of Conservatisms and Environmental Effects in ASME Code, Section III, Class 1 Fatigue Analysis," SAND94–0187, prepared by Structural Integrity Associates, San Jose, CA, under contract to Sandia National Laboratories, Albuquerque, NM, 1994.

115. Kooistra, L. F., E. A. Lange, and A. G. Pickett, "Full–Size Pressure Vessel Testing and Its Application to Design," J. Eng. Power 86, 419–428, 1964.

116. Scott, P. M., and G. M. Wilkowski, "A Comparison of Recent Full–Scale Component Fatigue Data with the ASME Section III Fatigue Design Curves," in Fatigue and Crack Growth: Environmental Effects, Modeling Studies, and Design Considerations, PVP Vol. 306, S. Yukawa, ed., American Society of Mechanical Engineers, New York, pp. 129–138, 1995.

117. Hechmer, J., "Evaluation Methods for Fatigue - A PVRC Project," in Fatigue, Environmental Factors, and New Materials, PVP Vol. 374, H. S. Mehta, R. W. Swindeman, J. A. Todd, S. Yukawa, M. Zako, W. H. Bamford, M. Higuchi, E. Jones, H. Nickel, and S. Rahman, eds., American Society of Mechanical Engineers, New York, pp. 191–199, 1998.

118. Manjoine, M. J., "Fatigue Damage Models for Annealed Type 304 Stainless Steel under Complex Strain Histories," Trans. 6th Intl. Conf. on Structural Mechanics in Reactor Technology (SMiRT), Vol. L, 8/1, North–Holland Publishing Co., pp. 1–13, 1981.

119. Nian, L., and Du Bai–Ping, "The Effect of Low–Stress High–Cycle Fatigue on the Microstructure and Fatigue Threshold of a 40Cr Steel," Int. J. Fatigue 17 (1), 43–48, 1995.

APPENDIX A

Incorporating Environmental Effects into Fatigue Evaluations

A1 Scope

This Appendix provides the environmental fatigue correction factor (F_{en}) methodology that is considered acceptable for incorporating the effects of reactor coolant environments on fatigue usage factor evaluations of metal components for new reactor construction. The methodology for performing fatigue evaluations for the three major categories of structural materials, e.g., carbon steel, low-alloy steels, and wrought and cast austenitic stainless steels, is described.

A2 Environmental Correction Factor (F_{en})

The effects of reactor coolant environments on the fatigue life of structural materials are expressed in terms of a nominal environmental fatigue correction factor, $F_{en,nom}$, which is defined as the ratio of fatigue life in air at room temperature ($N_{air,RT}$) to that in water at the service temperature (N_{water}).

$$F_{en,nom} = N_{air,RT}/N_{water} \tag{A.1}$$

The nominal environmental fatigue correction factor, $F_{en,nom}$, for carbon steels is expressed as

$$F_{en,nom} = \exp(0.632 - 0.101\ S^*\ T^*\ O^*\ \dot{\varepsilon}^*\ ), \tag{A.2}$$

and for low-alloy steels, it is expressed as

$$F_{en,nom} = \exp(0.702 - 0.101\ S^*\ T^*\ O^*\ \dot{\varepsilon}^*\ ), \tag{A.3}$$

where S^*, T^*, O^*, and $\dot{\varepsilon}^*$ are transformed S content, temperature, DO level, and strain rate, respectively, defined as:

$$
\begin{array}{lll}
S^* = S & (S \leq 0.015 \text{ wt.\%}) & \\
S^* = 0.015 & (S > 0.015 \text{ wt.\%}) & \text{(A.4)}
\end{array}
$$

$$
\begin{array}{lll}
T^* = 0 & (T < 150°C) & \\
T^* = T - 150 & (T = 150\text{–}350°C) & \text{(A.5)}
\end{array}
$$

$$
\begin{array}{lll}
O^* = 0 & (DO \leq 0.04 \text{ ppm}) & \\
O^* = \ln(DO/0.04) & (0.04 \text{ ppm} < DO \leq 0.5 \text{ ppm}) & \\
O^* = \ln(12.5) & (DO > 0.5 \text{ ppm}) & \text{(A.6)}
\end{array}
$$

$$
\begin{array}{lll}
\dot{\varepsilon}^* = 0 & (\dot{\varepsilon} > 1\%/s) & \\
\dot{\varepsilon}^* = \ln(\dot{\varepsilon}) & (0.001 \leq \dot{\varepsilon} \leq 1\%/s) & \\
\dot{\varepsilon}^* = \ln(0.001) & (\dot{\varepsilon} < 0.001\%/s). & \text{(A.7)}
\end{array}
$$

For both carbon and low-alloy steels, a threshold value of 0.07% for strain amplitude is defined below which environmental effects on the fatigue life of these steels do not occur. Thus,

$$F_{en,nom} = 1 \qquad\qquad (\varepsilon \le 0.07\%). \tag{A.8}$$

For wrought and cast austenitic stainless steels,

$$F_{en,nom} = \exp(0.734 - T' O' \dot{\varepsilon}') \tag{A.9}$$

where T', $\dot{\varepsilon}'$, and O' are transformed temperature, strain rate, and DO level, respectively, defined as:

$$
\begin{aligned}
T' &= 0 && (T < 150°C)\\
T' &= (T - 150)/175 && (150 \le T < 325°C)\\
T' &= 1 && (T \ge 325°C)
\end{aligned}
\tag{A.10}
$$

$$
\begin{aligned}
\dot{\varepsilon}' &= 0 && (\dot{\varepsilon} > 0.4\%/s)\\
\dot{\varepsilon}' &= \ln(\dot{\varepsilon}/0.4) && (0.0004 \le \dot{\varepsilon} \le 0.4\%/s)\\
\dot{\varepsilon}' &= \ln(0.0004/0.4) && (\dot{\varepsilon} < 0.0004\%/s)
\end{aligned}
\tag{A.11}
$$

$$O' = 0.281 \qquad\qquad (\text{all DO levels}). \tag{A.12}$$

For wrought and cast austenitic stainless steels, a threshold value of 0.10% for strain amplitude is defined below which environmental effects on the fatigue life of these steels do not occur. Thus,

$$F_{en,nom} = 1 \qquad\qquad (\varepsilon \le 0.10\%). \tag{A.13}$$

A3   Fatigue Evaluation Procedure

The evaluation method uses as its input the partial fatigue usage factors U_1, U_2, U_3, …U_n, determined in Class 1 fatigue evaluations. To incorporate environmental effects into the Section III fatigue evaluation, the partial fatigue usage factors for a specific stress cycle or load set pair, based on the current Code fatigue design curves, is multiplied by the environmental fatigue correction factor:

$$U_{en.1} = U_1 \cdot F_{en,1} \tag{A.14}$$

In the Class 1 design–by–analysis procedure, the partial fatigue usage factors are calculated for each type of stress cycle in paragraph NB-3222.4(e)(5). For Class 1 piping products designed using the NB–3600 procedure, Paragraph NB-3653 provides the procedure for the calculation of partial fatigue usage factors for each of the load set pairs. The partial usage factors are obtained from the Code fatigue design curves provided they are consistent, or conservative, with respect to the existing fatigue ε–N data. For example, the Code fatigue design curve for austenitic SSs developed in the 1960s is not consistent with the existing fatigue database and, therefore, will yield nonconservative estimates of usage factors for most heats of austenitic SSs that are used in the construction of nuclear reactor components. Examples of calculating partial usage factors are as follows:

(a)   For carbon and low–alloy steels with ultimate tensile strength ≤552 MPa (≤80 ksi), the partial fatigue usage factors are obtained from the ASME Code fatigue design curve, i.e., Fig. I–9.1 of the mandatory Appendix I to Section III of the ASME Code. As an alternative, to reduce conservatism in the current Code requirement of a factor of 20 on life, partial usage factors may be determined from the fatigue design curves that were developed from the ANL statistical model, i.e., Figs. 9 and 10 and Table 4

(b)   For wrought or cast austenitic SSs, the partial fatigue usage factors are obtained from the fatigue design curve proposed in the present report, i.e., Fig. 37 and Table 9.

The cumulative fatigue usage factor, U_{en}, considering the effects of reactor coolant environments is calculated as the following:

$$U_{en} = U_1 \cdot F_{en,1} + U_2 \cdot F_{en,2} + U_3 \cdot F_{en,3} + U_i \cdot F_{en,i} \ldots + U_n \cdot F_{en,n} \tag{A.15}$$

where $F_{en,i}$ is the nominal environmental fatigue correction factor for the "i"th stress cycle (NB-3200) or load set pair (NB-3600). Because environmental effects on fatigue life depend on parameters such as strain rate, temperature, dissolved oxygen in water, and for carbon and low–alloy steels S content, the values for these parameters are needed to calculate F_{en} for each stress cycle or load set pair. As discussed in Sections 4 and 5 of this report, the following guidance may be used to determine these parameters:

(1)   An average strain rate for the transient always yields a conservative estimate of F_{en}. The lower bound or saturation strain rate of 0.001%/s for carbon and low–alloy steels or 0.0004%/s for austenitic SSs can be used to perform the most conservative evaluation.

(2)   When the results of detailed transient analyses are available an average temperature (i.e., average of the maximum and minimum temperatures for the transients) may be used to calculate F_{en}. The maximum temperature can be used to perform the most conservative evaluation.

(3)   The DO value is obtained from each transient constituting the stress cycle. For carbon and low-alloy steels, the dissolved oxygen content, DO, associated with a stress cycle is the highest oxygen level in the transient, and for austenitic stainless steels, it is the lowest oxygen level in the transient. A value of 0.4 ppm for carbon and low-alloy steels and 0.05 ppm for austenitic stainless steels can be used for the DO content to perform a conservative evaluation.

(4)   The sulfur content, S, in terms of weight percent might be obtained from the certified material test report or an equivalent source. If the sulfur content is unknown, then its value shall be assumed as the maximum value specified in the procurement specification or the applicable construction Code.

The detailed procedures for incorporating environmental effects into the Code fatigue evaluations have been presented in several articles. The following two may be used for guidance:

(1)   Mehta, H. S., "An Update on the Consideration of Reactor Water Effects in Code Fatigue Initiation Evaluations for Pressure Vessels and Piping," Assessment Methodologies for Preventing Failure: Service Experience and Environmental Considerations, PVP Vol. 410-2, R. Mohan, ed., American Society of Mechanical Engineers, New York, pp. 45–51, 2000.

(2)   Nakamura, T., M. Higuchi, T. Kusunoki, and Y. Sugie, "JSME Codes on Environmental Fatigue Evaluation," Proc. of the 2006 ASME Pressure Vessels and Piping Conf., July 23–27, 2006, Vancouver, BC, Canada, paper # PVP2006–ICPVT11–93305.